

**Structural and functional analysis of the
human Rad50 and Mre11 DNA repair complex**

Reaching out for flexible solutions

Proefschrift

ter verkrijging van de graad van doctor
aan de Erasmus Universiteit Rotterdam
op gezag van de Rector Magnificus Prof.dr.ir. J.H. van Bommel
en volgens besluit van het College voor Promoties.

De openbare verdediging zal plaatsvinden op
woensdag 7 mei 2003 om 13.45 uur

door

Martijn de Jager

geboren te Gouda

Promotiecommissie

Promotoren:

Prof.dr. R. Kanaar
Prof.dr. J.H.J. Hoeijmakers

Overige leden:

Prof.dr. F. Grosveld
Prof.dr. C. Dekker
Prof.dr. I. Touw

Co-promotor:

Dr. C. Wyman

The studies described in this thesis have been performed at the department of Cell Biology and Genetics at the Erasmus Medical Centre in Rotterdam from 1998 to 2002. The research and this publication have been supported financially by the Dutch Cancer Society.

voor mijn ouders

voor Du

Contents

Scope and outline of the thesis	7
Chapter 1	9
DNA double-strand break repair and the Rad50 complex: essential from the beginning to the end(s)	
1. Occurrence and repair of DNA double-strand breaks	11
2. DNA double-strand break repair pathways	12
3. The Rad50 protein complex, at the crossroads of many DNA metabolic processes	18
4. Properties of the Rad50 complex	20
Chapter 2	35
DNA binding and strand-annealing activities of human Mre11: implications for its roles in DNA double-strand break repair pathways	
Chapter 3	57
Human Rad50/Mre11 is a flexible complex that can tether DNA ends	
Chapter 4	73
The coiled coil of the human Rad50 DNA repair protein contains specific segments of increased flexibility	

Chapter 5	87
DNA end-binding specificity of human Rad50/Mre11 is influenced by ATP	
Chapter 6	105
SMC family members: functional diversity through differential arrangements of conserved building blocks	
Chapter 7	123
Genome instability and <i>Rad50^S</i> : subtle yet severe	
Abbreviations	136
Summary of the thesis	137
Samenvatting van het proefschrift	139
List of publications	141
Curriculum vitae	142
Dankwoord	143

Scope and outline of the thesis

DNA, the genetic material, contains essential information for the proper function of cells. It is therefore of great importance that the integrity of the genome is carefully maintained during metabolic processes. Special challenges for genome maintenance pathways are DNA ends that arise in cells due to different causes. DNA ends, in the form of telomeres, naturally occur at the termini of the linear eukaryotic chromosomes. Random DNA double-strand breaks (DSBs) can be induced by various exogenous and endogenous DNA damaging agents. In contrast, the cell can intentionally induce site-specific DSBs in specialized processes to create genetic diversity during immune system development and meiosis. Improper processing of these DNA ends imposes a high risk for genetic rearrangements that can lead to cell death, cell malfunction or carcinogenesis. Therefore, it is of great importance that the DNA ends are processed and/or repaired accurately. For this purpose several mechanisms exist that depend on specific specialized protein machineries. The DSB repair pathway used depends on the circumstances under which the break occurs. One protein complex that is involved in multiple genome maintenance pathways that deal with DNA ends consists of three proteins: Rad50, Mre11 and Nbs1. The aim of this thesis is to gain insights in the role of this Rad50 protein complex in DNA end metabolism.

Chapter 1 briefly introduces the causes, consequences and the repair mechanisms of DSBs. Furthermore, it describes what is currently known about the Rad50 protein complex and its roles in DNA end metabolism. **Chapter 2** presents a biochemical analysis of Mre11. Mre11 binds to both single- and double-stranded DNA and can stimulate annealing of complementary DNA molecules.

Another approach to learn more about the function of the Rad50 protein complex is to analyze the structural features of the complex and its interaction with DNA. **Chapter 3** describes such an analysis for the complex of Rad50 and Mre11. Contrary to the prevailing dogma, scanning force microscopy (SFM) studies have revealed that Rad50 does not form intermolecular coiled coils but instead forms intramolecular coiled coils. Two Rad50 molecules associate with two Mre11 molecules, which results in an overall structure with a globular DNA binding and ATPase domain from which two flexible coiled-coil arms protrude. Large oligomers, containing multiple Rad50 complexes can tether different DNA molecules. The flexibility of the coiled-coil arms is analyzed in detail in **Chapter 4**. There, a method is developed to determine the local flexibility of biopolymers, exemplified by the Rad50 coiled coils. The Rad50 coiled coils contain segments of increased flexibility that correspond to amino acid sequences with a low predicted probability to form a coiled coil. The DNA binding properties of the Rad50 complex are further analyzed in **Chapter 5**. The complex requires a DNA end to

form large oligomers that can tether DNA molecules. The DNA binding properties are influenced by the DNA end structure and ATP.

Rad50 shares evolutionarily conserved sequence similarities with proteins from the structural maintenance of chromosomes (SMC) family. In **Chapter 6** a preliminary comparison of different SMC proteins is described. These proteins are all likely to have structural functions in different aspects of genome metabolism. The different proteins use universal components to assemble a structure that is similar but distinct, which allows them to perform their specialized functions. Finally, in **Chapter 7** a perspective is presented on the current knowledge of the Rad50 complex in relation to a Rad50 mouse model that has been generated to study the function of the complex *in vivo*.

Chapter

DNA double-strand break repair and the Rad50

complex: essential from the beginning to the end(s)

1

Chapter 1

DNA double-strand break repair and the Rad50 complex: essential from the beginning to the end(s)

Martijn de Jager¹, Claire Wyman^{1,2} and Roland Kanaar^{1,2}

¹Department of Cell Biology & Genetics, Erasmus MC, Dr. Molewaterplein 50, 3000 DR Rotterdam, The Netherlands, and ²Department of Radiation Oncology, Erasmus MC-Daniel, Rotterdam, The Netherlands

The Rad50 complex is an essential player in maintenance of genome integrity. In mammals, it is required from the beginning until the end of life. This protein complex is implicated in many different DNA metabolic processes, such as meiotic and mitotic DNA double-strand break repair, cell cycle regulation and telomere maintenance. Here we review the function of the Rad50 protein complex in the initial steps of DNA end metabolism.

1. Occurrence and repair of DNA double-strand breaks

During its life, a cell is continuously challenged by different factors that affect the integrity of its vital genetic material, the DNA. One of the most genotoxic DNA lesions is the double-stranded break (DSB). As depicted in Figure 1, this type of lesion can arise as a consequence of exposure to exogenous agents, such as ionizing radiation and chemicals. In addition to these exogenous sources, DSBs can also be created during normal cellular metabolism, for example due to processes that generate DSB-inducing free radicals. Other types of DNA damage such as crosslinks and single-stranded gaps can be converted to DSBs by DNA replication.

DNA double-strand break sources		
pathological		physiological
exogenous	endogenous	specialized
radiation	free radicals	meiotic recombination
chemicals	collapsed replication forks	V(D)J recombination
		somatic hypermutation
		IgG class switching

Figure 1. Causes of DNA double-strand breaks. Pathological DSBs can be induced by exogenous and endogenous sources. However, specialized cells also induce physiologically important DSBs that are necessary in processes that create genetic and immunogenic variation.

Apart from these pathological DSBs, the intentional creation of DSBs in specialized cellular processes is used to initiate genetic rearrangements (Figure 1). During meiosis, DSBs are induced in germ cells to promote exchange of genetic information between the paternal and maternal chromosomes to create genetic diversity. Other processes that rely on genetic rearrangements after the intentional induction of DSBs are found in the immune system. First, V(D)J recombination provides a means to create diversity by combinatorial arrangement and imprecise joining of different DNA segments to yield

functional immunoglobulin and T-cell receptor variable regions. The diversity in the immunoglobulin variable region gene segments is further enhanced by somatic hypermutation that induces point mutations at high frequency and that depends on the induction of DSBs. Second, different immunoglobulin isotypes are created by switch recombination that recombines a V(D)J gene segment with a different constant region.

If DSBs are not properly processed, this can lead to undesired genetic rearrangements. These can impair normal cellular function and eventually lead to cell death. Alternatively, abnormal cell function can lead to uncontrolled cell proliferation and tumor formation. In order to counteract the potential deleterious effects of exogenous and endogenous DNA damaging agents and to process programmed DSBs properly, different DSB repair pathways have evolved. The two major, mechanistically distinct, DSB repair pathways are homologous recombination and non-homologous end-joining (NHEJ). In addition to these major pathways, subpathways of each can be used, depending on the circumstances under which the break occurs.

2. DNA double-strand break repair pathways

Mechanisms of DNA double-strand break repair

Homologous recombination uses homologous DNA sequences, sister chromatids or homologous chromosomes, to precisely repair a DSB (Figure 2A). In addition to the repair of a break with two ends, homologous recombination is also used to restore collapsed, stalled and reversed replication forks. These rescue missions often involve the creation of single-end invasion intermediates (Figure 2B). A similar intermediate is found at the end of the chromosomes. At telomeres, the 3'-overhang single-stranded DNA is protected by looping back to form a recombination-like (Griffith et al., 1999; Figure 2C). In addition to these functions of homologous recombination in accurate repair and protection of DNA ends, homologous recombination is also used to recombine paternal and maternal chromosomes during meiosis.

NHEJ, on the other hand, is an error-prone pathway that directly links two DNA ends. Limited processing of the ends might be required for ligation, making this pathway error-prone (Figure 2D). In a distinct subset of the NHEJ events, small direct repeats at both ends of the DSB, so-called micro-homologies, are used to link the DNA ends, thereby resulting in small deletions (Figure 2E). The inaccuracy of NHEJ is used as a powerful tool to create additional diversity in V(D)J recombination by imprecise joining of V-, D- and J-segments that make up the variable regions of immunoglobulins and T-cell receptors, as described above.

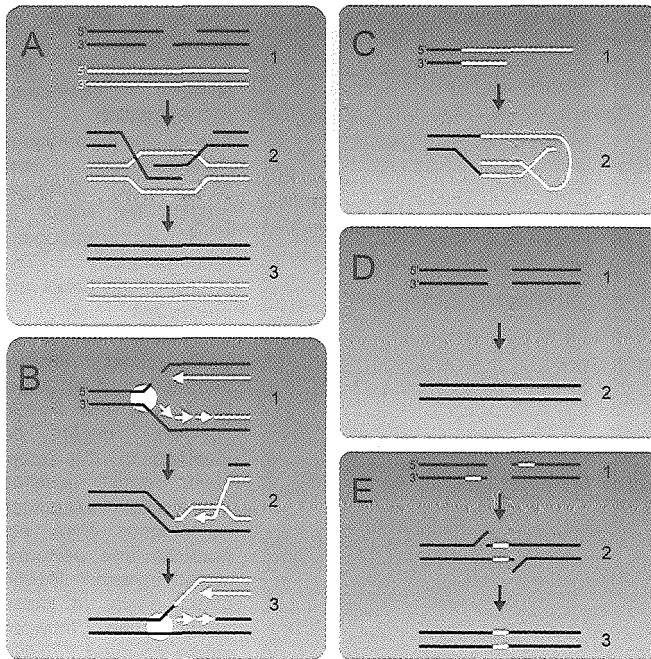


Figure 2. Processing of DNA ends. Schematic representation of different specialized mechanisms for DNA end processing. (A)

Homologous recombination of a DSB-containing DNA molecule (black) with a homologous template sequence (white). The DNA ends are processed (1) and the resulting single-stranded overhangs invade a homologous template DNA molecule (2), resulting in a so-called D-loop structure. Subsequently, the invaded strands are extended and the D-loop structure is resolved (3). (B) Restoration of a collapsed replication fork through recombination with the newly synthesized sister chromatid

(white sphere represents DNA replication complex; white strands represent newly synthesized DNA). After replication of a nicked template strand (1), the resulting DNA end can be processed and invades the homologous sister chromatid (2). After ligation of the Okazaki fragments this structure resembles a replication fork that can reinitiate replication by extension of the invaded strand (3). (C) Protection of telomeric DNA by a recombination intermediate between repeated sequences (white) at the end of chromosomal DNA. The long single-stranded overhang at the end of the chromosome (1) can invade the double-stranded region that contains many repeats to form a stable D-loop-like intermediate referred to as a T-loop (2). (D) Direct joining of a pair of DNA ends by NHEJ. Two ends of a DSB undergo no or limited processing (1) and are ligated (2). (E) Microhomology directed NHEJ using alignment of small direct repeats (white). The DNA ends are processed (1) to expose the direct repeats. The repeats can be annealed (2), after which this structure is further processed and ligated (3).

Homologous recombination

Eukaryotic homologous recombination is mediated through the Rad52 epistasis group of proteins. This group includes Rad51, Rad52, and Rad54, as well as the Rad50 complex (consisting of Rad50, Mre11 and Xrs2, the yeast homolog of mammalian Nbs1). Extensive genetic and biochemical analysis provided insights into the role of many players in homologous recombination (reviewed in Haber, 2000). A number of models for DSB repair through homologous recombination have been proposed. Two of these models, synthesis-dependent strand annealing and gene conversion, are schematically depicted in Figure 3A.

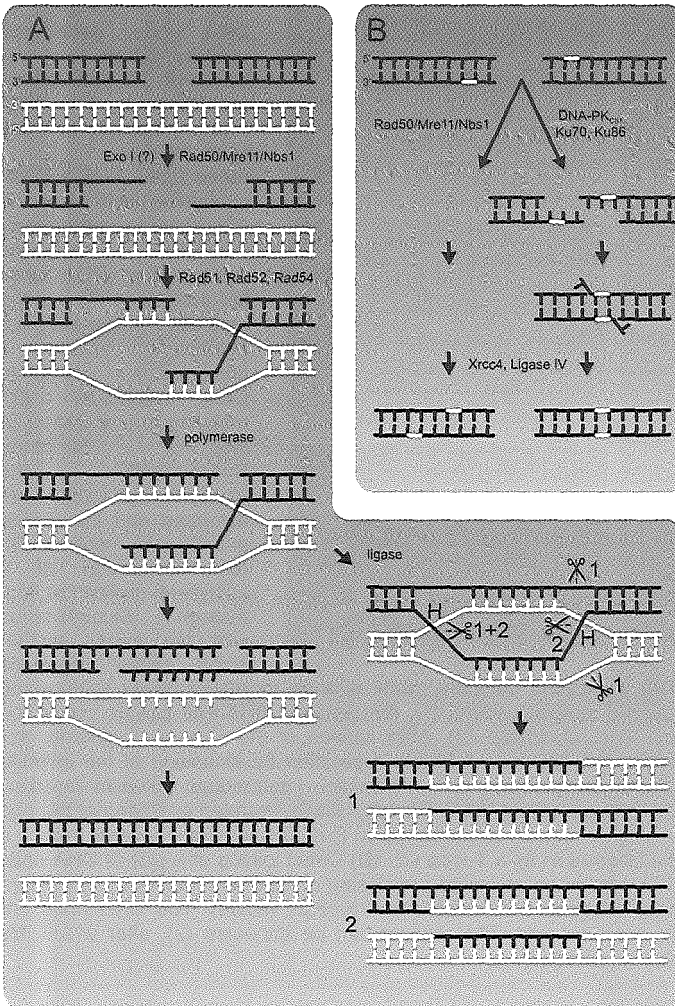


Figure 3. Models of homologous recombination and NHEJ.

Schematic representation of models for homologous recombination and NHEJ. (A) Different models for repair of DSBs by homologous recombination. The end(s) of the break are processed in a coordinated fashion to yield long single-stranded 3' overhangs. Exo1 and the Rad50 complex might be involved in this step. Next, Rad51 assisted by Rad52 recognizes homologous DNA sequences and performs strand invasion. Rad54 might assist in these steps. The invaded single-stranded DNA serves as a primer for extension by a DNA polymerase. In the next step the resulting D-loop structure is resolved. Here, two models are depicted. First, in synthesis-dependent strand annealing pathway (left branch) the two newly synthesized complementary DNA strands are separated from their templates and annealed

subsequently. It is unclear which enzymes are involved in this process. This type of resolution does not require any cleavage of the D-loop structure. Second, resolution of the D-loop can occur through gene conversion (right branch), in which the two Holliday junctions (H) are cleaved by a structure-specific endonuclease. Depending on the strands that are cleaved (indicated with 1 and 2), gene conversion can occur with or without cross over resulting in products 1 and 2, respectively. (B) In NHEJ, two ends are directly brought together and can undergo limited processing (right branch). Alternatively, short direct repeats are used to align the ends after limited processing (left branch). Candidates for these steps in both branches are the Rad50 complex as well as DNA-PK (consisting of Ku70, Ku80 and DNA-PK_{CS}). Next, the eventual flap-structures could be cleaved by Fen-1 endonuclease, and the ends are ligated through the activity of the ligase IV, Xrcc4 complex. More details about both pathways and the factors that are involved can be found in the text.

In the first step of both modes of homologous recombination, the DNA ends are resected to create extended 3' single-stranded overhangs. Exo1 is a processive exonuclease that is involved in processing of DNA ends (Tsubouchi and Ogawa, 2000). Although the Rad50 complex has also been implicated in the resection step (Usui et al., 1998; Tsubouchi and Ogawa, 1998), this complex might have a more structural function in organization of the DNA ends, as discussed below. Rad51 forms a nucleoprotein filament on single-stranded and double-stranded DNA molecules and can promote strand exchange between two homologous DNA molecules (Ogawa et al., 1993; reviewed in Baumann and West, 1998). Rad52 interacts with Rad51 and stimulates filament formation by removal of replication protein A (RPA) from the single-stranded DNA molecule generated at the break (Sung, 1997; Shinohara and Ogawa, 1998; New et al., 1998; Sugiyama and Kowalczykowski, 2002). Rad52 forms a heptameric ring structure that has been proposed to wrap DNA and can anneal complementary single-stranded DNA molecules (Shinohara et al., 1998; Stasiak et al., 2000; Singleton et al., 2002). Rad54 is also required for the strand invasion reaction, most likely through its ability to affect DNA topology (Petukhova et al., 1998; Petukhova et al., 1999; Van Komen et al., 2000; Mazin et al., 2000; Ristic et al., 2001; Essers et al., 2002). Rad54 is a member of the Swi2/Snf2 family of proteins that are involved in modulating protein-DNA interactions. Rad54 has chromatin remodeling activity (Alexiadis and Kadonaga, 2002; Jaskelioff et al., 2003; Alexeev et al., 2003). Recent reports indicate that Rad54 might have additional functions in both stabilization and disassembly of the Rad51-DNA filament (Solinger et al., 2002; Mazin et al., 2003). In addition to the proteins mentioned above, a number of other proteins involved in the early steps of homologous recombination, including homology recognition and joint molecule formation have been identified. They include the Rad51 paralogs Rad55 and 57 in *S. cerevisiae* and Rad51B-D, Xrcc2 and Xrcc3 in mammals, the Rad52 paralog Rad59 and the Rad54 paralog Rdh54 (reviewed in Symington, 2002).

The invasion of single-stranded DNA into the unwound homologous double-stranded DNA molecule by the proteins mentioned above results in a so-called D-loop structure (schematically depicted in Figure 3). After formation of a D-loop structure, the invading 3' end(s) can serve as a primer for extension by a DNA polymerase. In the synthesis-dependent strand-annealing pathway, the complementary newly synthesized strands are separated from their template strands and annealed. This type of resolution does not require any cleavage of the D-loop structure. In contrast, in the classical DSB repair model (Szostak et al., 1983) two Holliday junctions are formed (Figure 3). Their resolution requires strand cleavage to resolve recombination intermediates via gene conversion. Depending on the strands that are cleaved, gene conversion can occur with or without cross over. The nature of the Holliday junction resolvase is not known. Mus81 is a candidate nuclease that recognizes and resolves Holliday junctions (Boddy et al., 2001; Chen et al., 2001b). In cell free extracts Mus81 is present in one of the two fractions that contain Holliday junction resolvase activity. However, comparison of these two activities showed that a so far unidentified resolvase activity is more likely to resolve

Holliday junctions (Constantinou et al., 2002). Instead, Mus81 is more likely to cleave stalled replication fork structures in order to initiate replication restart (Kaliraman et al., 2001; Whitby et al., 2002).

Other models for DSB repair through homology-driven repair mechanisms are single-strand annealing and break-induced replication. Single-strand annealing occurs between direct repeated sequences on the same DNA molecule. Following a break and processing to expose homologous single-strands, one of the repeats and the intervening sequence are deleted. This pathway utilizes Rad52-mediated strand annealing. An additional requirement for this pathway is the Msh2 and Msh3 mismatch repair protein complex (Sugawara et al., 1997). Likely this complex recognizes the 3' flap structures that are formed by non-complementary single-stranded DNA adjacent to the annealed direct repeats. Subsequently, these flap structures can be cleaved by the Rad1/Rad10 structure-specific endonuclease (Ivanov and Haber, 1995). In break-induced replication a 3' overhang end invades the homologous template DNA and is extended by a polymerase. When the second end is missing or fails to engage, this intermediate (similar to the situation depicted in Figure 2B) can continue replication to the end of the chromosome (reviewed in Kraus et al., 2001).

Non-homologous end-joining

Like for homologous recombination, genetic and biochemical analysis identified and assigned functions to the key factors of the NHEJ process in eukaryotes: DNA-dependent kinase (DNA-PK; composed of Ku70, Ku86 and a catalytic subunit, DNA-PK_{CS}), ligase IV and Xrcc4 (for reviews see Lieber, 1999; Lewis and Resnick, 2000). A model for DSB repair through non-homologous end-joining is depicted in Figure 3B. Within the NHEJ pathway two subpathways exist: direct end-joining and microhomology-dependent end-joining. The first pathway directly joins the DNA ends after no or limited processing. The latter pathway uses small direct repeat sequences close to the DNA end to join the ends. The first step in NHEJ is limited processing of the ends to make them blunt or to reveal eventual microhomologies. The Rad50 complex has been implicated in this processing step, and in addition might have a structural function (as discussed below). Another protein complex important in an early step of the end-joining reaction is DNA-PK. The Ku heterodimer needs a DNA end for binding and forms a ring structure that can slide on DNA (Walker et al., 2001). DNA-PK_{CS} can interact with the Ku heterodimer bound at a DNA end and the resulting complex can promote tethering of two DNA ends (Cary et al., 1997; Yaneva et al., 1997). Next, DNA-PK can recruit the ligase IV and Xrcc4 protein complex and phosphorylate Xrcc4 (Chen et al., 2000; Calsou et al., 2003). Tethering of end-bound DNA-PK complexes can result in autophosphorylation of DNA-PK, which disrupts its DNA binding (Merkle et al., 2002). The elongated structure of Xrcc4 might be essential to link and position the DNA ends for ligation by ligase IV (Grawunder et al., 1997; Junop et al., 2000). In the case of joining through microhomologies, non-complementary short 3' or 5' overhangs would

result in 'flap structures'. The nature of the nuclease that processes 3' flap structures is so far unknown. The structure-specific endonuclease Fen-1 can remove 5' flap structures before ligation (Wu et al., 1999).

Contribution of homologous recombination and non-homologous end-joining

The fundamental mechanistic differences between homologous recombination and NHEJ have implications for the choice of DSB repair pathway in different cell types and cell cycle stages. For stem cells, embryonic cells, and unicellular organisms, having many divisions in view, it is essential that DSBs are accurately repaired to prevent accumulation of genetic rearrangements and mutations in their offspring. Because of their proliferative state, these cells have the opportunity to use homologous recombination between sister chromatids in S- and G₂-phase, resulting in accurate DSB repair. Conversely, non-dividing cells, in G₀- or G₁-phase of the cell cycle, have no sister chromatids available for recombination. In this case recombination between homologous chromosomes is dangerous since it can lead to loss of heterozygosity with undesirable consequences such as inactivation of tumor suppressor genes. Therefore, these cells depend more strongly on NHEJ. In multicellular organisms, somatic cells are not pluripotent and often have a determined limited life span, so that inaccurate repair is less likely to immediately impose risks to the organism.

Although the molecular mechanisms of DSB repair are highly conserved among species, the differences in the relative contribution of homologous recombination and NHEJ are reflected in the phenotype of the respective yeast and mammalian cell mutants. Deletion of yeast homologous recombination factors Rad52 or Rad54 results in extreme radiosensitivity (Game, 1993). In contrast, the murine deletion mutants have, depending on the cell type, only slightly reduced recombination frequencies and in case of Rad54 mild radiosensitivity (Essers et al., 1997; Rijkers et al., 1998). Deletion of factors involved in NHEJ has a relatively mild phenotype in yeast (Game, 1993; Siede et al., 1996; Boulton and Jackson, 1998), while the mammalian phenotype is severe. Strikingly, mutation of Rad50, Mre11 or Xrs2, has relatively mild effects in yeast, while deletion mutants of murine Rad50, Mre11 or Nbs1 are all incompatible with life (Xiao and Weaver, 1997; Luo et al., 1999; Zhu et al., 2001). Furthermore, deletion of either Xrcc4 or ligase IV are also embryonic lethal in the mouse (Frank et al., 1998; Barnes et al., 1998; Gao et al., 1998). Mutants in the components of DNA-PK display hypersensitivity to ionizing radiation and severe combined immunodeficiency (Blunt et al., 1995; Zhu et al., 1996; Gu et al., 1997). For Rad50 and Nbs1 viable murine hypomorphic mutants have been described (Bender et al., 2002; Williams et al., 2002). In humans a limited number of patients is known to have hypomorphic mutations in factors involved in DSB repair. This is the case in a patient with a mutation in DNA ligase IV (Riballo et al., 1999). Furthermore, patients suffering from Nijmegen breakage syndrome (NBS) and ataxia telangiectasia-like disorder (ATLD) have mutations in Nbs1 and Mre11, respectively. (Varon et al., 1998; Stewart et al., 1999; see below). The

biological importance of the Rad50 complex is underscored by the phenotype of these patients who are cancer prone and show cellular radiosensitivity.

3. The Rad50 protein complex, at the cross-roads of many DNA metabolic processes

Functions in mitotic and meiotic DSB repair

Nbs1 and Mre11 are components of a protein complex together with Rad50. Originally, the genes encoding the components of the Rad50, Mre11 and Xrs2 (the yeast homolog of mammalian Nbs1) protein complex were identified by screening of radiosensitive mutants in *Saccharomyces cerevisiae*. Epistasis analysis placed them within the group of mutants in homologous recombination as well as NHEJ pathways (Milne et al., 1996; Moore and Haber, 1996; Boulton and Jackson, 1998; Bressan et al., 1999). The Rad50 complex appears to be mostly involved in ionizing radiation induced sister-chromatid recombination, although a role in ionizing radiation induced interhomolog recombination is not ruled out (Bressan et al., 1999). The evidence for the involvement of the Rad50 complex in homologous recombination is supported by results with (inducible) knockout chicken DT40 cells. A knockout of Nbs1 in these cells shows that homologous recombination is affected (Tauchi et al., 2002). Furthermore, experiments with inducible Mre11 knockout cells show that Mre11 functions in homologous recombination, but most likely not in Ku70-dependent NHEJ (Yamaguchi-Iwai et al., 1999). However, evidence for the involvement of the Rad50 complex in NHEJ comes from reconstitution experiments with cell-free extracts. In this assay purified DNA-PK and the ligase IV / Xrcc4 complex are not sufficient for effective rejoining of a linearized plasmid. Efficient rejoining requires the addition of a fraction containing the Rad50 complex (Huang and Dynan, 2002).

In addition to its important role in the mitotic DSB repair, the yeast Rad50 complex is indispensable for progression of meiosis. In meiosis DSBs are created in the paternal and maternal chromatids during the prophase of the first meiotic division to initiate the chromosomal rearrangements that create genetic diversity. In the absence of any of the Rad50 complex components, meiotic DSBs are not created (Sun et al., 1991; Ivanov et al., 1992; Ajimura et al., 1993). Separation-of-function mutants of Rad50 or Mre11 do allow DSB formation, but the subsequent DNA resection does not occur (Alani et al., 1990; Nairz and Klein, 1997; Tsubouchi and Ogawa, 1998). In these mutants Spo11, that creates meiotic DSBs, remains covalently attached to the 5' DNA end

(Keeney and Kleckner, 1995). It thus appears that induction of meiotic DSBs and their repair are tightly coupled processes.

Additional roles in cell cycle control and telomere length maintenance

The progression of the cell through the different phases of mitotic division is tightly controlled by cell cycle checkpoints. In case of DNA damage, cells can pause the progression through the cell cycle at different phases to allow repair and to avoid genome rearrangements. A first clue to the function of the Rad50 complex in cell cycle regulation came from NBS patients that have hypomorphic mutations in Nbs1 (Shiloh, 1997; Varon et al., 1998; Carney et al., 1998). Cells of these patients are radiosensitive, which is likely to be a consequence of their improper response to DNA damage. In contrast to normal cells, NBS cells continue to replicate their DNA upon irradiation. This characteristic is referred to as a radio-resistant DNA synthesis (RDS) phenotype (Shiloh, 1997). Upon DSB induction, Nbs1 is one of the targets for phosphorylation by ataxia telangiectasia mutated (ATM) kinase. Genetic experiments showed that two branches exist in the intra-S checkpoint, one of them mediated through Nbs1 (Falck et al., 2002). Nbs1 associates with the Rad50 complex through Mre11 *in vivo* and *in vitro* (Carney et al., 1998). *In vivo*, Nbs1 is essential for relocalization of Rad50 and Mre11 to DSBs and colocalizes with Rad50 and Mre11 at the DSB sites (Carney et al., 1998; Desai-Mehta et al., 2001; Tauchi et al., 2001). The hypothesis that the Rad50 complex is involved in cell cycle regulation through the association of Nbs1 is confirmed by the phenotype of patients with hypomorphic mutations in Mre11. They suffer from ATLD, which is, like NBS, hallmarked by cellular RDS and radiosensitivity (Stewart et al., 1999). The hypomorphic mutations of ATLD patients can be mapped onto the structure of a archaeal Mre11 homolog at a potential interaction interface between Mre11 and Nbs1 (Hopfner et al., 2001). The impaired cell cycle response in ATLD patients could thus be a consequence of a disrupted Mre11 and Nbs1 interaction.

Components of the Rad50 complex are also involved in telomere length maintenance as indicated by the observation that yeast deletion mutants in any of the three complex components have shorter telomeres (Nugent et al., 1998). The involvement in telomere length maintenance is further supported by genetic experiments that show that the components of the yeast Rad50 complex are in the same epistasis group as telomerase (Kironmai and Muniyappa, 1997; Nugent et al., 1998). In mammalian cells the Rad50 complex is also implicated in telomere metabolism. Nbs1-deficient cells have shorter telomeres (Ranganathan et al., 2001) and recent experiments show that the Rad50 complex interacts *in vivo* through Mre11 with Trf2, a protein component of telomeres (Zhu et al., 2000). Trf2 binds double-stranded telomere repeats and is thought to be involved in creation or stabilization of the 3'-overhangs at telomeres (Broccoli et al., 1997; van Steensel et al., 1998). The exact function of the Rad50 complex in telomere length maintenance is unknown. One function might be to create the 3'-overhang single-stranded overhang that is required for telomerase-

mediated telomere elongation (Diede and Gottschling, 2001). However, a direct role in the creation of these single-stranded overhangs is unlikely, since a nuclease deficient Mre11 mutant in yeast has normal telomere length (Moreau et al., 1999). Indeed, genetic experiments indicate that the complex functions in a telomerase-independent pathway that elongates telomeres through a recombination-mediated process (Le et al., 1999; Teng et al., 2000; Chen et al., 2001a).

The essential function of the Rad50 complex in the different processes mentioned above is reflected in the inviability of mammalian deletion mutants in any of the three complex components (Xiao and Weaver, 1997; Luo et al., 1999; Zhu et al., 2001). In humans hypomorphic mutants for Mre11 and Nbs1 have been described (Varon et al., 1998; Stewart et al., 1999). For Rad50 and Nbs1, hypomorphic mouse models have been developed (Bender et al., 2002; Kang et al., 2002; Williams et al., 2002; discussed in Chapter 7). In view of the dramatic effect of null mutants, the phenotype of these hypomorphic mutants is likely to reflect only part their essential functions. The phenotypic heterogeneity between the different hypomorphic mutants confirms that subtle mutations affect different functions of the complex (reviewed in Chapter 7).

4. Properties of the Rad50 complex

Biochemical activities of the Rad50 complex

Despite the essential functions of all three components of the Rad50 complex, the biochemistry of the complex is still poorly understood. Rad50 homologs possess a weak ATPase activity, but the biological relevance of this activity remains unclear (Chapter 5; Hopfner et al., 2000b). More data are available for the various Mre11 homologs. These have both 3' to 5' exonuclease as well as weak endonuclease activities (Sharples and Leach, 1995; Usui et al., 1998; Paull and Gellert, 1998; Hopfner et al., 2000a). The exonuclease activity may not be directly involved in homologous recombination as it does not have the polarity needed to produce the required 3' single-stranded overhang (Sugawara and Haber, 1992). Furthermore, genetic experiments show that the nuclease activity is not required for the role of Mre11 in mitotic homologous recombination (Bressan et al., 1999; Moreau et al., 1999). In contrast, the nuclease activity of Mre11 is required for meiotic recombination and, in addition, might be important for its role in micro-homology dependent NHEJ (Moreau et al., 1999; Paull and Gellert, 2000). This activity might be modified in the presence of other proteins. One *in vitro* finding, consistent with this idea is that the nuclease activity of yeast Mre11 is different in the context of the Rad50 complex. The complex can partially unwind DNA and, through its

Mre11 endonuclease activity, degrade the DNA in 5' to 3' direction (Trujillo and Sung, 2001). So far it is unclear which type of end-processing is required for (micro-homology directed) NHEJ, leaving the possibility that the 3' to 5' nuclease activity is relevant for this pathway. After limited degradation, the resulting short single-stranded tails could anneal at the exposed micro-homologies through the annealing activity that is associated with Mre11 (Paull and Gellert, 2000; Chapter 2). To date, no enzymatic activity has been described for Nbs1.

Rad50 complex architecture

One remarkable feature of Rad50 can be deduced from its predicted secondary structure. Rad50 contains a bipartite ATPase domain that is split between the amino- and carboxy-terminal ends of the protein, containing Walker A- and B-type motifs of an ATPase domain, respectively. Similar bipartite ATPase domains have been observed in proteins of the ABC transporter family, where these separated motifs come together to form a functional ATPase (Lowe et al., 2001). Furthermore, structure prediction of Rad50 shows that a domain having a high tendency to form a α -helix separates the ATPase motifs. These structural properties make Rad50 a member of the structural maintenance of chromosomes (SMC) protein family (Aravind et al., 1999; Strunnikov and Jessberger, 1999). These proteins were thought to form homodimers with an anti-parallel orientation. Thus, the α -helices would wind around each other, forming an intermolecular coiled coil, bringing the Walker A- and B-type motifs from different monomers together to form two active ATPase domains on either end of an extended coiled coil. This arrangement results in an overall structure resembling a dumbbell, as schematically depicted in Figure 4A.

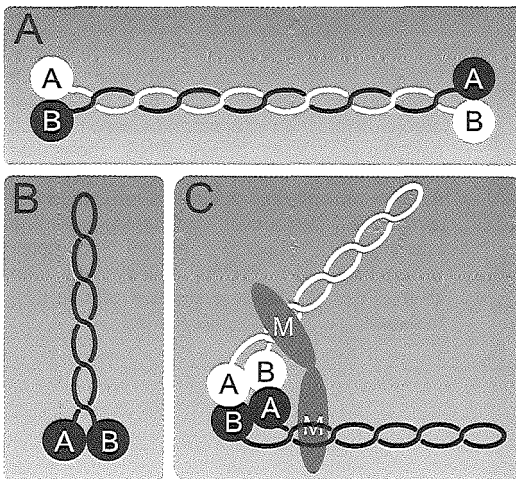


Figure 4. Possible arrangements of Rad50 protomers. Different models for the arrangement of Rad50 and the interaction with Mre11. (A) Dimerization of two Rad50 molecules in an anti-parallel intermolecular coiled coil forms two functional ATPase domains through association of Walker A- and B-type ATPase motifs (A and B, respectively). (B) Rad50 arrangement in an intramolecular coiled coil, forming one functional ATPase domain through association of a Walker A- and B-type ATPase motifs. (C) Rad50 complex arrangement. Two Rad50 molecules arranged as intramolecular coiled coils associate with two Mre11 molecules (M) to form a functional Rad50 complex molecule.

Indeed, structures resembling this overall architecture have been observed by electron microscopy of SMC family members and bacterial Rad50 homologs (Melby et al., 1998; Connelly et al., 1998). The crystal structure of the ATPase domain of an archaeal Rad50 homolog shows that two Rad50 molecules dimerize to form two functional ATPase domains (Hopfner et al., 2000b).

The coiled-coil regions were not present in the crystal structure of the Rda50 ATPase domain, leaving the possibilities of intermolecular and intramolecular coiled coils open. However, for the human Rad50/Mre11 complex SFM images are only consistent with intramolecular coiled coils in which the α -helix is folded back halfway and wound around itself, as schematically depicted in Figure 4B (Chapter 3). Combining data obtained from crystals of parts of Rad50 and Mre11 homologs (Hopfner et al., 2000b; Hopfner et al., 2001) with the overall complex architecture observed by SFM (Chapter 3) results in a model of the complex architecture as a heterotetramer containing two Rad50 and two Mre11 molecules, as depicted in Figure 4C. The organization as intramolecular coiled coils now appears to be the rule rather than the exception for the SMC family of proteins. The crystal structure of the apex of the coiled-coil arms of the *Pyrococcus furiosus* Rad50 homolog shows a similar intramolecular coiled-coil arrangement (Hopfner et al., 2002). Furthermore, electron microscopic experiments with the *S. cerevisiae* cohesin complex as well as the crystal structure of the *Thermotoga maritima* SMC1 and SMC3 hinge domains shows that these SMC family members are arranged as intramolecular coiled coils as well (Haering et al., 2002).

From structure to function

SFM studies of the interaction of the human Rad50 complex with DNA revealed that the protein complex forms oligomers on linear DNA, with the arms protruding away from the DNA. The Rad50 complex can tether different DNA molecules through multiple

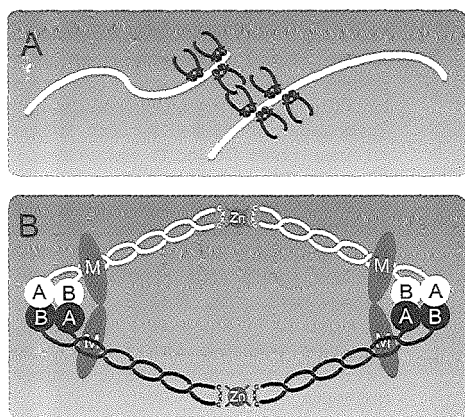


Figure 5. Interactions between Rad50 complexes. Model for the molecular mechanism of the interaction between Rad50 complexes that brings DNA molecules together. (A) Tethering of DNA molecules through multiple interactions of the coiled-coil arms. (B) Molecular mechanism of the interaction between Rad50 complex molecules. Two Rad50 coiled coils can interact through the coordination of zinc (Zn) between two CXXC-motifs (CXXC).

interactions of the coiled-coil arms (Chapter 3), as depicted in Figure 5A. A possible molecular mechanism for the interactions between the Rad50 arms became clear with the crystal structure of the tip of the arm of the *P. furiosus* Rad50 homolog. It appears that the apex of each Rad50 arm is half of a zinc finger, the so-called CXXC-motif, where 'C' stands for cysteine and 'X' for any amino acid (Hopfner et al., 2002). Two properly oriented Rad50 arms can coordinate a zinc atom, thus providing a link between two complex molecules as depicted in Figure 5B. SFM studies show that the protein complex requires a DNA end to form oligomers. Furthermore, these oligomers do not necessarily stay attached to the very end of the DNA, but can also be found at internal positions on the DNA (Chapter 5). This inward movement might be essential for function since it keeps DNA molecules in close proximity while leaving the ends accessible for other proteins to perform their function.

Model for the function of SMC proteins in sister chromatid cohesion and chromosome condensation have often assumed that the arms of the SMC proteins are stiff levers. SFM images show however that the coiled-coil arms of the Rad50 complex can adapt different conformations. Time-resolved SFM experiments in buffer with Rad50 complex that was partially immobilized directly show that individual coiled-coil arms are flexible structures that can adopt different conformations (Chapter 3). The development of a method that can measure local flexibility from high-resolution SFM images led to the finding that there are two segments that have increased flexibility within the coiled coil. The source of this increased flexibility can be found in the amino acid sequence of the coiled-coil arms. The segment between the amino- and carboxy-terminal globular domains is in general highly likely to form a coiled coil. However, there are two segments where in both strands the formation of a coiled coil is less likely. These segments coincide with the experimentally determined positions of increased flexibility (Chapter 4). The segments with increased flexibility are likely to be important for the function of the Rad50 complex. Since the protein can tether DNA molecules through multiple flexible interactions of, presumably, the tips of the coiled-coils arms, it is essential that the arms are bendable enough to adopt different conformations. The intrinsic flexibility of ordered coiled coils might not be big enough and could therefore be enhanced by disruptions in the coiled coil to achieve the required elasticity within a reasonable length.

Rad50 complex homologs: conservation of building blocks

Based on the structural properties described above, Rad50 is a member of the structural maintenance of chromosomes (SMC) family of proteins. The common structural properties of this class of proteins are similar, as summarized in Figure 6. First, they contain a globular ATPase domain of the Rad50 homolog that interacts with a partner protein. This partner is a homolog of Mre11 in case of the human, *S. cerevisiae*, *E. coli* and *P. furiosus* Rad50/Mre11 complexes (Sharples and Leach, 1995; Usui et al., 1998; Paull and Gellert, 1998; Hopfner et al., 2000a). *S. cerevisiae* Rad50 and the

ATPase domains of *P. furiosus* Rad50 can directly interact with DNA in the presence of ATP (Raymond and Kleckner, 1993; Hopfner et al., 2000b). The *S. cerevisiae* SMC1/SMC3 cohesin complex interacts with Scc1 through its ATPase domains. Scc1 does not directly interact with DNA but is hypothesized to form a ring structure with SMC1 and SMC3 that embraces DNA (Haering et al., 2002; see below). Second an extended coiled coil protrudes from the ATPase domain. This is arranged as an intramolecular coiled coil for the human and *P. furiosus* Rad50 homologs as well as for *S. cerevisiae* and *T. maritima* SMC1/SMC3 cohesin complex (Chapter 3; Hopfner et al., 2002; Haering et al., 2002). The length and likely the flexibility of the coiled-coil region varies among SMC family members (Chapter 6). Third, the apex of the coiled-coil arms is a dimerization domain. The human, yeast, bacterial and archaeal homologs of Rad50

have a CXXC-motif. For the *P. furiosus* Rad50 homolog this motif functions in the interaction between two coiled-coil arms through the orientation of a zinc atom, as described above (Hopfner et al., 2002). The different cohesin homologs have a globular domain at this position that provides a strong dimerization interface for two SMC protein molecules (Haering et al., 2002).

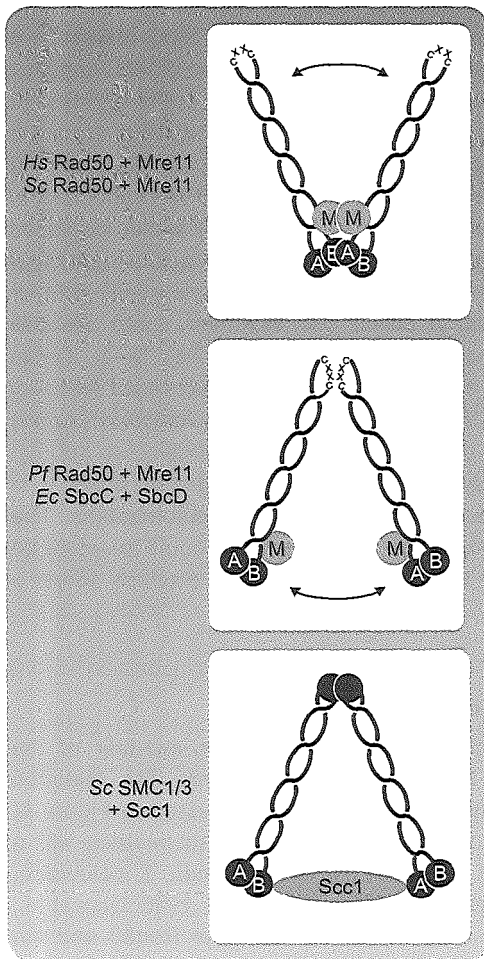


Figure 6. SMC family proteins are composed of universal 'building blocks'. Comparison of *Homo sapiens* (Hs), *Saccharomyces cerevisiae* (Sc), *Pyrococcus furiosus* (Pf), *Escherichia coli* (Ec) Rad50 and Mre11 homologs, and the *S. cerevisiae* cohesin complex (SMC1, SMC3 and Scc1). 'Building blocks' of the homologs: ATPase domain consisting of Walker A- and B-type ATPase motifs (A and B, respectively), intramolecular coiled coils with either a CXXC-motif (CXXC) or a globular domain at the apex, and the partner protein of the complex Mre11 or Scc1 (M and Scc1, respectively). Assembly of family members from their 'building blocks' yields similar but distinct architectures. Double-headed arrows indicate the flexibility of the coiled-coil arms that can result in different conformations.

Despite the similarities in these 'building blocks' the overall architecture of the Rad50 complexes from different species is different, as summarized in Figure 6. The human and *S. cerevisiae* Rad50 heterodimeric complexes form heterotetramers through the interaction of the globular domains and partner proteins (Chapter 3; Chapter 6; Anderson et al., 2001). In contrast, the *P. furiosus* and *E. coli* complexes appear to have stronger interactions through the apexes of the coiled-coil arms (Connelly et al., 1998; Chapter 6). These differences in conformation might be a consequence of the relative strength of interactions through the globular domains versus CXXC-motifs. The architecture of the complexes likely reflects the DNA binding properties of the different homologs. The human Rad50 complex interacts with DNA through the globular domain, with the coiled-coil arms protruding away from the DNA (Chapter 3). In view of the comparable complex architecture, the *S. cerevisiae* Rad50 complex might interact similarly with DNA. In contrast, the architecture of the archaeal and bacterial Rad50 complexes implies that these have two independent DNA binding domains that can interact with different DNA sites. The archaeal and bacterial complexes have so far not been implicated in DSB repair.

Dimerization through the apexes of the coiled-coil arms is also observed for the cohesin complex of different species. The coiled coils of these proteins contain a globular domain that provides a very strong dimerization domain. Biochemical experiments show that the ATPase domain of SMC1 and SMC3 interact separately with different domains of Scc1, thus forming a ring structure (Figure 6). It has been hypothesized that this ring embraces sister chromatids to prevent them from drifting apart before cell division (Haering et al., 2002).

It thus appears that the different members of the SMC family of proteins use very similar but distinct building blocks to assemble unique architectures. These differences in protein architecture are likely to reflect the diverse functions of these family members in DNA metabolism.

References

- Ajimura, M., Leem, S. H., and Ogawa, H. (1993). Identification of new genes required for meiotic recombination in *Saccharomyces cerevisiae*. *Genetics* 133, 51-66.
- Alani, E., Padmore, R., and Kleckner, N. (1990). Analysis of wild-type and rad50 mutants of yeast suggests an intimate relationship between meiotic chromosome synapsis and recombination. *Cell* 61, 419-436.
- Alexeev, A., Mazin, A., and Kowalczykowski, S. C. (2003). Rad54 protein possesses chromatin-remodeling activity stimulated by the Rad51-ssDNA nucleoprotein filament. *Nat. Struct. Biol.* 10, 82-86.

- Alexiadis, V., and Kadonaga, J. T.** (2002). Strand pairing by Rad54 and Rad51 is enhanced by chromatin. *Genes Dev.* *16*, 2767-2771.
- Anderson, D. E., Trujillo, K. M., Sung, P., and Erickson, H. P.** (2001). Structure of the Rad50 x Mre11 DNA repair complex from *Saccharomyces cerevisiae* by electron microscopy. *J. Biol. Chem.* *276*, 37027-37033.
- Aravind, L., Walker, D. R., and Koonin, E. V.** (1999). Conserved domains in DNA repair proteins and evolution of repair systems. *Nucleic Acids Res.* *27*, 1223-1242.
- Barnes, D. E., Stamp, G., Rosewell, I., Denzel, A., and Lindahl, T.** (1998). Targeted disruption of the gene encoding DNA ligase IV leads to lethality in embryonic mice. *Curr. Biol.* *8*, 1395-1398.
- Baumann, P., and West, S. C.** (1998). Role of the human RAD51 protein in homologous recombination and double-stranded-break repair. *Trends Biochem. Sci.* *23*, 247-251.
- Bender, C. F., Sikes, M. L., Sullivan, R., Huye, L. E., Le Beau, M. M., Roth, D. B., Mirzoeva, O. K., Oltz, E. M., and Petrini, J. H.** (2002). Cancer predisposition and hematopoietic failure in Rad50^{S/S} mice. *Genes Dev.* *16*, 2237-2251.
- Blunt, T., Finnie, N. J., Taccioli, G. E., Smith, G. C., Demengeot, J., Gottlieb, T. M., Mizuta, R., Varghese, A. J., Alt, F. W., Jeggo, P. A.** (1995). Defective DNA-dependent protein kinase activity is linked to V(D)J recombination and DNA repair defects associated with the murine scid mutation. *Cell* *80*, 813-823.
- Boddy, M. N., Gaillard, P. H., McDonald, W. H., Shanahan, P., Yates, J. R., 3rd, and Russell, P.** (2001). Mus81-Eme1 are essential components of a Holliday junction resolvase. *Cell* *107*, 537-548.
- Boulton, S. J., and Jackson, S. P.** (1998). Components of the Ku-dependent non-homologous end-joining pathway are involved in telomeric length maintenance and telomeric silencing. *EMBO J.* *17*, 1819-1828.
- Bressan, D. A., Baxter, B. K., and Petrini, J. H.** (1999). The Mre11-Rad50-Xrs2 protein complex facilitates homologous recombination-based double-strand break repair in *Saccharomyces cerevisiae*. *Mol. Cell. Biol.* *19*, 7681-7687.
- Broccoli, D., Smogorzewska, A., Chong, L., and de Lange, T.** (1997). Human telomeres contain two distinct Myb-related proteins, TRF1 and TRF2. *Nat. Genet.* *17*, 231-235.
- Calsou, P., Delteil, C., Frit, P., Drouet, J., and Salles, B.** (2003). Coordinated Assembly of Ku and p460 Subunits of the DNA-dependent Protein Kinase on DNA Ends is Necessary for XRCC4-ligase IV Recruitment. *J. Mol. Biol.* *326*, 93-103.
- Carney, J. P., Maser, R. S., Olivares, H., Davis, E. M., Le Beau, M., Yates, J. R., 3rd, Hays, L., Morgan, W. F., and Petrini, J. H.** (1998). The hMre11/hRad50 protein complex and Nijmegen breakage syndrome: linkage of double-strand break repair to the cellular DNA damage response. *Cell* *93*, 477-486.
- Cary, R. B., Peterson, S. R., Wang, J., Bear, D. G., Bradbury, E. M., and Chen, D. J.** (1997). DNA looping by Ku and the DNA-dependent protein kinase. *Proc. Natl. Acad. Sci. USA* *94*, 4267-4272.
- Chen, L., Trujillo, K., Sung, P., and Tomkinson, A. E.** (2000). Interactions of the DNA ligase IV-XRCC4 complex with DNA ends and the DNA-dependent protein kinase. *J. Biol. Chem.* *275*, 26196-26205.

Chen, Q., Ijima, A., and Greider, C. W. (2001a). Two survivor pathways that allow growth in the absence of telomerase are generated by distinct telomere recombination events. *Mol. Cell Biol.* *21*, 1819-1827.

Chen, X. B., Melchionna, R., Denis, C. M., Gaillard, P. H., Blasina, A., Van de Weyer, I., Boddy, M. N., Russell, P., Vialard, J., and McGowan, C. H. (2001b). Human Mus81-associated endonuclease cleaves Holliday junctions *in vitro*. *Mol. Cell* *8*, 1117-1127.

Connelly, J. C., Kirkham, L. A., and Leach, D. R. (1998). The SbcCD nuclease of *Escherichia coli* is a structural maintenance of chromosomes (SMC) family protein that cleaves hairpin DNA. *Proc. Natl. Acad. Sci. USA* *95*, 7969-7974.

Constantinou, A., Chen, X. B., McGowan, C. H., and West, S. C. (2002). Holliday junction resolution in human cells: two junction endonucleases with distinct substrate specificities. *EMBO J.* *21*, 5577-5585.

de Jager, M., Dronkert, M. L., Modesti, M., Beerens, C. E., Kanaar, R., and van Gent, D. C. (2001a). DNA-binding and strand-annealing activities of human Mre11: implications for its roles in DNA double-strand break repair pathways. *Nucleic Acids Res.* *29*, 1317-1325.

de Jager, M., van Noort, J., van Gent, D. C., Dekker, C., Kanaar, R., and Wyman, C. (2001b). Human Rad50/Mre11 is a flexible complex that can tether DNA ends. *Mol. Cell* *8*, 1129-1135.

de Jager, M., Wyman, C., van Gent, D. C., and Kanaar, R. (2002). DNA end-binding specificity of human Rad50/Mre11 is influenced by ATP. *Nucleic Acids Res.* *30*, 4425-4431.

Desai-Mehta, A., Cerosaletti, K. M., and Concannon, P. (2001). Distinct functional domains of nibrin mediate Mre11 binding, focus formation, and nuclear localization. *Mol. Cell Biol.* *21*, 2184-2191.

Diede, S. J., and Gottschling, D. E. (2001). Exonuclease activity is required for sequence addition and Cdc13p loading at a de novo telomere. *Curr. Biol.* *11*, 1336-1340.

Essers, J., Hendriks, R. W., Swagemakers, S. M., Troelstra, C., de Wit, J., Bootsma, D., Hoeijmakers, J. H., and Kanaar, R. (1997). Disruption of mouse RAD54 reduces ionizing radiation resistance and homologous recombination. *Cell* *89*, 195-204.

Essers, J., Hendriks, R. W., Wesoly, J., Beerens, C. E., Smit, B., Hoeijmakers, J. H., Wyman, C., Dronkert, M. L., and Kanaar, R. (2002). Analysis of mouse Rad54 expression and its implications for homologous recombination. *DNA Repair* *1*, 779-793.

Falck, J., Petrini, J. H., Williams, B. R., Lukas, J., and Bartek, J. (2002). The DNA damage-dependent intra-S phase checkpoint is regulated by parallel pathways. *Nat. Genet.* *30*, 290-294.

Frank, K. M., Sekiguchi, J. M., Seidl, K. J., Swat, W., Rathbun, G. A., Cheng, H. L., Davidson, L., Kangaloo, L., and Alt, F. W. (1998). Late embryonic lethality and impaired V(D)J recombination in mice lacking DNA ligase IV. *Nature* *396*, 173-177.

Game, J. C. (1993). DNA double-strand breaks and the RAD50-RAD57 genes in *Saccharomyces*. *Semin. Cancer Biol.* *4*, 73-83.

Gao, Y., Sun, Y., Frank, K. M., Dikkes, P., Fujiwara, Y., Seidl, K. J., Sekiguchi, J. M., Rathbun, G. A., Swat, W., Wang, J., Bronson, R. T., Malynn, B. A., Bryans, M., Zhu, C., Chaudhuri, J., Davidson, L., Ferrini, R., Stamato, T., Orkin, S. H., Greenberg, M. E., and Alt, F. W. (1998). A critical role for DNA end-joining proteins in both lymphogenesis and neurogenesis. *Cell* *95*, 891-902.

- Grawunder, U., Wilm, M., Wu, X., Kulesza, P., Wilson, T. E., Mann, M., and Lieber, M. R.** (1997). Activity of DNA ligase IV stimulated by complex formation with XRCC4 protein in mammalian cells. *Nature* 388, 492-495.
- Griffith, J. D., Comeau, L., Rosenfield, S., Stansel, R. M., Bianchi, A., Moss, H., and de Lange, T.** (1999). Mammalian telomeres end in a large duplex loop. *Cell* 97, 503-514.
- Gu, Y., Seidl, K. J., Rathbun, G. A., Zhu, C., Manis, J. P., van der Stoep, N., Davidson, L., Cheng, H. L., Sekiguchi, J. M., Frank, K., Stanhope-Baker, P., Schlissel, M. S., Roth, D. B., and Alt, F. W.** (1997). Growth retardation and leaky SCID phenotype of Ku70-deficient mice. *Immunity* 7, 653-665.
- Haber, J. E.** (2000). Lucky breaks: analysis of recombination in *Saccharomyces*. *Mutat. Res.* 451, 53-69.
- Haering, C. H., Lowe, J., Hochwagen, A., and Nasmyth, K.** (2002). Molecular architecture of SMC proteins and the yeast cohesin complex. *Mol. Cell* 9, 773-788.
- Hopfner, K. P., Karcher, A., Shin, D., Fairley, C., Tainer, J. A., and Carney, J. P.** (2000a). Mre11 and Rad50 from *Pyrococcus furiosus*: cloning and biochemical characterization reveal an evolutionarily conserved multiprotein machine. *J. Bacteriol.* 182, 6036-6041.
- Hopfner, K. P., Karcher, A., Shin, D. S., Craig, L., Arthur, L. M., Carney, J. P., and Tainer, J. A.** (2000b). Structural biology of Rad50 ATPase: ATP-driven conformational control in DNA double-strand break repair and the ABC-ATPase superfamily. *Cell* 101, 789-800.
- Hopfner, K. P., Karcher, A., Craig, L., Woo, T. T., Carney, J. P., and Tainer, J. A.** (2001). Structural biochemistry and interaction architecture of the DNA double-strand break repair Mre11 nuclease and Rad50-ATPase. *Cell* 105, 473-485.
- Hopfner, K. P., Craig, L., Moncalian, G., Zinkel, R. A., Usui, T., Owen, B. A., Karcher, A., Henderson, B., Bodmer, J. L., McMurray, C. T., Carney, J. P., Petrini, J. H., and Tainer, J. A.** (2002). The Rad50 zinc-hook is a structure joining Mre11 complexes in DNA recombination and repair. *Nature* 418, 562-566.
- Huang, J., and Dynan, W. S.** (2002). Reconstitution of the mammalian DNA double-strand break end-joining reaction reveals a requirement for an Mre11/Rad50/NBS1-containing fraction. *Nucleic Acids Res.* 30, 667-674.
- Ivanov, E. L., and Haber, J. E.** (1995). RAD1 and RAD10, but not other excision repair genes, are required for double-strand break-induced recombination in *Saccharomyces cerevisiae*. *Mol. Cell Biol.* 15, 2245-2251.
- Ivanov, E. L., Korolev, V. G., and Fabre, F.** (1992). XRS2, a DNA repair gene of *Saccharomyces cerevisiae*, is needed for meiotic recombination. *Genetics* 132, 651-664.
- Jaskelioff, M., Van Komen, S., Krebs, J. E., Sung, P., and Peterson, C. L.** (2003). Rad54p is a chromatin remodeling enzyme required for heteroduplex DNA joint formation with chromatin. *J. Biol. Chem.* 278, 3.
- Junop, M. S., Modesti, M., Guarne, A., Ghirlando, R., Gellert, M., and Yang, W.** (2000). Crystal structure of the Xrcc4 DNA repair protein and implications for end joining. *EMBO J.* 19, 5962-5970.
- Kaliraman, V., Mullen, J. R., Fricke, W. M., Bastin-Shanower, S. A., and Brill, S. J.** (2001). Functional overlap between Sgs1-Top3 and the Mms4-Mus81 endonuclease. *Genes Dev.* 15, 2730-2740.

Kang, J., Bronson, R. T., and Xu, Y. (2002). Targeted disruption of NBS1 reveals its roles in mouse development and DNA repair. *EMBO J.* 21, 1447-1455.

Keeney, S., and Kleckner, N. (1995). Covalent protein-DNA complexes at the 5' strand termini of meiosis-specific double-strand breaks in yeast. *Proc. Natl. Acad. Sci. USA* 92, 11274-11278.

Kironmai, K. M., and Muniyappa, K. (1997). Alteration of telomeric sequences and senescence caused by mutations in RAD50 of *Saccharomyces cerevisiae*. *Genes Cells* 2, 443-455.

Kraus, E., Leung, W. Y., and Haber, J. E. (2001). Break-induced replication: a review and an example in budding yeast. *Proc. Natl. Acad. Sci. USA* 98, 8255-8262.

Le, S., Moore, J. K., Haber, J. E., and Greider, C. W. (1999). RAD50 and RAD51 define two pathways that collaborate to maintain telomeres in the absence of telomerase
Cell cycle and genetic requirements of two pathways of nonhomologous end-joining repair of double-strand breaks in *Saccharomyces cerevisiae*. *Genetics* 152, 143-152.

Lewis, L. K., and Resnick, M. A. (2000). Tying up loose ends: nonhomologous end-joining in *Saccharomyces cerevisiae*. *Mutat. Res.* 451, 71-89.

Lieber, M. R. (1999). The biochemistry and biological significance of nonhomologous DNA end joining: an essential repair process in multicellular eukaryotes. *Genes Cells* 4, 77-85.

Lowe, J., Cordell, S. C., and van den Ent, F. (2001). Crystal structure of the SMC head domain: an ABC ATPase with 900 residues antiparallel coiled-coil inserted. *J. Mol. Biol.* 306, 25-35.

Luo, G., Yao, M. S., Bender, C. F., Mills, M., Bladl, A. R., Bradley, A., and Petrini, J. H. (1999). Disruption of mRad50 causes embryonic stem cell lethality, abnormal embryonic development, and sensitivity to ionizing radiation. *Proc. Natl. Acad. Sci. USA* 96, 7376-7381.

Mazin, A. V., Alexeev, A. A., and Kowalczykowski, S. C. (2003). A novel function of RAD54 protein: Stabilization of the RAD51 nucleoprotein filament. *J. Biol. Chem.* 3, 3.

Mazin, A. V., Bornarth, C. J., Solinger, J. A., Heyer, W. D., and Kowalczykowski, S. C. (2000). Rad54 protein is targeted to pairing loci by the Rad51 nucleoprotein filament. *Mol. Cell* 6, 583-592.

Melby, T. E., Ciampaglio, C. N., Briscoe, G., and Erickson, H. P. (1998). The symmetrical structure of structural maintenance of chromosomes (SMC) and MukB proteins: long, antiparallel coiled coils, folded at a flexible hinge. *J. Cell. Biol.* 142, 1595-1604.

Merkle, D., Douglas, P., Moorhead, G. B., Leonenko, Z., Yu, Y., Cramb, D., Bazett-Jones, D. P., and Lees-Miller, S. P. (2002). The DNA-dependent protein kinase interacts with DNA to form a protein-DNA complex that is disrupted by phosphorylation. *Biochemistry* 41, 12706-12714.

Milne, G. T., Jin, S., Shannon, K. B., and Weaver, D. T. (1996). Mutations in two Ku homologs define a DNA end-joining repair pathway in *Saccharomyces cerevisiae*. *Mol. Cell. Biol.* 16, 4189-4198.

Moore, J. K., and Haber, J. E. (1996). Cell cycle and genetic requirements of two pathways of nonhomologous end-joining repair of double-strand breaks in *Saccharomyces cerevisiae*. *Mol. Cell. Biol.* 16, 2164-2173.

Moreau, S., Ferguson, J. R., and Symington, L. S. (1999). The nuclease activity of Mre11 is required for meiosis but not for mating type switching, end joining, or telomere maintenance. *Mol. Cell. Biol.* 19, 556-566.

Nairz, K., and Klein, F. (1997). mre11S - a yeast mutation that blocks double-strand-break processing and permits nonhomologous synapsis in meiosis. *Genes Dev.* 11, 2272-2290.

- New, J. H., Sugiyama, T., Zaitseva, E., and Kowalczykowski, S. C.** (1998). Rad52 protein stimulates DNA strand exchange by Rad51 and replication protein A. *Nature* 391, 407-410.
- Nugent, C. I., Bosco, G., Ross, L. O., Evans, S. K., Salinger, A. P., Moore, J. K., Haber, J. E., and Lundblad, V.** (1998). Telomere maintenance is dependent on activities required for end repair of double-strand breaks. *Curr. Biol.* 8, 657-660.
- Ogawa, T., Yu, X., Shinohara, A., and Egelman, E. H.** (1993). Similarity of the yeast RAD51 filament to the bacterial RecA filament. *Science* 259, 1896-1899.
- Paull, T. T., and Gellert, M.** (1998). The 3' to 5' exonuclease activity of Mre 11 facilitates repair of DNA double-strand breaks. *Mol. Cell* 1, 969-979.
- Paull, T. T., and Gellert, M.** (2000). A mechanistic basis for Mre11-directed DNA joining at microhomologies. *Proc. Natl. Acad. Sci. USA* 97, 6409-6414.
- Petukhova, G., Stratton, S., and Sung, P.** (1998). Catalysis of homologous DNA pairing by yeast Rad51 and Rad54 proteins. *Nature* 393, 91-94.
- Petukhova, G., Van Komen, S., Vergano, S., Klein, H., and Sung, P.** (1999). Yeast Rad54 promotes Rad51-dependent homologous DNA pairing via ATP hydrolysis-driven change in DNA double helix conformation. *J. Biol. Chem.* 274, 29453-29462.
- Ranganathan, V., Heine, W. F., Ciccone, D. N., Rudolph, K. L., Wu, X., Chang, S., Hai, H., Ahearn, I. M., Livingston, D. M., Resnick, I., Rosen, F., Seemanova, E., Jarolim, P., Depinho, R. A., and Weaver, D. T.** (2001). Rescue of a telomere length defect of Nijmegen breakage syndrome cells requires NBS and telomerase catalytic subunit. *Curr. Biol.* 11, 962-966.
- Raymond, W. E., and Kleckner, N.** (1993). RAD50 protein of *S. cerevisiae* exhibits ATP-dependent DNA binding. *Nucleic Acids Res.* 21, 3851-3856.
- Riballo, E., Critchlow, S. E., Teo, S. H., Doherty, A. J., Priestley, A., Broughton, B., Kysela, B., Beamish, H., Plowman, N., Arlett, C. F., Lehmann, A. R., Jackson, S. P., and Jeggo, P. A.** (1999). Identification of a defect in DNA ligase IV in a radiosensitive leukaemia patient. *Curr. Biol.* 9, 699-702.
- Rijkers, T., Van Den Ouweland, J., Morolli, B., Rolink, A. G., Baarends, W. M., Van Sloun, P. P., Lohman, P. H., and Pastink, A.** (1998). Targeted inactivation of mouse RAD52 reduces homologous recombination but not resistance to ionizing radiation. *Mol. Cell. Biol.* 18, 6423-6429.
- Ristic, D., Wyman, C., Paulusma, C., and Kanaar, R.** (2001). The architecture of the human Rad54-DNA complex provides evidence for protein translocation along DNA. *Proc. Natl. Acad. Sci. USA* 98, 8454-8460.
- Sharples, G. J., and Leach, D. R.** (1995). Structural and functional similarities between the SbcCD proteins of *Escherichia coli* and the RAD50 and MRE11 (RAD32) recombination and repair proteins of yeast. *Mol. Microbiol.* 17, 1215-1217.
- Shiloh, Y.** (1997). Ataxia-telangiectasia and the Nijmegen breakage syndrome: related disorders but genes apart. *Annu. Rev. Genet.* 31, 635-662.
- Shinohara, A., and Ogawa, T.** (1998). Stimulation by Rad52 of yeast Rad51-mediated recombination. *Nature* 391, 404-407.
- Shinohara, A., Shinohara, M., Ohta, T., Matsuda, S., and Ogawa, T.** (1998). Rad52 forms ring structures and co-operates with RPA in single-strand DNA annealing. *Genes Cells* 3, 145-156.

- Siede, W., Friedl, A. A., Dianova, I., Eckardt-Schupp, F., and Friedberg, E. C.** (1996). The *Saccharomyces cerevisiae* Ku autoantigen homologue affects radiosensitivity only in the absence of homologous recombination. *Genetics* 142, 91-102.
- Singleton, M. R., Wentzell, L. M., Liu, Y., West, S. C., and Wigley, D. B.** (2002). Structure of the single-strand annealing domain of human RAD52 protein. *Proc. Natl. Acad. Sci. USA* 99, 13492-13497.
- Solinger, J. A., Kiiianitsa, K., and Heyer, W. D.** (2002). Rad54, a Swi2/Snf2-like recombinational repair protein, disassembles Rad51:dsDNA filaments. *Mol. Cell* 10, 1175-1188.
- Stasiak, A. Z., Larquet, E., Stasiak, A., Muller, S., Engel, A., Van Dyck, E., West, S. C., and Egelman, E. H.** (2000). The human Rad52 protein exists as a heptameric ring. *Curr. Biol.* 10, 337-340.
- Stewart, G. S., Maser, R. S., Stankovic, T., Bressan, D. A., Kaplan, M. I., Jaspers, N. G., Raams, A., Byrd, P. J., Petrini, J. H., and Taylor, A. M.** (1999). The DNA double-strand break repair gene hMRE11 is mutated in individuals with an ataxia-telangiectasia-like disorder. *Cell* 99, 577-587.
- Strunnikov, A. V., and Jessberger, R.** (1999). Structural maintenance of chromosomes (SMC) proteins: conserved molecular properties for multiple biological functions. *Eur. J. Biochem.* 263, 6-13.
- Sugawara, N., and Haber, J. E.** (1992). Characterization of double-strand break-induced recombination: homology requirements and single-stranded DNA formation. *Mol. Cell. Biol.* 12, 563-575.
- Sugawara, N., Paques, F., Colaiacovo, M., and Haber, J. E.** (1997). Role of *Saccharomyces cerevisiae* Msh2 and Msh3 repair proteins in double-strand break-induced recombination. *Proc. Natl. Acad. Sci. USA* 94, 9214-9219.
- Sugiyama, T., and Kowalczykowski, S. C.** (2002). Rad52 protein associates with replication protein A (RPA)-single-stranded DNA to accelerate Rad51-mediated displacement of RPA and presynaptic complex formation. *J. Biol. Chem.* 277, 31663-31672.
- Sun, H., Treco, D., and Szostak, J. W.** (1991). Extensive 3'-overhanging, single-stranded DNA associated with the meiosis-specific double-strand breaks at the ARG4 recombination initiation site. *Cell* 64, 1155-1161.
- Sung, P.** (1997). Function of yeast Rad52 protein as a mediator between replication protein A and the Rad51 recombinase. *J. Biol. Chem.* 272, 28194-28197.
- Symington, L. S.** (2002). Role of RAD52 epistasis group genes in homologous recombination and double-strand break repair. *Microbiol. Mol. Biol. Rev.* 66, 630-670.
- Szostak, J. W., Orr-Weaver, T. L., Rothstein, R. J., and Stahl, F. W.** (1983). The double-strand-break repair model for recombination. *Cell* 33, 25-35.
- Tauchi, H., Kobayashi, J., Morishima, K., Matsuura, S., Nakamura, A., Shiraishi, T., Ito, E., Masnada, D., Delia, D., and Komatsu, K.** (2001). The forkhead-associated domain of NBS1 is essential for nuclear foci formation after irradiation but not essential for hRAD50[middle dot]hMRE11[middle dot]NBS1 complex DNA repair activity. *J. Biol. Chem.* 276, 12-15.
- Tauchi, H., Kobayashi, J., Morishima, K., van Gent, D. C., Shiraishi, T., Verkaik, N. S., vanHeems, D., Ito, E., Nakamura, A., Sonoda, E., Takata, M., Takeda, S., Matsuura, S., and**

- Komatsu, K.** (2002). Nbs1 is essential for DNA repair by homologous recombination in higher vertebrate cells. *Nature* 420, 93-98.
- Teng, S. C., Chang, J., McCowan, B., and Zakian, V. A.** (2000). Telomerase-independent lengthening of yeast telomeres occurs by an abrupt Rad50p-dependent, Rif-inhibited recombinational process. *Mol. Cell* 6, 947-952.
- Trujillo, K. M., and Sung, P.** (2001). DNA structure-specific nuclease activities in the *Saccharomyces cerevisiae* Rad50.Mre11 complex. *J. Biol. Chem.* 276, 35458-35464.
- Tsubouchi, H., and Ogawa, H.** (1998). A novel mre11 mutation impairs processing of double-strand breaks of DNA during both mitosis and meiosis. *Mol. Cell. Biol.* 18, 260-268.
- Tsubouchi, H., and Ogawa, H.** (2000). Exo1 roles for repair of DNA double-strand breaks and meiotic crossing over in *Saccharomyces cerevisiae*. *Mol. Biol. Cell* 11, 2221-2233.
- Usui, T., Ohta, T., Oshiumi, H., Tomizawa, J., Ogawa, H., and Ogawa, T.** (1998). Complex formation and functional versatility of Mre11 of budding yeast in recombination. *Cell* 95, 705-716.
- Van Komen, S., Petukhova, G., Sigurdsson, S., Stratton, S., and Sung, P.** (2000). Superhelicity-driven homologous DNA pairing by yeast recombination factors Rad51 and Rad54. *Mol. Cell* 6, 563-572.
- van Steensel, B., Smogorzewska, A., and de Lange, T.** (1998). TRF2 protects human telomeres from end-to-end fusions. *Cell* 92, 401-413.
- Varon, R., Vissinga, C., Platzer, M., Cerosaletti, K. M., Chrzanowska, K. H., Saar, K., Beckmann, G., Seemanova, E., Cooper, P. R., Nowak, N. J., Stumm, M., Weemaes, C. M., Gatti, R. A., Wilson, R. K., Digweed, M., Rosenthal, A., Sperling, K., Concannon, P., and Reis, A.** (1998). Nibrin, a novel DNA double-strand break repair protein, is mutated in Nijmegen breakage syndrome. *Cell* 93, 467-476.
- Walker, J. R., Corpina, R. A., and Goldberg, J.** (2001). Structure of the Ku heterodimer bound to DNA and its implications for double-strand break repair. *Nature* 412, 607-614.
- Whitby, M. C., Osman, F., and Dixon, J.** (2003). Cleavage of model replication forks by fission yeast Mus81-Eme1 and budding yeast Mus81-Mms4. *J. Biol. Chem.* 278, 6928-6935.
- Williams, B. R., Mirzoeva, O. K., Morgan, W. F., Lin, J., Dunnick, W., and Petrini, J. H.** (2002). A murine model of Nijmegen breakage syndrome. *Curr. Biol.* 12, 648-653.
- Wu, X., Wilson, T. E., and Lieber, M. R.** (1999). A role for FEN-1 in nonhomologous DNA end joining: the order of strand annealing and nucleolytic processing events. *Proc. Natl. Acad. Sci. USA* 96, 1303-1308.
- Xiao, Y., and Weaver, D. T.** (1997). Conditional gene targeted deletion by Cre recombinase demonstrates the requirement for the double-strand break repair Mre11 protein in murine embryonic stem cells. *Nucleic Acids Res.* 25, 2985-2991.
- Yamaguchi-Iwai, Y., Sonoda, E., Sasaki, M. S., Morrison, C., Haraguchi, T., Hiraoka, Y., Yamashita, Y. M., Yagi, T., Takata, M., Price, C., Kakazu, N., and Takeda, S.** (1999). Mre11 is essential for the maintenance of chromosomal DNA in vertebrate cells. *EMBO J.* 18, 6619-6629.
- Yaneva, M., Kowalewski, T., and Lieber, M. R.** (1997). Interaction of DNA-dependent protein kinase with DNA and with Ku: biochemical and atomic-force microscopy studies. *EMBO J.* 16, 5098-5112.

Zhu, C., Bogue, M. A., Lim, D. S., Hasty, P., and Roth, D. B. (1996). Ku86-deficient mice exhibit severe combined immunodeficiency and defective processing of V(D)J recombination intermediates. *Cell* *86*, 379-389.

Zhu, J., Petersen, S., Tessarollo, L., and Nussenzweig, A. (2001). Targeted disruption of the Nijmegen breakage syndrome gene NBS1 leads to early embryonic lethality in mice. *Curr. Biol.* *11*, 105-109.

Zhu, X. D., Kuster, B., Mann, M., Petrini, J. H., and Lange, T. (2000). Cell-cycle-regulated association of RAD50/MRE11/NBS1 with TRF2 and human telomeres. *Nat. Genet.* *25*, 347-352.

Chapter

**DNA binding and strand-annealing activities of
human Mre11: implications for its roles in DNA
double-strand break repair pathways**

2

DNA binding and strand-annealing activities of human Mre11: implications for its roles in DNA double-strand break repair pathways

Martijn de Jager ¹, Mies L.G. Dronkert ¹, Mauro Modesti ¹, Cecile E. M. T. Beerens ^{1,2}, Roland Kanaar ^{1,2} and Dik C. van Gent ¹

¹Department of Cell Biology & Genetics, Erasmus MC, Dr. Molewaterplein 50, 3000 DR Rotterdam, The Netherlands, and ²Department of Radiation Oncology, Erasmus MC-Daniel, Rotterdam, The Netherlands

Modified from: *Nucleic Acids Research*, 2001, Vol. 29, No. 6, 1317-1325

DNA double-strand breaks (DSBs) in eukaryotic cells can be repaired by non-homologous end-joining or homologous recombination. The complex containing the Mre11, Rad50 and Nbs1 proteins has been implicated in both DSB repair pathways, even though they are mechanistically different. To get a better understanding of the properties of the human Mre11 (hMre11) protein, we investigated some of its biochemical activities. We found that hMre11 binds both single-stranded and double-stranded DNA, with a preference for single-stranded DNA. hMre11 does not require DNA ends for efficient binding. Interestingly, hMre11 mediates the annealing of complementary single-stranded DNA molecules. In contrast to the annealing activity of the homologous recombination protein hRad52, the activity of hMre11 is abrogated by the single-stranded DNA binding protein hRPA. We discuss the possible implications of the results for the role(s) of hMre11 in both DSB repair pathways.

Introduction

DNA double-strand breaks (DSBs) can be required intermediates in specialized aspects of DNA metabolism such as immunoglobulin gene rearrangements and meiosis. In contrast to these programmed DSBs, potentially harmful DSBs can be induced by endogenous or exogenous DNA damaging agents. Unrepaired DSBs can be lethal, whereas misrepaired DSBs can cause chromosomal fragmentation, translocations and deletions. Such lesions are potential inducers of carcinogenesis through activation of proto-oncogenes, inactivation of tumor suppressor genes or loss of heterozygosity. Therefore, effective repair of DSBs is of great importance for the maintenance of genome stability and prevention of carcinogenesis (Kanaar et al., 1998).

A number of fundamentally different DSB repair pathways are available in eukaryotic cells, two of which will be discussed further. First, non-homologous end-joining (NHEJ) mediates joining of DSB ends after no or limited processing. DSB repair through NHEJ can result in deletions through the use of short direct repeats on either side of the break, referred to as microhomologies (Roth et al., 1985; Roth and Wilson, 1986; Thode et al., 1990; Thacker et al., 1992; Kramer et al., 1994; Pfeiffer et al., 1994; Moore and Haber, 1996; Mason et al., 1996; Ducau et al., 2000). Genes involved in NHEJ, most of them first identified in mutant rodent cell lines, are *XRCC4* to *XRCC7* (encoding Xrcc4, Ku80, Ku70 and DNA-PK_{cs} proteins, respectively) and *LIG4* (encoding DNA ligase IV) (Tsukamoto and Ikeda, 1998; Kanaar et al., 1998; Lewis and Resnick, 2000). Subsequent analysis of the homologous genes in yeast identified a NHEJ pathway in this organism as well. Interestingly, in addition to the Ku and ligase IV

homologs, the *RAD50*, *MRE11* and *XRS2* genes were also found to be involved in NHEJ (Moore and Haber, 1996; Tsukamoto et al., 1997; Wilson et al., 1999).

In the second repair pathway, homologous recombination, the repair machinery uses a homologous DNA molecule, i.e. the sister chromatid or the homologous chromosome, as a template for accurate repair of both programmed DSBs in meiosis and induced DSBs during mitosis. Homologous recombination requires the products of the *RAD52* epistasis group of genes, first identified in the yeast *Saccharomyces cerevisiae*. This epistasis group includes *RAD50*, *RAD51*, *RAD52*, *RAD54*, *RAD55*, *RAD57*, *RAD59*, *MRE11* and *XRS2* (Kanaar et al., 1998; Paques and Haber, 1999). The *RAD50*, *MRE11* and *XRS2* gene products function in the initial steps of meiotic recombination but are also thought to be involved in recombination processes in mitotic cells (Alani et al., 1990; Sugawara and Haber, 1992; Ivanov et al., 1994; Johzuka and Ogawa, 1995; Ogawa et al., 1995; Usui et al., 1998; Furuse et al., 1998; Bressan et al., 1998; Tsubouchi and Ogawa, 1998; Bressan et al., 1999; Yamaguchi-Iwai et al., 1999).

The Rad50/Mre11/Xrs2 protein complex, like many other DNA repair factors, has been conserved from yeast to mammals (Sharples and Leach, 1995; Petrini et al., 1995; Tavassoli et al., 1995; Dolganov et al., 1996; Matsuura et al., 1998; Carney et al., 1998; Varon et al., 1998). Disruption of the mammalian *RAD50* or *MRE11* genes results in inviable cells (Xiao and Weaver, 1997; Luo et al., 1999). Mutations in the human ortholog of *XRS2*, the *NBS1* gene, can result in Nijmegen breakage syndrome (NBS), a recessive disorder with some phenotypic similarities to ataxia telangiectasia (AT) (Shiloh, 1997; Matsuura et al., 1998; Varon et al., 1998; Ito et al., 1999; Digweed et al., 1999). Furthermore, non-null mutations in human *MRE11* (hMRE11) have been linked to ataxia telangiectasia-like disorder (ATLD) (Stewart et al., 1999). Cells from NBS, AT, and ATLD patients are hypersensitive to DSB-inducing agents and show radioresistant DNA synthesis after exposure to ionizing radiation. Recent experiments have shown that ATM, the kinase defective in AT cells, phosphorylates Nbs1 upon the induction of DNA damage (Kim et al., 1999; Gatei et al., 2000; Zhao et al., 2000; Lim et al., 2000). These observations provide a rationale for the similarities between the NBS, ATLD and AT phenotypes and suggest a link between DNA-damage signaling and the Rad50/Mre11/Nbs1 complex. Except for functions in recombination processes, NHEJ and DNA damage sensing, the complex is thought to have additional functions in telomere maintenance (Boulton and Jackson, 1998; Bertuch and Lundblad, 1998; Wilson et al., 1999; Chamankhah and Xiao, 1999; Moreau et al., 1999; Lombard and Guarente, 2000; Zhu et al., 2000).

Biochemical studies of the yeast and human protein complexes have shown that Mre11 has a 3' to 5' Mn²⁺-dependent exonuclease activity on DNA substrates with blunt or 5' protruding ends and endonuclease activity on single-stranded and hairpin DNA substrates (Furuse et al., 1998; Trujillo et al., 1998; Paull and Gellert, 1998; Moreau et al., 1999). The complex containing hRad50 and Nbs1 in addition to the hMre11 protein can also mediate limited DNA duplex unwinding and more efficient

hairpin opening, stimulated by ATP. The presence of ATP also allows the complex to endonucleolytically cut a 3' overhang at a single-strand double-strand transition (Paull and Gellert, 1999). In combination with DNA ligase I or IV, hMre11 stimulates the use of microhomologies in an *in vitro* joining reaction (Paull and Gellert, 1998). The exonuclease activity of hMre11 is stimulated by mismatched ends, but inhibited if cohesive ends are present and delayed if an internal microhomology is found (Paull and Gellert, 2000). This suggests that hMre11 might be a nuclease that stimulates the use of microhomology during NHEJ.

Although the details of the biochemical activities of the hMre11 protein are now beginning to emerge, several questions remain about its precise functions in microhomology-dependent NHEJ and homologous recombination. In this study, we further characterize the interactions of hMre11 protein with DNA. In addition to binding of both single-stranded and double-stranded DNA, the protein can mediate annealing of complementary single-stranded DNA molecules. This annealing activity is both quantitatively and qualitatively different from the annealing activity of another DSB repair protein, hRad52. We discuss a possible common function of the hMre11-containing complex in both microhomology-dependent NHEJ and homologous recombination.

Results

DNA binding of hMre11

Recombinant proteins were produced in Sf21 insect cells using a baculovirus expression system or in *E. coli*. Figure 1 shows an SDS-PAGE analysis of the purified proteins. Titration and time course experiments showed that the specific nuclease activity of the hMre11 preparation was similar to the activity reported previously (Paull and Gellert, 1998).

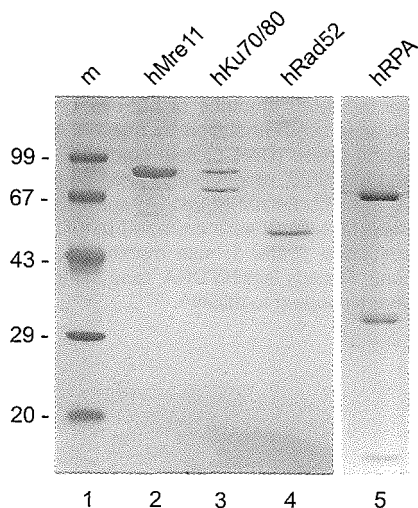


Figure 1. Purified protein preparations. Protein preparations were analyzed by SDS-PAGE and Coomassie Blue staining. Lane 1, molecular size marker (m; molecular mass indicated in kDa), lane 2, hMre11-his₆ preparation; lane 3, hKu70-his₆/hKu80 preparation; lane 4, hRad52-his₆ preparation; lane 5, hRPA preparation.

To investigate the complex formation of hMre11 and DNA, the protein was incubated with radiolabeled 50 nucleotide (nt) single-stranded (ss) DNA and blunt-ended 50 basepair (bp) double-stranded (ds) DNA oligonucleotides without addition of divalent cations. As shown in Figure 2A, hMre11 formed distinct complexes with ssDNA molecules (lane 1 to 5) and with dsDNA molecules (lane 6 to 10). Incubation with dsDNA resulted in at least two distinct protein-DNA complexes at the higher concentrations of hMre11. Two-dimensional gel analysis of the protein-DNA complexes (native PAGE in the first dimension and SDS-PAGE for separation of ss- and dsDNA in the second dimension), showed that both bands in the dsDNA bandshift contain indeed only dsDNA (data not shown) suggesting that these bands represent protein-dsDNA complexes that differ in amount of protein and/or DNA molecules or in conformation. Similar protein-DNA complex formation was also observed with at least eight other ssDNA or dsDNA oligonucleotides that varied in length from 20 to 60 nt or bp and that were unrelated in nt sequence (data not shown). The presence of the divalent cations Mg^{2+} or Ca^{2+} did not result in different reaction products (data not shown).

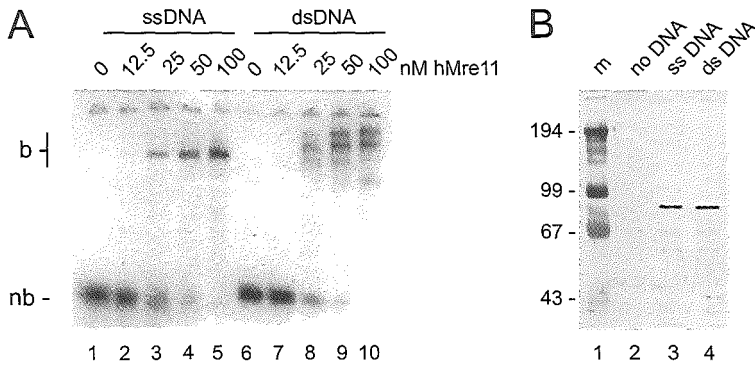


Figure 2. hMre11 binds to single-stranded and double-stranded DNA molecules. (A) Radiolabeled 50 nucleotide (nt) ssDNA or blunt-ended dsDNA (MJ19 and MJ19/20, respectively) were incubated at 1.25 nM with

the indicated amounts of hMre11 under standard conditions in the absence of divalent cations. Samples were analyzed by native PAGE, followed by autoradiography. 'nb', non-bound probe, 'b', bound probe (DNA-protein complex). (B) Biotinylated 50 nt ssDNA or blunt-ended dsDNA (MJ29 and MJ29/20, respectively) were coupled to streptavidin-coated magnetic beads and incubated at 20 nM with 24 nM hMre11 preparation under standard conditions supplemented with 0.1% NP40. Bound fractions were analyzed by SDS-PAGE and immunoblotting with affinity purified anti-hMre11 antibodies. Lane 1, size marker (m, molecular mass indicated in kDa); lane 2, incubation with control beads lacking DNA; lane 3, incubation with beads coupled to ssDNA; lane 4, incubation with beads coupled to dsDNA.

To confirm that the observed protein-DNA complexes were due to hMre11 binding to both ssDNA and dsDNA molecules, biotinylated ssDNA or blunt-ended dsDNA oligonucleotides were coupled to streptavidin coated magnetic beads. These beads were incubated with the hMre11 preparation under conditions that resulted in protein-DNA complex formation. Subsequently, the beads were washed with binding buffer and bound proteins were analyzed by SDS-PAGE and immunoblotting. As shown in Figure 2B, incubation of the beads coupled to either ssDNA or dsDNA with the hMre11 protein preparation resulted in recovery of hMre11 (lanes 3 and 4, respectively), whereas no hMre11 protein was recovered in the absence of DNA (lane 2). We conclude that the hMre11 protein binds both ssDNA and dsDNA in a sequence independent manner.

Characterization of hMre11 DNA-binding properties

The exonuclease activity of hMre11 might suggest a binding preference for DNA ends. We therefore determined whether hMre11 requires free DNA ends to bind its substrate molecule. A competition experiment was performed in which hMre11 was first incubated with a radiolabeled 50-nt ssDNA oligonucleotide under standard assay conditions. Subsequently, non-labeled ssDNA oligonucleotide or circular Φ X174 ssDNA was added on equal nucleotide basis and the incubation was continued (Figure 3A, left panel). Circular Φ X174 DNA competed even better than ssDNA oligonucleotides, suggesting that hMre11 might load more efficiently on longer DNA molecules. A similar result was obtained when the complex of hMre11 and dsDNA oligonucleotide was competed with dsDNA oligonucleotide or circular Φ X174 dsDNA (Figure 3B, right panel). No difference was observed between circular and linearized Φ X174 molecules (data not shown). Therefore, we conclude that hMre11 does not preferentially bind DNA ends.

The relative affinity of hMre11 for ssDNA and dsDNA was investigated in competition experiments. After incubation of hMre11 with a radiolabeled 50-nt ssDNA oligonucleotide, non-identical ssDNA or dsDNA competitor oligonucleotide was titrated in and the reaction was continued. The fraction of radiolabeled DNA oligonucleotide bound by hMre11 was determined and normalized to the fraction of probe bound in the absence of competitor DNA. The inverse of this normalized fraction is a linear function of the molar excess of competitor DNA added (Figure 3B). The slope of the line is indicative of the effectiveness of the competitor. We conclude that hMre11 had an approximately 9-fold higher binding affinity for ssDNA than for dsDNA molecules. The presence of short (4-nt) 3' or 5' ssDNA overhangs did not result in a higher affinity compared to blunt-ended dsDNA (data not shown).

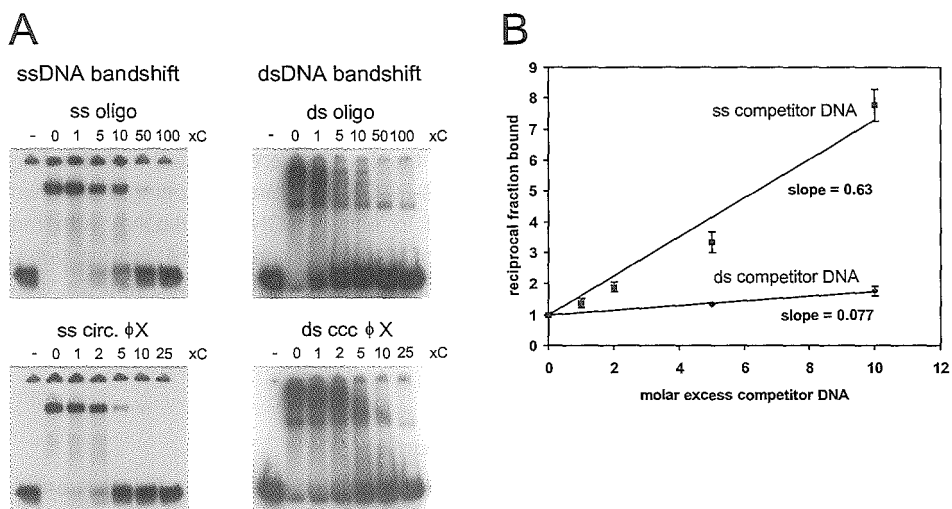


Figure 3. Characterization of hMre11 DNA-binding properties. (A) Radiolabeled 50 nt ssDNA (MJ19; left) or dsDNA (MJ19/MJ20; right) was incubated at 1.25 nM with hMre11 at 50 nM. After 15 min incubation, the indicated nucleotide excess non-radioactively labeled competitor DNA was added and incubation was continued for an additional 15 min. Competitor DNA was single-stranded oligonucleotide (MJ19) or circular ϕ X174 ssDNA (left) and blunt-ended double-stranded oligonucleotide (MJ19/MJ20) or circular ϕ X174 dsDNA (right). Lane $-$, incubation without hMre11. Samples were analyzed by native PAGE, followed by autoradiography. (B) Radiolabeled 50 nt ssDNA (MJ19) was incubated at 1.25 nM with 50 nM hMre11 as in (A). Non-labeled, non-identical ssDNA (DG73) or dsDNA (DG73/DG74) oligonucleotide DNA was used as a competitor. Values on Y-axis are reciprocal fractions of DNA-protein complex, normalized to the fraction of DNA-protein complex in non-competed reactions (see Materials and Methods). Bars indicate standard deviations of mean values of triplicate reactions. Slopes of linear regression lines through the datapoints are indicated.

Strand annealing by hMre11

In competition assays with complementary DNA, formation of dsDNA was observed. To investigate this effect in more detail, two complementary 50-nt ssDNA oligonucleotides were incubated with hMre11 without addition of divalent cations. After deproteinization samples were analyzed by native PAGE. As shown in Figure 4, hMre11 stimulated annealing of the two complementary single-strands. As negative and positive controls for these experiments we used the hKu70/80 and hRad52 proteins. The hKu70/80 heterodimer did not support annealing. In contrast, the hRad52 protein displayed a robust annealing activity consistent with previous reports for both the *S. cerevisiae* and human Rad52 proteins (Mortensen et al., 1996; Reddy et al., 1997; Shinohara et al., 1998; Sugiyama et al., 1998). The annealing activities for both hMre11 and hRad52 were also observed with other sets of complementary ssDNA oligonucleotides that were unrelated in nt sequence to the oligonucleotide shown in Figure 4 (data not shown).

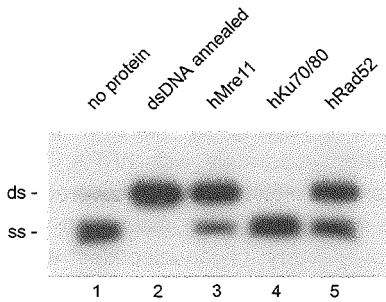


Figure 4. hMre11 anneals complementary ssDNA molecules. Two complementary 50 nt ssDNAs (MJ19 and MJ20), one of which was radiolabeled, were incubated with 10 nM hMre11, hKu70/80, hRad52 or without protein. After deproteinization, samples were analyzed by native PAGE and autoradiography. Lane 1, incubation without protein; lane 2, dsDNA, annealed by heating and slow cooling; lane 3, incubation with hMre11; lane 4, incubation with hKu70/80 heterodimer; lane 5, incubation with hRad52. The positions of ssDNA and dsDNA are indicated.

Kinetics of strand annealing by hMre11 and hRad52

The kinetics of the annealing reaction were determined in a time-course experiment in which two complementary 50-nt oligonucleotides were incubated in the presence of

hMre11, hRad52 or hKu70/80 or in the absence of protein. The percentage of dsDNA as a function of time was determined (Figure 5A). Although both hMre11 and hRad52 efficiently annealed complementary DNA molecules, the annealing rate of hRad52 was approximately two-fold higher than that of hMre11. To further quantify this difference, the initial reaction rates were determined for different concentrations of hMre11 and hRad52 (Figure 5B). The maximal annealing rate of hRad52 was approximately twice as high as that of hMre11.

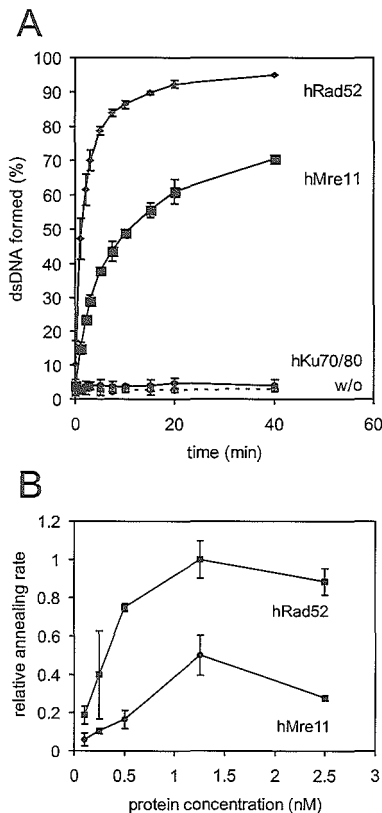


Figure 5. Kinetics of hMre11-mediated oligonucleotide annealing. (A) Two complementary 50 nt ssDNAs (MJ19 and MJ20), one of which was radiolabeled, were incubated at 0.5 nM with hMre11, hRad52 or hKu70/80, at 1.25 nM, or without protein. Samples were taken at 0, 1, 2, 3, 5, 7.5, 10, 15, 20 and 40 min. Annealing was analyzed as in Figure 4. Bars indicate standard deviation of mean values of triplicate experiments. (B) Annealing reactions as in (A), with the indicated concentrations of either hMre11 or hRad52. Samples were taken at 0, 1 and 2 min. Initial annealing rates, normalized to highest measured annealing rate of hRad52, were determined from the slopes of the time courses. Bars indicate standard deviations of mean values of triplicate reactions.

hMre11-mediated strand annealing is inhibited by hRPA

Probably most ssDNA *in vivo* is covered by ssDNA binding proteins, such as the human RPA heterotrimer. We therefore investigated whether coating of the ssDNA oligonucleotides with hRPA would influence strand annealing by hMre11. 61-nt complementary ssDNA molecules were first incubated separately with hRPA. The concentration of hRPA (3.4 nM) was such that all substrate molecules were covered by hRPA, as determined by mobility shift assays (data not shown). After incubation with hRPA, the reaction mixtures containing the complementary oligonucleotides were combined, hMre11 was added at 10 nM and the incubation was continued. As shown in Figure 6A, preincubation of hRPA with the oligonucleotides completely inhibited the strand annealing activity of hMre11. In contrast, the strand annealing activity of hRad52 was much less affected. As expected, the presence of hRPA had no effect on the absence of annealing activity by hKu70/80.

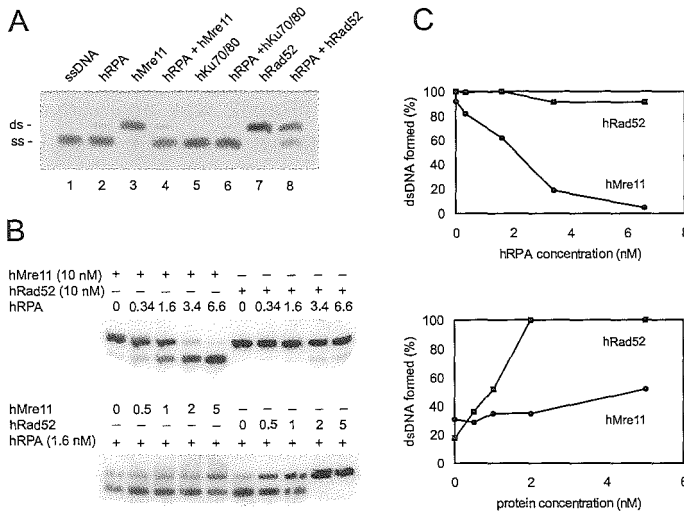


Figure 6. hMre11 but not hRad52 annealing activity is inhibited by pre-coating of substrate oligonucleotides with hRPA. (A) Complementary 61 nt ssDNAs (DG61 and DG62) were incubated separately at 1 nM with 3.4 nM hRPA for 15 min at 25 °C. Reaction mixtures were combined and incubations were continued for 60 min at 16 °C after addition of hMre11, hRad52 or hKu70/80 at 10 nM each, or without protein, as indicated.

Annealing was analyzed by native PAGE after deproteinization, followed by autoradiography. Lane 1, no proteins added; lane 2, preincubation with hRPA only; lane 3, incubation with hMre11 only; lane 4, preincubation with hRPA, followed by addition of hMre11; lane 5, incubation with hKu70/80 only; lane 6, preincubation with hRPA, followed by addition of hKu70/80; lane 7, incubation with hRad52 only; lane 8, preincubation with hRPA, followed by addition of hRad52. (B) Complementary 61 nt ssDNAs (DG61 and DG62) were incubated separately at 1 nM with the indicated concentrations of hRPA in the top panel or 1.6 nM hRPA in the bottom panel for 15 min at 25 °C. Reaction mixtures were combined and incubations were continued after addition of hMre11 or hRad52 at 10 nM in the top panel or at the indicated concentrations in the bottom panel, for 60 min at 16 °C. Annealing was analyzed by native PAGE after deproteinization. (C) Quantification of the percentages dsDNA formed in (B). Values are expressed as percentages dsDNA for hMre11 and hRad52.

The effect of precoating the substrate oligonucleotides with hRPA was further analyzed by titration of hRPA, while keeping the concentrations of hMre11 or hRad52 constant (Figure 6B, upper panel). Alternatively, different concentrations of hMre11 or hRad52 were added after preincubation with a fixed concentration of hRPA (Figure 6B, lower panel). The presence of hRPA at 2 nM reduced hMre11-mediated strand annealing by 50% compared to the absence of hRPA, while hRad52-mediated strand annealing was not affected. Higher concentrations of hRPA only mildly affected hRad52-mediated annealing (Figure 6C, upper graph). Similarly, preincubation with 1.6 nM hRPA inhibited strand annealing at a low concentration of hMre11, while increasing amounts of hMre11 could only partially overcome the inhibitory effect (50% annealing activity at 5 nM hMre11). In contrast, the hRad52 annealing activity was completely restored at 2 nM (Figure 6C, lower graph).

Discussion

In this paper we describe a number of biochemical properties of the human Mre11 protein. We show that hMre11 forms complexes with both ssDNA and dsDNA. The affinity for ssDNA is higher than for dsDNA and hMre11 binds to DNA without the need for free DNA ends. Furthermore, hMre11 can promote annealing of complementary ssDNA molecules, with a slightly slower rate than hRad52. The hMre11 annealing activity is, in contrast to hRad52, inhibited by the presence of hRPA. Although strand-annealing activity has been reported for a number of proteins, the biological significance cannot always readily be assessed. However, strand-annealing activity is a key feature of certain DSB repair pathways. Below we will discuss how this activity of hMre11 might contribute to the repair of DSB's.

The importance of the Mre11 protein in DSB repair is highlighted by a number of observations implicating Mre11 in both major DSB repair pathways in yeast as well as vertebrate cells. In yeast the involvement of Mre11 in NHEJ and homologous recombination has been revealed by plasmid rejoining assays and genetic experiments, respectively (Ivanov et al., 1994; Johzuka and Ogawa, 1995; Tavassoli et al., 1995; Ogawa et al., 1995; Moore and Haber, 1996; Tsukamoto et al., 1997; Usui et al., 1998; Furuse et al., 1998; Bressan et al., 1998; Tsubouchi and Ogawa, 1998; Wilson et al., 1999; Bressan et al., 1999; Gerecke and Zolan, 2000). In vertebrate cells a requirement for Mre11 in NHEJ and homologous recombination has been inferred from biochemical experiments and epistasis analysis, respectively (Paull and Gellert, 1998; Yamaguchi-Iwai et al., 1999; Paull and Gellert, 2000). Below we discuss the implications of the DNA binding and complementary ssDNA annealing activities of hMre11 for its potential roles in both NHEJ and homologous recombination.

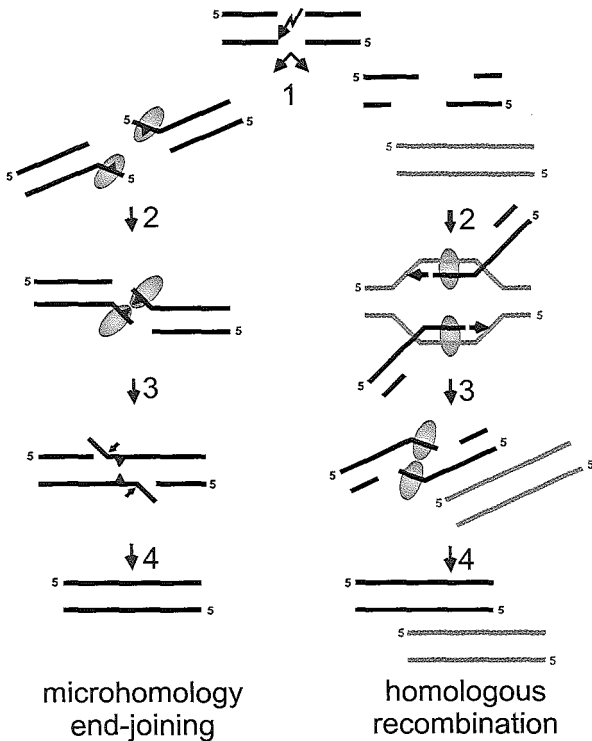


Figure 7. Proposed models for the possible functions of the Mre11 complex in end-joining and homologous recombination. If a DSB is repaired via microhomology-directed end-joining, both ends can be either nucleolytically processed or partially unwound (left, step 1, microhomologies symbolized by triangle). The Mre11-containing complex (symbolized by the oval) may bind the short ssDNA tails. The tails could be kept in close proximity through interaction between two Mre11 protomers either directly or as constituents of the same Rad50/Mre11 complex (left, step 2). The single-strand annealing activity of Mre11 promotes base pairing between complementary DNA sequences (left, step 3). In the last step the activities of processing enzymes such as flap-endonucleases, polymerases and ligase(s) are required to restore the continuity of the DNA molecule (left, step 4). If the DSB is repaired via homologous recombination,

extensive degradation of both ends results in long 3' ssDNA tails (right, step 1). After strand invasion and homologous pairing (right, step 2) by the Rad52 epistasis group proteins and RPA (not indicated), new DNA is synthesized (arrowhead). Restoration of the lost sequence information will be complete when both newly synthesized strands overlap (right, step 3). A possible resolution step of this recombination intermediate would involve unwinding of the newly synthesized strand from the template DNA followed by annealing of the complementary newly synthesized strands, possibly by Mre11. Finally, single-strand gaps are filled in and ligated, completing the repair of the damaged DNA molecule (right, step 4).

First, we will consider the role of Mre11 in NHEJ. *In vivo* plasmid rejoining assays have shown that DNA ends are preferentially joined on short direct repeats (i.e. microhomologies) on either side of the DSB in cells from the fission yeast *Schizosaccharomyces pombe*. Studies with *rad32* deletion mutants, the *S. pombe* homologue of *hMRE11*, have revealed that this gene is required for microhomology-dependent end-joining (Wilson et al., 1999). *In vitro* experiments have shown that DNA ligase I or IV can join DNA molecules using microhomologies when combined with the hMre11 protein (Paull and Gellert, 1998). Furthermore, the hMre11 exonuclease activity

is stimulated by mismatched ends, but inhibited by cohesive ends and delayed when an internal microhomology is present (Paull and Gellert, 2000). The initial step in the microhomology-dependent end-joining pathway could be formation of protruding ssDNA tails to expose the microhomologies. These tails could be created by the 3' to 5' exonuclease activity of the Rad50/Mre11/Nbs1 complex (Furuse et al., 1998; Trujillo et al., 1998; Paull and Gellert, 1998; Moreau et al., 1999). Alternatively, the DNA ends could be partially unwound by the Rad50/Mre11/Nbs1 complex and annealed on microhomologies. Subsequently, the displaced ssDNA tails could be removed endonucleolitically (Paull and Gellert, 1999; Figure 7). The human ssDNA binding protein RPA will probably not be able to inhibit hMre11 strand annealing activity, since the microhomology-containing tails are presumably too short for recognition by hRPA (Roth et al., 1985; Roth and Wilson, 1986; Thacker et al., 1992; Tsukamoto et al., 1996). The two DNA ends could be held in proximity by the Rad50 protein, which has similarities to the SMC family of proteins. Members of this protein family are involved in processes that require bridging of distant sites on DNA, such as cohesion between chromatids or condensation of DNA (Melby et al., 1998; Hopfner et al., 2000). Further processing of this intermediate in DSB repair could occur by other nucleases, DNA polymerases, ligases, and their respective accessory factors.

The alternative major DSB repair pathway in eukaryotes is homologous recombination. Genetic experiments with *S. cerevisiae* clearly implicate ScMre11 in both meiotic and mitotic homologous recombination (Ivanov et al., 1994; Johzuka and Ogawa, 1995; Tavassoli et al., 1995; Ogawa et al., 1995; Usui et al., 1998; Furuse et al., 1998; Bressan et al., 1998; Tsubouchi and Ogawa, 1998; Bressan et al., 1999; Gerecke and Zolan, 2000). The protein plays an early role during meiotic recombination because its nuclease activity is required for the processing of meiosis-specific DSBs made by the Spo11 protein (Moreau et al., 1999). Although ScMre11 plays a role in the initiation of meiotic recombination, an early role in mitotic recombination is less likely. An early event in mitotic DSB repair through homologous recombination is the processing of the DSB ends into 3' ssDNA tails that are required for the invasion of the broken DNA into the duplex homologous repair template DNA. However, its polarity of exonuclease activity make the Mre11 protein a less likely candidate to generate these recombination intermediates (Furuse et al., 1998; Trujillo et al., 1998; Paull and Gellert, 1998). Another possible early role in homologous recombination could be similar to the proposed annealing activity of the Rad52 protein in joint molecule formation (Shinohara et al., 1992; Mortensen et al., 1996; Reddy et al., 1997; Sung, 1997; New et al., 1998; Shinohara et al., 1998; Shinohara and Ogawa, 1998; Sugiyama et al., 1998). However, the ssDNA tail intermediates will most probably be covered by RPA *in vivo*, which would strongly inhibit the hMre11-mediated annealing activity but not the annealing activity of hRad52. Therefore, a role for hMre11 in this step is less likely, although it is still possible that the presence of the other complex components or additional factors could overcome the inhibitory effect of hRPA.

Instead of an early role in mitotic DSB repair, it is possible that the Mre11 complex functions at a later stage of recombination such as resolution (see Figure 7). If one or both 3' ssDNA tails invade the intact homologous strands of the sister chromatid or the homologous chromosome, the intermediate structure would consist of an intact chromosome with one or two 3' ends from which DNA synthesis can start (Paques and Haber, 1999). If synthesis proceeds beyond the point of the original break, all lost sequence information has been regained. However, the two ends from the broken chromatid or chromosome have to find each other to restore the continuity of the chromosome. This would require melting of the newly synthesized strands from their templates and annealing to each other. The unwinding activity detected for the purified human Rad50/Mre11/Nbs1 complex might be useful to initiate the unwinding of the newly synthesized strands from the template strand (Paull and Gellert, 1999). Then, hMre11 could be loaded preferentially on the resulting ssDNA and subsequently anneal the complementary newly synthesized strands. During this reaction the ssDNA could be of limited length, thereby preventing RPA from binding and inhibiting Mre11 annealing activity or the unwinding and annealing could be accomplished in a concerted reaction. The signal for inducing this activity of the Rad50/Mre11/Nbs1 complex could be the proximity of the two DNA polymerase complexes that are moving towards each other.

This potential role for the Mre11 strand annealing activity, but not necessarily the Mre11 nuclease activity, in resolution of recombination intermediates is consistent with the lack of a recombination and DNA repair-deficient phenotype of nuclease defective *mre11* mutants in *S. cerevisiae* (Bressan et al., 1999). According to the model presented above (Figure 7), the usual interstrand short track gene conversion events might not be resolved in *mre11Δ* cells. Instead, they could result in replication of a large part of the homologous chromosome (or sister chromatid) and therefore an increased rate of recombination between markers on different ends of a chromosome would result. This so-called 'hyper-recombination' phenotype has been observed in mitotic *mre11Δ* and *rad50Δ* cells (Malone et al., 1990; Bressan et al., 1998). In addition to the proposed role of the strand annealing activity of Mre11 in restoring DNA damage induced by exogenous agents, this activity could also be required for the rescue of collapsed replication forks. While Mre11 is dispensable in yeast cells, it is essential for growth of vertebrate cells (Glasunov et al., 1989; Tavassoli et al., 1995; Xiao and Weaver, 1997; Yamaguchi-Iwai et al., 1999). Because *S. cerevisiae* chromosomes are in general much shorter than vertebrate chromosomes, *S. cerevisiae mre11Δ* cells could be viable because the break induced replication can more easily continue to the end of the chromosome in *S. cerevisiae* cells than in vertebrate cells.

The proposed functions for the hMre11 complex in end-joining and homologous recombination are not mutually exclusive. Most of the activities described in both models are conceptually similar; first to disrupt base pairing at the DSB end in NHEJ or with the template strand in homologous recombination and subsequently to anneal homologous ssDNA strands which are held in close proximity (see Figure 7).

Therefore, these fundamentally different repair processes might both rely on the use of a similar enzymatic activity of the Rad50/Mre11/Nbs1 complex.

Materials and Methods

Protein expression and purification

Human Mre11 protein was produced by infection of Sf21 cells with baculoviruses expressing hMre11 containing a C-terminal 6-histidine (his₆) tag (a generous gift of T. Paull and M. Gellert). Sf21 cells were infected at MOI 10 and harvested after 48 hours. The purification protocol was based on a method described previously (Paull and Gellert, 1998). Briefly, infected cells were collected, washed three times in PBS and frozen in liquid nitrogen. Cells were thawed and resuspended in 5 ml (5 packed cell volumes) buffer A (20 mM Tris-HCl, pH 7.9, 500 mM NaCl, 2 mM β-mercaptoethanol) containing 5 mM imidazole and 1 mM Pefablock (Merck). Then, the cells were disrupted by 30 strokes of a type B pestle in a Dounce homogenizer. After one hour centrifugation at 80,000 x g, the soluble fraction was loaded on a 1 ml Ni²⁺-NTA agarose column (Qiagen), equilibrated in buffer A. The column was washed with 10 volumes buffer A, then with 10 volumes buffer A containing 40 mM imidazole and subsequently with 10 volumes buffer B (20 mM Tris-HCl, pH 7.9, 100 mM NaCl, 2 mM β-mercaptoethanol) containing 40 mM imidazole. Bound proteins were eluted in buffer B containing 200 mM imidazole and diluted 1:1 in buffer B containing 2 mM dithiothreitol (DTT). This preparation was loaded on a 1 ml MonoQ column (Pharmacia) equilibrated in buffer B containing 2 mM DTT. After washing the column with 10 column volumes, the proteins were eluted by a 10 ml linear salt gradient from 100 mM to 500 mM NaCl. Fractions were analyzed by Coomassie-stained SDS polyacrylamide gel electrophoresis (PAGE). Fractions containing hMre11 were pooled and dialyzed against dialysis buffer (25 mM Tris-HCl, pH 8.0, 150 mM KCl, 10% glycerol, 2 mM β-mercaptoethanol and 2 mM dithiothreitol). The resulting protein preparation was aliquoted, frozen in liquid nitrogen and stored at -80°C. The nuclease activity of the hMre11 preparation was assayed as described (Paull and Gellert, 1998).

The human Ku70/80 heterodimer was produced and purified using a protocol similar to the one described above for hMre11. The proteins were produced by co-infection of Sf21 cells with baculoviruses expressing hKu70 containing a C-terminal his₆ tag and hKu80 (Ono et al., 1994). Sf21 cells were infected at MOI 2 and 6 for the hKu70 and hKu80 producing viruses, respectively, to ensure that all recovered hKu70 would be complexed with hKu80. The human RPA heterotrimer was produced by co-expression of its three subunits in *Escherichia coli* from a polycistronic messenger RNA and purified as described previously (Henricksen et al., 1994). Human Rad52 protein containing an N-terminal his₆ tag was produced in *E. coli* and purified as described (Benson et al., 1998).

DNA substrates

Oligonucleotides used in this study were MJ19 (GGATGATTATGGTTATACGTGAT-TAGTAGCGACGAACATTTTGTAGCAGC) and the complementary oligonucleotide MJ20, MJ21 = MJ19 + 3' TTTT, MJ22 = MJ20 + 3' TTTT, MJ23 = MJ19 + 5' TTTT, MJ24 = MJ20 + 5' TTTT, MJ29 = 5'-end biotinylated MJ19, DG61 (GATCTGGCCTGTCTTACACAGTGGTAGTACTCCAC-TGTCTGGCTGTACAAAACCCTCGGG) and the complementary DG62, DG73 (CTAGACCGACAGCTGGTGTCACGATGTCTGACCTT-GTTTTGGGACGTC) and the complementary DG74. Circular single-stranded (ss) DNA used in this study was Φ X174 virion DNA (NEB). Circular double-stranded (ds) DNA was Φ X174 RF-I DNA. Φ X174 RF-I DNA was digested with *Apa*I to generate linear dsDNA, which was denatured and subsequently chilled on ice to generate linear ssDNA. Oligonucleotides were 5'-end labeled with 32 P using polynucleotide kinase and purified through a 1-ml G25 sepharose column.

Generation of anti-hMre11 antibodies

A 1.9 kb *Xho*I-*Pst*I fragment from the *hMRE11* cDNA, obtained by RT-PCR using HeLa cell mRNA, was subcloned into pMal-C2 (New England Biolabs). The fusion protein derived from this plasmid contained the maltose binding protein fused to the C-terminal 634 amino acids of hMre11 and was produced in *E. coli* strain FB810. The protein was present in the insoluble fraction and was dissolved in 6 M urea. It was purified by preparative PAGE, and used to immunize two rabbits. The antibodies were affinity purified using fusion protein immobilized on a nitrocellulose filter.

DNA binding reactions

To analyze the DNA binding properties of hMre11, 32 P 5'-end labeled DNA substrate molecules (MJ19 or MJ19 annealed to MJ20), were incubated at 2.5 nM with hMre11 at 50 nM or the indicated concentrations in binding buffer (50 mM Hepes-KOH, pH 8.0, 10 mM Tris-HCl, 100 mM KCl, 4.2% glycerol and 0.5 mg/ml BSA) for 15 min at 25°C in a volume of 20 μ l. In competition experiments, 5 μ l of non-labeled competitor DNA solution was added to 15 μ l of initial binding reaction and incubation was continued for 15 min at 25 °C. Subsequently, reaction mixtures were analyzed on a 4% native polyacrylamide gel in 0.5 x TBE. Gels were analyzed by autoradiography or phosphor imaging. To compare the affinity for different DNA substrates, the remaining percentage of DNA-protein complex was determined and normalized to non-competed reactions. Reciprocal values of these percentages yield a straight line with slope 1 as a function of molar excess for identical competitor DNA. Therefore, the slopes of the curves for different competitor DNA molecules indicate the competitive capacity of the specific competitor.

To recover hMre11 bound to DNA, the 5'-biotinylated MJ29 was incubated for 30 min at room temperature in coupling buffer (5 mM Tris-HCl, pH 7.5, 0.5 mM EDTA and 1 M NaCl) with streptavidin coated magnetic beads (Dynal) that had been prewashed in coupling buffer. The beads were washed three times with coupling buffer, once with non-fat milk and incubated for two hours with non-fat milk at room temperature. Then, the beads were washed three times with

binding buffer as used for standard binding experiments supplemented with 0.1% NP40. Next, hMre11 was incubated at 24 nM with the DNA coupled to the beads at 20 nM for 30 min in standard binding buffer. Beads were collected and washed three times with binding buffer containing 0.1% NP40. Bound fractions were analyzed on an 8% SDS-PAGE gel followed by immunoblotting using affinity purified anti-hMre11 antisera.

Strand annealing reactions

To assay for strand annealing activities, ³²P 5'-end labeled MJ19 was incubated with MJ20 (both at 0.5 nM) and hMre11, hRad52 or hKu70/80 at a concentration of 10 nM. Reactions were done in annealing buffer (50 mM Hepes-KOH, pH 8.0, 10 mM KCl, 0.5 mg/ml BSA) for 1 hour at 16 °C in a volume of 100 µl. To determine the effect of hRPA on the annealing reactions, ³²P 5'-end labeled DG61 and unlabeled DG62 were incubated separately at 1.0 nM with 3.4 nM or the indicated concentrations of hRPA for 15 min at 25 °C in annealing buffer. Then, the reaction mixtures were combined and the reaction was continued for 1 hour at 16 °C after addition of 10 nM or indicated concentrations of hMre11, hRad52 or hKu70/80. Reactions were terminated by phenol extraction and analyzed on native 10% polyacrylamide gels, containing 0.5x TBE. Reaction products were visualized and quantified by autoradiography or phosphor imaging.

Acknowledgements

We thank T. Paull and M. Gellert for the generous gift of the hMre11-producing baculovirus and J.H.J. Hoeijmakers for carefully reading the manuscript. This work was supported by grants from the Dutch Cancer Society (KWF), the Dutch Organisation for Scientific Research (NWO) and the Human Frontiers Science Project Organization (HFSPO). D.C.v.G. is an academy fellow of the Royal Netherlands Academy for Arts and Sciences (KNAW).

References

- Alani, E., Padmore, R., and Kleckner, N.** (1990). Analysis of wild-type and rad50 mutants of yeast suggests an intimate relationship between meiotic chromosome synapsis and recombination. *Cell* 61, 419-436.
- Benson, F. E., Baumann, P., and West, S. C.** (1998). Synergistic actions of Rad51 and Rad52 in recombination and DNA repair. *Nature* 391, 401-404.

- Bertuch, A., and Lundblad, V.** (1998). Telomeres and double-strand breaks: trying to make ends meet. *Trends Cell Biol.* *8*, 339-342.
- Boulton, S. J., and Jackson, S. P.** (1998). Components of the Ku-dependent non-homologous end-joining pathway are involved in telomeric length maintenance and telomeric silencing. *EMBO J.* *17*, 1819-1828.
- Bressan, D. A., Baxter, B. K., and Petrini, J. H.** (1999). The Mre11-Rad50-Xrs2 protein complex facilitates homologous recombination-based double-strand break repair in *Saccharomyces cerevisiae*. *Mol. Cell. Biol.* *19*, 7681-7687.
- Bressan, D. A., Olivares, H. A., Nelms, B. E., and Petrini, J. H.** (1998). Alteration of N-terminal phosphoesterase signature motifs inactivates *Saccharomyces cerevisiae* Mre11. *Genetics* *150*, 591-600.
- Carney, J. P., Maser, R. S., Olivares, H., Davis, E. M., Le Beau, M., Yates, J. R., 3rd, Hays, L., Morgan, W. F., and Petrini, J. H.** (1998). The hMre11/hRad50 protein complex and Nijmegen breakage syndrome: linkage of double-strand break repair to the cellular DNA damage response. *Cell* *93*, 477-486.
- Chamankhah, M., and Xiao, W.** (1999). Formation of the yeast Mre11-Rad50-Xrs2 complex is correlated with DNA repair and telomere maintenance. *Nucleic Acids Res.* *27*, 2072-2079.
- Digweed, M., Reis, A., and Sperling, K.** (1999). Nijmegen breakage syndrome: consequences of defective DNA double strand break repair. *Bioessays* *21*, 649-656.
- Dolganov, G. M., Maser, R. S., Novikov, A., Tosto, L., Chong, S., Bressan, D. A., and Petrini, J. H.** (1996). Human Rad50 is physically associated with human Mre11: identification of a conserved multiprotein complex implicated in recombinational DNA repair. *Mol. Cell. Biol.* *16*, 4832-4841.
- Ducau, J., Bregliano, J., and de La Roche Saint-Andre, C.** (2000). Gamma-irradiation stimulates homology-directed DNA double-strand break repair in *Drosophila* embryo. *Mutat. Res.* *460*, 69-80.
- Furuse, M., Nagase, Y., Tsubouchi, H., Murakami-Murofushi, K., Shibata, T., and Ohta, K.** (1998). Distinct roles of two separable *in vitro* activities of yeast Mre11 in mitotic and meiotic recombination. *EMBO J.* *17*, 6412-6425.
- Gatei, M., Young, D., Cerosaletti, K. M., Desai-Mehta, A., Spring, K., Kozlov, S., Lavin, M. F., Gatti, R. A., Concannon, P., and Khanna, K.** (2000). ATM-dependent phosphorylation of nibrin in response to radiation exposure. *Nat. Genet.* *25*, 115-119.
- Gerecke, E. E., and Zolan, M. E.** (2000). An mre11 mutant of *Coprinus cinereus* has defects in meiotic chromosome pairing, condensation and synapsis. *Genetics* *154*, 1125-1139.
- Glasunov, A. V., Glaser, V. M., and Kapultsevich, Y. G.** (1989). Two pathways of DNA double-strand break repair in G1 cells of *Saccharomyces cerevisiae*. *Yeast* *5*, 131-139.
- Henricksen, L. A., Umbricht, C. B., and Wold, M. S.** (1994). Recombinant replication protein A: expression, complex formation, and functional characterization. *J. Biol. Chem.* *269*, 11121-11132.
- Hopfner, K. P., Karcher, A., Shin, D. S., Craig, L., Arthur, L. M., Carney, J. P., and Tainer, J. A.** (2000). Structural biology of Rad50 ATPase: ATP-driven conformational control in DNA double-strand break repair and the ABC-ATPase superfamily. *Cell* *101*, 789-800.
- Ito, A., Tauchi, H., Kobayashi, J., Morishima, K., Nakamura, A., Hirokawa, Y., Matsuura, S., Ito, K., and Komatsu, K.** (1999). Expression of full-length NBS1 protein restores normal radiation

responses in cells from Nijmegen breakage syndrome patients. *Biochem. Biophys. Res. Commun.* 265, 716-721.

Ivanov, E. L., Sugawara, N., White, C. I., Fabre, F., and Haber, J. E. (1994). Mutations in XRS2 and RAD50 delay but do not prevent mating-type switching in *Saccharomyces cerevisiae*. *Mol. Cell Biol.* 14, 3414-3425.

Johzuka, K., and Ogawa, H. (1995). Interaction of Mre11 and Rad50: two proteins required for DNA repair and meiosis-specific double-strand break formation in *Saccharomyces cerevisiae*. *Genetics* 139, 1521-1532.

Kanaar, R., Hoeijmakers, J. H., and van Gent, D. C. (1998). Molecular mechanisms of DNA double strand break repair. *Trends Cell Biol.* 8, 483-489.

Kim, S. T., Lim, D. S., Canman, C. E., and Kastan, M. B. (1999). Substrate specificities and identification of putative substrates of ATM kinase family members. *J. Biol. Chem.* 274, 37538-37543.

Kramer, K. M., Brock, J. A., Bloom, K., Moore, J. K., and Haber, J. E. (1994). Two different types of double-strand breaks in *Saccharomyces cerevisiae* are repaired by similar RAD52-independent, nonhomologous recombination events. *Mol. Cell Biol.* 14, 1293-1301.

Lewis, L. K., and Resnick, M. A. (2000). Tying up loose ends: nonhomologous end-joining in *Saccharomyces cerevisiae*. *Mutat. Res.* 451, 71-89.

Lim, D. S., Kim, S. T., Xu, B., Maser, R. S., Lin, J., Petrini, J. H., and Kastan, M. B. (2000). ATM phosphorylates p95/nbs1 in an S-phase checkpoint pathway. *Nature* 404, 613-617.

Lombard, D. B., and Guarente, L. (2000). Nijmegen breakage syndrome disease protein and MRE11 at PML nuclear bodies and meiotic telomeres. *Cancer Res.* 60, 2331-2334.

Luo, G., Yao, M. S., Bender, C. F., Mills, M., Bladl, A. R., Bradley, A., and Petrini, J. H. (1999). Disruption of mRad50 causes embryonic stem cell lethality, abnormal embryonic development, and sensitivity to ionizing radiation. *Proc. Natl. Acad. Sci. USA* 96, 7376-7381.

Malone, R. E., Ward, T., Lin, S., and Waring, J. (1990). The RAD50 gene, a member of the double strand break repair epistasis group, is not required for spontaneous mitotic recombination in yeast. *Curr. Genet.* 18, 111-116.

Mason, R. M., Thacker, J., and Fairman, M. P. (1996). The joining of non-complementary DNA double-strand breaks by mammalian extracts. *Nucleic Acids Res.* 24, 4946-4953.

Matsuura, S., Tsuchi, H., Nakamura, A., Kondo, N., Sakamoto, S., Endo, S., Smeets, D., Solder, B., Belohradsky, B. H., Der Kaloustian, V. M., Oshimura, M., Isomura, M., Nakamura, Y., and Komatsu, K. (1998). Positional cloning of the gene for Nijmegen breakage syndrome. *Nat. Genet.* 19, 179-181.

Melby, T. E., Ciampaglio, C. N., Briscoe, G., and Erickson, H. P. (1998). The symmetrical structure of structural maintenance of chromosomes (SMC) and MukB proteins: long, antiparallel coiled coils, folded at a flexible hinge. *J. Cell Biol.* 142, 1595-1604.

Moore, J. K., and Haber, J. E. (1996). Cell cycle and genetic requirements of two pathways of nonhomologous end-joining repair of double-strand breaks in *Saccharomyces cerevisiae*. *Mol. Cell Biol.* 16, 2164-2173.

- Moreau, S., Ferguson, J. R., and Symington, L. S.** (1999). The nuclease activity of Mre11 is required for meiosis but not for mating type switching, end joining, or telomere maintenance. *Mol. Cell. Biol.* 19, 556-566.
- Mortensen, U. H., Bendixen, C., Sunjevaric, I., and Rothstein, R.** (1996). DNA strand annealing is promoted by the yeast Rad52 protein. *Proc. Natl. Acad. Sci. USA* 93, 10729-10734.
- New, J. H., Sugiyama, T., Zaitseva, E., and Kowalczykowski, S. C.** (1998). Rad52 protein stimulates DNA strand exchange by Rad51 and replication protein A. *Nature* 391, 407-410.
- Ogawa, H., Johzuka, K., Nakagawa, T., Leem, S. H., and Hagihara, A. H.** (1995). Functions of the yeast meiotic recombination genes, MRE11 and MRE2. *Adv. Biophys.* 31, 67-76.
- Ono, M., Tucker, P. W., and Capra, J. D.** (1994). Production and characterization of recombinant human Ku antigen. *Nucleic Acids Res.* 22, 3918-3924.
- Paques, F., and Haber, J. E.** (1999). Multiple pathways of recombination induced by double-strand breaks in *Saccharomyces cerevisiae*. *Microbiol Mol Biol Rev.* 63, 349-404.
- Paull, T. T., and Gellert, M.** (1998). The 3' to 5' exonuclease activity of Mre 11 facilitates repair of DNA double-strand breaks. *Mol. Cell* 1, 969-979.
- Paull, T. T., and Gellert, M.** (1999). Nbs1 potentiates ATP-driven DNA unwinding and endonuclease cleavage by the Mre11/Rad50 complex. *Genes Dev.* 13, 1276-1288.
- Paull, T. T., and Gellert, M.** (2000). A mechanistic basis for Mre11-directed DNA joining at microhomologies. *Proc. Natl. Acad. Sci. USA* 97, 6409-6414.
- Petrini, J. H., Walsh, M. E., DiMare, C., Chen, X. N., Korenberg, J. R., and Weaver, D. T.** (1995). Isolation and characterization of the human MRE11 homologue. *Genomics* 29, 80-86.
- Pfeiffer, P., Thode, S., Hancke, J., and Vielmetter, W.** (1994). Mechanisms of overlap formation in nonhomologous DNA end joining. *Mol. Cell. Biol.* 14, 888-895.
- Reddy, G., Golub, E. I., and Radding, C. M.** (1997). Human Rad52 protein promotes single-strand DNA annealing followed by branch migration. *Mutat. Res.* 377, 53-59.
- Roth, D. B., Porter, T. N., and Wilson, J. H.** (1985). Mechanisms of nonhomologous recombination in mammalian cells. *Mol. Cell. Biol.* 5, 2599-2607.
- Roth, D. B., and Wilson, J. H.** (1986). Nonhomologous recombination in mammalian cells: role for short sequence homologies in the joining reaction. *Mol. Cell. Biol.* 6, 4295-4304.
- Sharples, G. J., and Leach, D. R.** (1995). Structural and functional similarities between the SbcCD proteins of *Escherichia coli* and the RAD50 and MRE11 (RAD32) recombination and repair proteins of yeast. *Mol. Microbiol.* 17, 1215-1217.
- Shiloh, Y.** (1997). Ataxia-telangiectasia and the Nijmegen breakage syndrome: related disorders but genes apart. *Annu. Rev. Genet.* 31, 635-662.
- Shinohara, A., Ogawa, H., and Ogawa, T.** (1992). Rad51 protein involved in repair and recombination in *S. cerevisiae* is a RecA-like protein. *Cell* 69, 457-470.
- Shinohara, A., and Ogawa, T.** (1998). Stimulation by Rad52 of yeast Rad51-mediated recombination. *Nature* 391, 404-407.
- Shinohara, A., Shinohara, M., Ohta, T., Matsuda, S., and Ogawa, T.** (1998). Rad52 forms ring structures and co-operates with RPA in single-strand DNA annealing. *Genes Cells* 3, 145-156.
- Stewart, G. S., Maser, R. S., Stankovic, T., Bressan, D. A., Kaplan, M. I., Jaspers, N. G., Raams, A., Byrd, P. J., Petrini, J. H., and Taylor, A. M.** (1999). The DNA double-strand break

repair gene hMRE11 is mutated in individuals with an ataxia-telangiectasia-like disorder. *Cell* 99, 577-587.

Sugawara, N., and Haber, J. E. (1992). Characterization of double-strand break-induced recombination: homology requirements and single-stranded DNA formation. *Mol. Cell. Biol.* 12, 563-575.

Sugiyama, T., New, J. H., and Kowalczykowski, S. C. (1998). DNA annealing by RAD52 protein is stimulated by specific interaction with the complex of replication protein A and single-stranded DNA. *Proc. Natl. Acad. Sci. USA* 95, 6049-6054.

Sung, P. (1997). Function of yeast Rad52 protein as a mediator between replication protein A and the Rad51 recombinase. *J. Biol. Chem.* 272, 28194-28197.

Tavassoli, M., Shayeghi, M., Nasim, A., and Watts, F. Z. (1995). Cloning and characterisation of the *Schizosaccharomyces pombe* rad32 gene: a gene required for repair of double strand breaks and recombination. *Nucleic Acids Res.* 23, 383-388.

Thacker, J., Chalk, J., Ganesh, A., and North, P. (1992). A mechanism for deletion formation in DNA by human cell extracts: the involvement of short sequence repeats. *Nucleic Acids Res.* 20, 6183-6188.

Thode, S., Schafer, A., Pfeiffer, P., and Vielmetter, W. (1990). A novel pathway of DNA end-to-end joining. *Cell* 60, 921-928.

Trujillo, K. M., Yuan, S. S., Lee, E. Y., and Sung, P. (1998). Nuclease activities in a complex of human recombination and DNA repair factors Rad50, Mre11, and p95. *J. Biol. Chem.* 273, 21447-21450.

Tsubouchi, H., and Ogawa, H. (1998). A novel mre11 mutation impairs processing of double-strand breaks of DNA during both mitosis and meiosis. *Mol. Cell. Biol.* 18, 260-268.

Tsukamoto, Y., and Ikeda, H. (1998). Double-strand break repair mediated by DNA end-joining. *Genes Cells* 3, 135-144.

Tsukamoto, Y., Kato, J., and Ikeda, H. (1996). Effects of mutations of RAD50, RAD51, RAD52, and related genes on illegitimate recombination in *Saccharomyces cerevisiae*. *Genetics* 142, 383-391.

Tsukamoto, Y., Kato, J., and Ikeda, H. (1997). Budding yeast Rad50, Mre11, Xrs2, and Hdf1, but not Rad52, are involved in the formation of deletions on a dicentric plasmid. *Mol. Gen. Genet* 255, 543-547.

Usui, T., Ohta, T., Oshiumi, H., Tomizawa, J., Ogawa, H., and Ogawa, T. (1998). Complex formation and functional versatility of Mre11 of budding yeast in recombination. *Cell* 95, 705-716.

Varon, R., Vissinga, C., Platzer, M., Cerosaletti, K. M., Chrzanoska, K. H., Saar, K., Beckmann, G., Seemanova, E., Cooper, P. R., Nowak, N. J., Stumm, M., Weemaes, C. M., Gatti, R. A., Wilson, R. K., Digweed, M., Rosenthal, A., Sperling, K., Concannon, P., and Reis, A. (1998). Nibrin, a novel DNA double-strand break repair protein, is mutated in Nijmegen breakage syndrome. *Cell* 93, 467-476.

Wilson, S., Warr, N., Taylor, D. L., and Watts, F. Z. (1999). The role of *Schizosaccharomyces pombe* Rad32, the Mre11 homologue, and other DNA damage response proteins in non-homologous end joining and telomere length maintenance. *Nucleic Acids Res.* 27, 2655-2661.

Xiao, Y., and Weaver, D. T. (1997). Conditional gene targeted deletion by Cre recombinase demonstrates the requirement for the double-strand break repair Mre11 protein in murine embryonic stem cells. *Nucleic Acids Res.* 25, 2985-2991.

Yamaguchi-Iwai, Y., Sonoda, E., Sasaki, M. S., Morrison, C., Haraguchi, T., Hiraoka, Y., Yamashita, Y. M., Yagi, T., Takata, M., Price, C. C., Kakazu, N., and Takeda, S. (1999). Mre11 is essential for the maintenance of chromosomal DNA in vertebrate cells. *EMBO J.* 18, 6619-6629.

Zhao, S., Weng, Y. C., Yuan, S. S., Lin, Y. T., Hsu, H. C., Lin, S. C., Gerbino, E., Song, M. H., Zdzienicka, M. Z., Gatti, R. A., Shay, J. W., Ziv, Y., Shiloh, Y., and Lee, E. Y. (2000). Functional link between ataxia-telangiectasia and Nijmegen breakage syndrome gene products. *Nature* 405, 473-477.

Zhu, X. D., Kuster, B., Mann, M., Petrini, J. H., and Lange, T. (2000). Cell-cycle-regulated association of RAD50/MRE11/NBS1 with TRF2 and human telomeres. *Nat. Genet.* 25, 347-352.

Chapter

Human Rad50/Mre11 is a flexible complex

that can tether DNA ends

3

Human Rad50/Mre11 is a flexible complex that can tether DNA ends

Martijn de Jager¹, John van Noort², Dik C. van Gent¹, Cees Dekker², Roland Kanaar^{1,3} and Claire Wyman¹

¹Department of Cell Biology & Genetics, Erasmus MC, Dr. Molewaterplein 50, 3000 DR Rotterdam, The Netherlands, ²Delft University of Technology, Department of Applied Physics and DIMES, Lorentzweg 1, 2628 CJ Delft, The Netherlands, and ³Department of Radiation Oncology, Erasmus MC-Daniel, Rotterdam, The Netherlands

Modified from: *Molecular Cell*, 2001, Vol. 8, No. 5, 1129-1135

The human Rad50 protein, classified as a structural maintenance of chromosome (SMC) family member, is complexed with Mre11 (R/M) and has important functions in at least two distinct double-strand break repair pathways. To find out what the common function of R/M in these pathways might be, we investigated its architecture. Scanning force microscopy showed that the complex architecture is distinct from the described SMC family members. R/M consisted of two highly flexible intramolecular coiled coils emanating from a central globular DNA-binding domain. DNA end-bound R/M oligomers could tether linear DNA molecules. These observations suggest that a unified role for R/M in multiple aspects of DNA repair and chromosome metabolism is to provide a flexible, possibly dynamic, link between DNA ends.

Introduction

DNA double-strand breaks (DSBs) are necessary intermediates in a number of normal aspects of DNA metabolism, such as V(D)J recombination and meiosis (Modesti and Kanaar, 2001). In addition, DSBs can be caused by endogenous or exogenous DNA damaging agents. Unrepaired DSBs can be lethal, whereas misrepaired DSBs can cause chromosomal fragmentation, translocations and deletions. Eukaryotic cells primarily repair DSBs by one of two distinct pathways, non-homologous end-joining or homologous recombination (Baumann and West, 1998; Kanaar et al., 1998; Karran, 2000; Sung et al., 2000). These two pathways process and repair DSBs in different ways but both require a protein complex containing Rad50, Mre11 and Nbs1 (or Xrs2 in yeast) (Ogawa et al., 1995; Dolganov et al., 1996; Trujillo et al., 1998; Usui et al., 1998; Paques and Haber, 1999; Paull and Gellert, 2000; Lewis and Resnick, 2000). The essential role of these gene products in mammals is underscored by the fact that disruption of *RAD50*, *MRE11* or *NBS1* genes results either in cell inviability or embryonic lethality (Xiao and Weaver, 1997; Luo et al., 1999; Zhu et al., 2001). Furthermore, mutations in the human *MRE11* and *NBS1* genes cause the cancer predisposition syndromes ataxia telangiectasia-like disorder and Nijmegen breakage syndrome, respectively (Carney et al., 1998; Stewart et al., 1999). A unified function for the Rad50, Mre11 and Nbs1 proteins in the distinct DSB repair pathways has not yet been identified.

One clue towards understanding the function(s) of R/M comes from sequence analysis which places Rad50 in the structural maintenance of chromosomes (SMC) family of proteins (Sharples and Leach, 1995; Saitoh et al., 1995; Aravind et al., 1999; Strunnikov and Jessberger, 1999). The paradigm proteins in this class are involved in DNA condensation and structural chromosome

maintenance and they all have an interesting predicted architecture consisting of globular amino (N)- and carboxy (C)- termini separated by an extended coiled-coil domain (Strunnikov and Jessberger, 1999; Fousteri and Lehmann, 2000; Holmes and Cozzarelli, 2000). This architecture has been beautifully confirmed by electron microscopy (EM) studies of the bacterial family members *E. coli* MukB, *Bacillus subtilis* SMC (Melby et al., 1998) and *E. coli* SbcCD (Connelly et al., 1998). For *E. coli* MukB and *B. subtilis* SMC the coiled-coil domain has been shown to contain an anti-parallel arrangement of two protomers with a flexible central hinge (Melby et al., 1998). It has been suggested that this structure has specific relevance for chromosome condensation by binding distant DNA sites with the terminal globular domains and effecting rearrangement of the intervening DNA through movement of the hinge (Melby et al., 1998; Holmes and Cozzarelli, 2000). Atomic level structure determination of the catalytic domain of two structural Rad50 homologues from archaea and bacteria confirmed the association of N- and C-terminal domains to form a functional ATPase active site (Hopfner et al., 2000; Lowe et al., 2001). Additional data from the crystal structure of the *P. furiosus* Mre11 and Rad50 structural homologues resulted in a model for the arrangement of Rad50 and Mre11 in a complex that is a variation of the general model for SMC proteins (Hopfner et al., 2001). Though the structural models of bacterial and archaeal SMC proteins and R/M homologues provide a starting point for understanding function, the structure of human R/M is not known and differences from those already proposed could have important functional consequences.

We describe the architecture of human R/M and complexes of this protein with DNA using scanning force microscopy (SFM). SFM images showed human R/M to have a striking architecture that shares some features of, but is distinct from, the bacterial and archaeal SMC proteins so far described. Human R/M consisted of a large central globular domain from which two rod-like 'arms' protruded. We observed a variety of conformations for the arms and demonstrated their remarkable flexibility by time-resolved SFM of single molecules in buffer. DNA was bound by the central globular domain of R/M. SFM images revealed preferential binding to linear DNA and accumulation of R/M oligomers at DNA ends. Different DNA molecules could be held together by interaction of the arms of the end-bound R/M oligomers. These data suggest that the architecture of R/M bound to DNA ends allows association of DNA through multiple interactions of the flexible arms. This ability to hold different DNA molecules together in a relatively non-specific and flexible manner can explain the importance of R/M in the variety of DNA metabolic pathways.

Results

Human Rad50 forms an intramolecular coiled coil

To study the structure of the human Rad50 and Mre11 complex (hereafter referred to as R/M), it was purified from Sf21 cells coinfecting with baculoviruses expressing histidine-tagged hRad50 and untagged hMre11. The identity of the proteins in the final fraction was confirmed by immunoblotting, and size fractionation confirmed that the purified hRad50 and hMre11 are present in a complex (data not shown). As shown for hMre11 alone, purified R/M bound to DNA and promoted annealing of complementary oligonucleotides (de Jager et al., 2001; Chapter 2; data not shown). As expected, R/M also possessed an ATP-independent, but manganese-dependent, 3' to 5' exonuclease activity on blunt-ended double-stranded DNA substrates (Paull and Gellert, 1998; data not shown).

The amino acid sequence of hRad50 predicts that this protein would have a structure similar to bacterial SMC class molecules with N- and C-terminal globular domains connected by a 960 amino acid long heptad repeat, likely to form a coiled-coil structure. We used SFM to determine the architecture of the purified human R/M complex. Human R/M indeed had a distinct architecture consisting of a large globular domain, from which two 40 to 50 nm-long arms protruded (Figure 1).

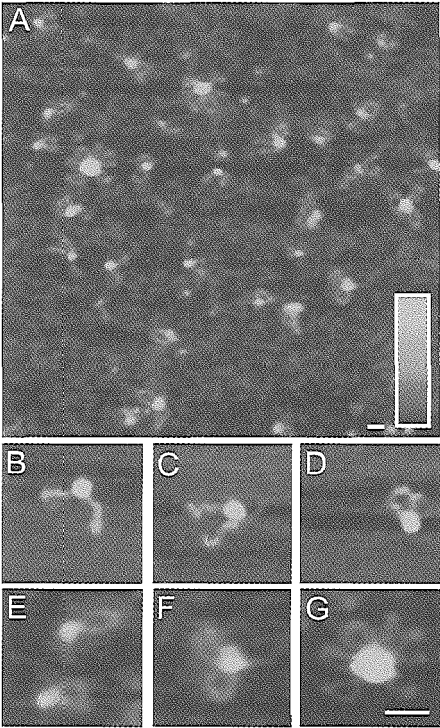


Figure 1. SFM analysis of human R/M. Purified R/M was deposited on mica and imaged by tapping mode SFM in air. (A) A typical field of complexes (1 μm x 1 μm scan). R/M exhibited a distinct architecture with a central globular domain and from which arms of 40 to 50 nm long protruded. The arms were observed in a variety of conformations (B to E), and multimeric forms (F and G). The scale bars are 50 nm. Color represents height, from 0 to 1 nm (dark to light), as shown by the key insert in (A).

The length of the arms was half of that expected for a 960 amino acid long coiled-coil structure. To determine whether the individual arms consisted of a single hRad50 molecule folded back on itself or a complex of more than one coiled coil, we estimated the width of the arms. Dimensions of biomolecules measured by SFM are subject to distortions (Bustamante, 1993). Therefore, we compared the width of the arms to the width of DNA in the same image. Within the error of measurements, the R/M arms were about the same width as double-stranded DNA. Based on a width of 2 nm for B form DNA and 3 nm for a coiled coil, determined by X-ray crystallography (O'Shea et al., 1991), we believe the R/M arms are a single coiled coil.

The arms appeared in a variety of conformations varying from completely splayed (Figure 1B) to closed structures with the ends touching (Figure 1D, and 1E). The individual arms appeared in straight, bent and kinked conformations, which cannot simply be due to rotation around the globular domain. Open and closed arms appeared with a frequency of about 60% and 40%, respectively, which was not significantly influenced by the presence of Mg^{2+} , or Mn^{2+} and/or ATP.

R/M appeared in different oligomeric forms (Figure 1). The most abundant form (80% of all molecules) consisted of a single globular domain with two arms (Figure 1B to 1E) which we refer to as a 'monomer' complex. We never observed a globular domain with only one arm. Though in some cases the arms were almost parallel or almost on top of each other, there were always clearly two arms. Based on the width and length of the arms and the composition of an archaeal R/M complex (Hopfner et al., 2001), we believe this form contains two hRad50 molecules and two hMre11 molecules. Other oligomeric forms were dimer complexes having 4 arms (14% of all molecules; Figure 1F) and some larger multimers, usually consisting of 4 to 6 monomers (6% of all molecules; Figure 1G). Multimers always contained an even number of arms, confirming that the two-armed version (Figure 1B to 1E) is the unit structure. Larger protein aggregates were only very rarely observed in the absence of DNA.

The coiled-coil arms of the human R/M complex are flexible

The different conformations of the protein complex, observed by SFM imaging in air (Figure 1B to 1E), suggested flexibility of the R/M arms. However, the different conformations observed could also be due to the presence of a mixture of static forms. In order to see if individual molecules were flexible we used SFM imaging of partially immobilized R/M in buffer. This method allows time-resolved analysis of single molecules. Figure 2 shows 4 consecutive frames, taken at 3 min intervals, of 4 individual molecules. The molecules were only partially immobilized and moved during the time it took to collect an image, thus the images appear less clear. However, it was obvious that each individual R/M molecule adopted a variety of conformations over the time intervals measured. Both joining and un-joining of the tips of the arms (Figure 2A, and 2D), as well as changes in curvature (Figure 2B,

and 2D) were observed for individual molecules, showing that the arms were indeed highly flexible. The flexibility of long polymer molecules can be expressed in persistence length (Rivetti et al., 1998). Though we do not know if the Rad50 arms can be accurately modeled as uniform polymers, as a first estimate of their flexibility we determined their persistence length. The Rad50 arms have a calculated persistence length of 35 nm, making them more flexible than double-stranded DNA (persistence length 50 nm).

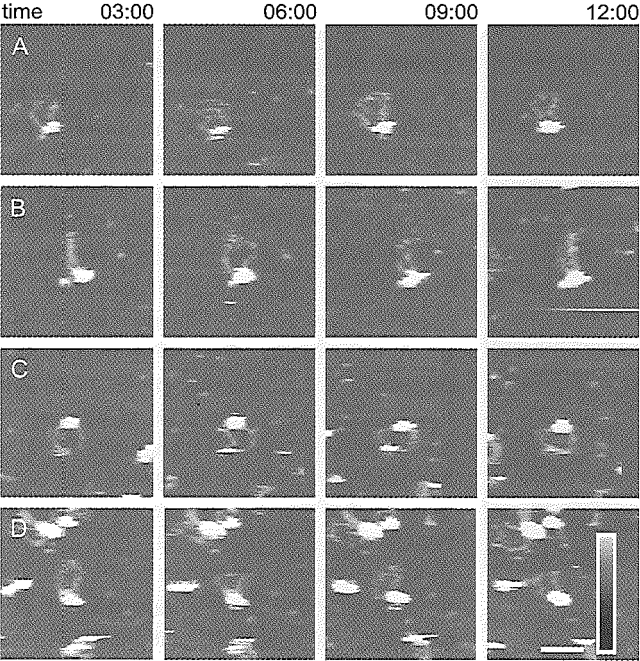


Figure 2. Time-resolved SFM imaging reveals R/M to be a highly flexible structure. Purified R/M was deposited on mica and imaged by tapping mode in buffer. Each series of panels, (A to D), shows a different single R/M complex observed over time. The panels are sequential images collected at 3 min intervals. The scale bar is 50 nm. Color represents height, from 0 to 5 nm (dark to light), as shown by the key insert at the bottom right.

The human R/M complex binds DNA ends

The cellular roles of this protein and its relation to SMC proteins suggest that R/M could work by organizing broken DNA molecules for further processing. How R/M would do this will depend on which part of the protein binds to DNA and possible interactions between DNA-bound proteins. We used SFM to investigate the architectural features of R/M-DNA complexes. R/M bound to DNA via the globular domain while the arms protruded from DNA (Figure 3B, 3C and 3E). Significantly, DNA binding via the arms was not observed. On linear DNA, R/M bound almost exclusively to the ends (Figure 3C and 3D, and see below). Increased protein concentrations resulted in the accumulation of large R/M oligomers at DNA ends (Figure 3D compared to 3C). Although the protein oligomers could become quite large and individual R/M molecules were difficult to resolve, in all cases the arms

were extending away from the DNA. We did not observe objects with the height of the large globular domain at the periphery of the DNA-bound protein oligomers. At protein concentrations resulting in large R/M oligomers at DNA ends, we often observed tethering of DNA molecules (Figure 3D and 3F). Interestingly, tethering of DNA molecules appeared to occur via interactions of R/M arms and apparently required multiple contacts (see below).

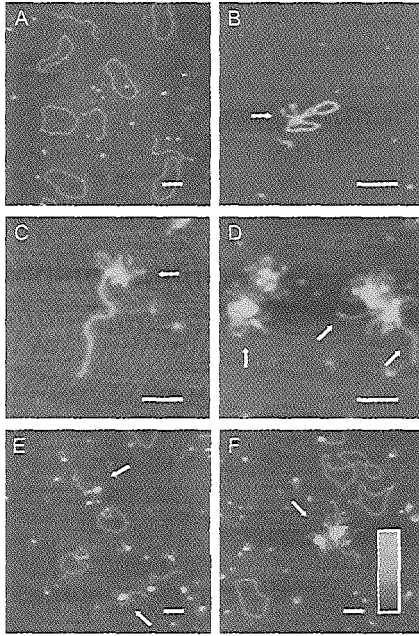


Figure 3. SFM analysis of R/M-DNA complexes. Reactions mixtures including the purified R/M and DNA were deposited on mica and imaged by tapping mode SFM in air. (A) The 1 kb linear and 1.8 kb circular DNA molecules that were used (either separately or together) in binding reactions. (B) R/M bound to the 1.8 kb circular DNA. (C and D) Reactions with 1 kb linear DNA at 15 nM of fragment, incubated with either 50 nM R/M (C) or 100 nM R/M (D). (E and F) Reaction mixtures including both the 1 kb linear DNA fragment and 1.8 kb relaxed circular DNA at 45 nM and 70 nM of fragments, respectively, incubated with 200 nM R/M complex. Arrows indicate protein molecules bound to DNA (B, C, E and F) or DNA (D). The scale bars are 100 nm. Color represents height, from 0 to 1 nm (dark to light), as shown by the key insert in (F).

To directly test if free DNA ends are a preferred substrate, we analyzed binding of R/M to a mixture of linear and circular DNA molecules. A preference for binding to DNA ends was not observed in gel retardation experiments (data not shown). For SFM we used a molar ratio of 3:1 to 6:1 protein to DNA molecules. These protein concentrations are much lower than the minimal required to observe any DNA binding in a gel retardation assay. For SFM in air, the protein-DNA complexes present in the reaction mixture at the time of deposition are effectively frozen for imaging. Thus, it is possible to observe complexes by SFM that do not survive gel electrophoresis-based assays (Wyman et al., 1997). Using SFM we observed a strong preference for binding of R/M to DNA ends (Figure 3E, and 3F); 29% (105/357) of linear DNA was bound by protein, versus 7% (43/624) for circular DNA. In addition, the complexes on circular DNA were very different from those on linear DNA. Almost all (92%) of the R/M complex bound to circular DNA was in its monomeric state. In contrast, about half (53%) of the linear DNA-R/M complexes included protein oligomers. In addition, multiple linear DNA molecules were often tethered together, accounting for 27% of the protein-bound DNA. We never observed circular DNA molecules tethered together. Tethering of DNA molecules was not observed with one or a

few R/M monomers. Association of DNA bound R/M appeared to occur through interaction of the arms. Although individual arms at the junctions were not resolved, the protein in the obvious junction regions was not as high as the globular domains.

Discussion

Human R/M is an essential cellular component that functions in several aspects of DNA metabolism. R/M has direct roles in both major pathways of DSB repair, homologous recombination and non-homologous end-joining. The amino acid sequence of Rad50 places it in the SMC class of proteins that in general affect chromosome condensation, DNA organization and reorganization through the cell cycle. We have described the architecture of human R/M and elements of this architecture that are important for DNA binding. The ability to observe individual protein complexes in buffer allowed us to demonstrate the remarkable flexibility of the hRad50 coiled-coil domains. We believe that our data indicate a general role for R/M in tethering DNA molecules together via multiple, presumable individually weak, interactions of the flexible arms as a sort of molecular Velcro. Below, we discuss this model and compare this R/M architecture to that of other SMC proteins.

Our SFM images of human R/M reveal an architecture that is different from those so far proposed for SMC proteins or the bacterial and archaeal R/M structural homologues. This architecture has important implications for the interaction of R/M with DNA and between DNA molecules. The architecture of bacterial SMC proteins is shown in Figure 4A (Melby et al., 1998). This architecture is often presented as general for SMC proteins (Strunnikov and Jessberger, 1999; Hopfner et al., 2000). A variation of this, specific for archaeal and bacterial R/M structural homologues (Hopfner et al., 2000; 2001; Lowe et al., 2001), is shown in Figure 4B. Our proposed arrangement for human R/M is shown in Figure 4C. We do not observe globular domains at the ends of the arms, ruling out the bacterial SMC type architecture (Figure 4A). Qualitatively, the arrangement in Figure 4B could be possible for human R/M, if the structures we observe consist of two such units. We do not believe this is the case for two reasons. First, we never see structures with one arm emanating from a globular domain. Second, the measured width of the arms is close to the measured width of DNA, likely representing one coiled coil. Third, biophysical characterization of the *P. furiosus* R/M homologue suggests that the unit form of the complex is R_2/M_2 (Hopfner et al., 2001). Interestingly, it has recently been demonstrated that altering the hinge region of *B. subtilis* SMC can convert this protein from an intermolecular dimer to intramolecular monomers, such as we propose here for human wild-type R/M (Hirano et al., 2001). In our proposed R/M

structure a functional ATPase is formed by interaction of N- and C-terminal domains from the same polypeptide folded in an intramolecular coiled coil. An Mre11 dimer is shown associated with Rad50 at the position predicted from the *P. furiosus* Rad50 and Mre11 structures (Hopfner et al., 2001). Though SFM does not provide information on the protein interfaces, because Mre11 itself forms dimers and based on the *P. furiosus* Mre11 and Rad50 interactions (Hopfner et al., 2001) we have indicated dimerization of the complex via Mre11.

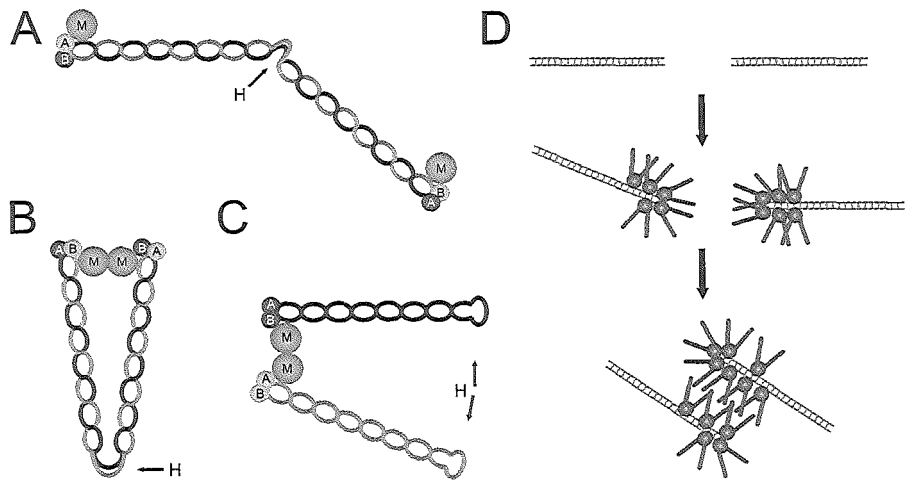


Figure 4. Possible architectural arrangements of Rad50 and Mre11 in the complex and implications for its roles in DNA double-strand break repair. (A) Hypothetical arrangement of R/M based on bacterial SMC proteins. Two anti-parallel Rad50 molecules in an intermolecular coiled coil with distal ATPase domains, formed by combining an N- and C-terminal part of two different Rad50 molecules and Mre11 interacting with these domains. (B) The arrangement proposed for the *P. furiosus* R/M structural homologue. Similar to (A) except that the two ATPase domains associate through an Mre11 dimer. (C) Proposed arrangement for human R/M. Two folded Rad50 arms as intramolecular coiled coils associated with an Mre11 dimer. Rad50 molecules are represented as light and dark grey spheres, with their two bipartite ATPase domains marked 'A' and 'B'. Mre11 is represented as a grey sphere, marked 'M'. The putative flexible hinge region in the middle of the coiled coil is indicated by 'H'. (D) Schematic representation of one of the hypothesized functions of R/M in DSB repair. R/M oligomers accumulate at broken DNA ends and keep the ends in close proximity by interaction of the end-bound R/M oligomers. The distinct architecture of the R/M complex could coordinate steps in end-processing and -joining by providing a flexible connection via multiple interaction sites. During non-homologous end-joining the R/M complex could provide a tether between the two ends of the same sister chromatid, while during homologous recombination it could in addition provide a tether between a broken end and the intact sister chromatid.

The architecture of R/M has important implications for its interactions with DNA. In contrast to the proposed direct connection of DNA molecules by a single coiled coil of an SMC-type molecule (Melby et al., 1998; Strunnikov and Jessberger, 1999; Hopfner et al., 2000; Holmes and Cozzarelli, 2000; Hirano et al., 2001), we observe indirect tethering of DNA molecules via multiple interactions of coiled-coil arms from complexes bound to separate DNA molecules. In accordance, recent data imply that the DNA aggregation activity of *B. subtilis* SMC is likely to require interaction between coiled-coil domains (Hirano et al., 2001). It seems likely that the individual interactions between R/M and DNA and between the R/M arms are relatively weak. The R/M DNA complexes we observe by SFM (at low protein concentrations) are not stable in gel mobility shift assays and we do not observe DNA tethering unless many R/M molecules are bound to each DNA molecule. Because the hRad50 arms are very flexible, their interactions could be dynamic. Thus, we propose that two DNA molecules are kept in contact through the net positive effect of association and dissociation of multiple hRad50 arms (Figure 4D). In addition, the flexibility of the individual arms would allow multiple arms to interact without forcing their bound DNA molecules into a rigid conformation relative to each other. *In vivo*, during non-homologous end-joining the R/M complex could provide a tether between the two ends of the same sister chromatid. During homologous recombination it could, in addition, provide a tether between a broken end and the intact sister chromatid (see also Cromie and Leach, 2001). The flexible connections between DNA molecules would allow a variety of orientations of the DNA molecules and access for more tenaciously binding factors with specific functions in DSB repair. We believe this defines a new type of connection between DNA molecules that gains strength of functional diversity through the details of structural weakness.

Materials and Methods

Scanning force microscopy

For SFM analysis of R/M, 20 μ l containing 400 ng of protein in protein buffer (150 mM KCl, 25 mM Tris-HCl [pH 7.8], and 10% glycerol) was deposited on freshly cleaved mica. After about 1 min the mica was washed with water (glass distilled, SIGMA) and dried in a stream of filtered air. Samples were imaged in air at room temperature and humidity using a NanoScope IIIa (Digital Instruments), operating in tapping mode with a type E scanner. Silicon tips (Nanoprobes) were from Digital Instruments.

Images of R/M in buffer were obtained by depositing protein onto mica as described above. Without rinsing or drying, the sample was mounted onto the SFM and 50 μ l of protein

buffer was added to the liquid cell. Olympus oxide-sharpened silicon nitride tips were used for tapping mode in buffer, operated at 18 kHz.

DNA substrates and binding reactions

The 1 kb fragment used for SFM experiments was obtained by a PCR reaction on M13 ssDNA template using 22 nt primers complementary to positions 5570 and 6584. The 1.8 kb nicked circular was produced as described (Ristic et al., 2001).

DNA-protein complexes for SFM were formed in 20 μ l reactions as described for gel retardation experiments (de Jager et al., 2001; Chapter 2) without BSA. DNA and protein concentrations were as described in the figure legend. Reactions were diluted 10-fold in deposition buffer (10 mM Hepes-KOH [pH 7.5] and 10 mM $MgCl_2$), deposited and imaged by SFM as described above.

Image processing and measurements

SFM images were processed only by flattening to remove background slope using NanoScope software. Measurements were done using NanoScope software. The persistence length of the hRad50 coiled coil was calculated from the measured end to end distance as described (Rivetti et al., 1998). We defined the end to end distance of the coiled coil as the distance between the end of the arm and the point at which that arm joined the central globular domain. The maximal measured end to end distance was used as the contour length in persistence length calculation.

Acknowledgements

We thank M. Modesti for discussion. We are grateful to T. Paull and M. Gellert for providing the Rad50 and Mre11 expression constructs. This work was supported by grants from the Dutch Cancer Society (KWF) and the section Chemical Sciences (CW) of the Netherlands Organisation for Scientific Research (NWO).

References

- Aravind, L., Walker, D. R., and Koonin, E. V.** (1999). Conserved domains in DNA repair proteins and evolution of repair systems. *Nucleic Acids Res.* *27*, 1223-1242.
- Baumann, P., and West, S.C.** (1998). Role of the human RAD51 protein in homologous recombination and double-stranded-break repair. *Trends Biochem. Sci.* *23*, 247-251.
- Bustamante, C., Keller, D., Yang, G.** (1993). Scanning force microscopy of nucleic acids and nucleoprotein assemblies. *Curr. Opin. Struct. Biol.* *3*, 363-372.
- Carney, J. P., Maser, R. S., Olivares, H., Davis, E. M., Le Beau, M., Yates, J. R., Connelly, J. C., Kirkham, L. A., and Leach, D. R.** (1998). The SbcCD nuclease of *Escherichia coli* is a structural maintenance of chromosomes (SMC) family protein that cleaves hairpin DNA. *Proc. Natl. Acad. Sci. USA* *95*, 7969-7974.
- Cromie, G. A., and Leach, D. R. F.** (2001). Recombinational repair of chromosomal DNA double-strand breaks generated by a restriction endonuclease. *Mol. Microbiol.* *41*, in press.
- de Jager, M., Dronkert, M. L., Modesti, M., Beerens, C. E., Kanaar, R., and van Gent, D. C.** (2001). DNA-binding and strand-annealing activities of human Mre11: implications for its roles in DNA double-strand break repair pathways. *Nucleic Acids Res.* *29*, 1317-1325.
- Dolganov, G. M., Maser, R. S., Novikov, A., Tosto, L., Chong, S., Bressan, D. A., and Petrini, J. H.** (1996). Human Rad50 is physically associated with human Mre11: identification of a conserved multiprotein complex implicated in recombinational DNA repair. *Mol. Cell. Biol.* *16*, 4832-4841.
- Fousteri, M. I., and Lehmann, A. R.** (2000). A novel SMC protein complex in *Schizosaccharomyces pombe* contains the Rad18 DNA repair protein. *EMBO J.* *19*, 1691-1702.
- Hirano, M., Anderson, D. E., Erickson, H. P., and Hirano, T.** (2001). Bimodal activation of SMC ATPase by intra- and inter-molecular interactions. *EMBO J.* *20*, 3238-3250.
- Holmes, V. F., and Cozzarelli, N. R.** (2000). Closing the ring: links between SMC proteins and chromosome partitioning, condensation, and supercoiling. *Proc. Natl. Acad. Sci. USA* *97*, 1322-1324.
- Hopfner, K., Karcher, A., Craig, L., Woo, T. T., Carney, J. P., and Tainer, J. A.** (2001). Structural biochemistry and interaction architecture of the DNA double-strand break repair mre11 nuclease and rad50-atpase. *Cell* *105*, 473-485.
- Hopfner, K. P., Karcher, A., Shin, D. S., Craig, L., Arthur, L. M., Carney, J. P., and Tainer, J. A.** (2000). Structural biology of Rad50 ATPase: ATP-driven conformational control in DNA double-strand break repair and the ABC-ATPase superfamily. *Cell* *101*, 789-800.
- Kanaar, R., Hoeijmakers, J.H.J., and van Gent, D.C.** (1998). Molecular mechanisms of DNA double strand break repair. *Trends Cell Biol.* *8*, 483-489.
- Karran, P.** (2000). DNA double strand break repair in mammalian cells. *Curr. Opin. Genet. Dev.* *10*, 144-150.

- Lewis, L.K., and Resnick, M.A.** (2000). Tying up loose ends: nonhomologous end-joining in *Saccharomyces cerevisiae*. *Mutat. Res.* *451*, 71-89.
- Lowe, J., Cordell, S. C., and van den Ent, F.** (2001). Crystal structure of the SMC head domain: an ABC ATPase with 900 residues antiparallel coiled-coil inserted. *J. Mol. Biol.* *306*, 25-35.
- Luo, G., Yao, M. S., Bender, C. F., Mills, M., Bladi, A. R., Bradley, A., and Petrini, J. H.** (1999). Disruption of mRad50 causes embryonic stem cell lethality, abnormal embryonic development, and sensitivity to ionizing radiation. *Proc. Natl. Acad. Sci. USA* *96*, 7376-7381.
- Melby, T. E., Ciampaglio, C. N., Briscoe, G., and Erickson, H. P.** (1998). The symmetrical structure of structural maintenance of chromosomes (SMC) and MukB proteins: long, antiparallel coiled coils, folded at a flexible hinge. *J. Cell. Biol.* *142*, 1595-1604.
- Modesti, M., and Kanaar, R.** (2001). DNA repair: Spot(light)s on chromatin. *Curr. Biol.* *11*, R229-232.
- Ogawa, H., Johzuka, K., Nakagawa, T., Leem, S. H., and Hagihara, A. H.** (1995). Functions of the yeast meiotic recombination genes, MRE11 and MRE2. *Adv. Biophys.* *31*, 67-76.
- O'Shea, E. K., Klemm, J. D., Kim, P. S., and Alber, T.** (1991). X-ray structure of the GCN4 leucine zipper, a two-stranded, parallel coiled coil. *Science* *254*, 539-544.
- Paques, F., and Haber, J. E.** (1999). Multiple pathways of recombination induced by double-strand breaks in *Saccharomyces cerevisiae*. *Microbiol. Mol. Biol. Rev.* *63*, 349-404.
- Paull, T. T., and Gellert, M.** (1998). The 3' to 5' exonuclease activity of Mre 11 facilitates repair of DNA double-strand breaks. *Mol. Cell* *1*, 969-979.
- Paull, T. T., and Gellert, M.** (2000). A mechanistic basis for Mre11-directed DNA joining at microhomologies. *Proc. Natl. Acad. Sci. USA* *97*, 6409-6414.
- Ristic, D., Wyman, C., Paulusma, C., and Kanaar, R.** (2001). The architecture of the human Rad54-DNA complex provides evidence for protein translocation along DNA. *Proc. Natl. Acad. Sci. USA* *98*, 8454-8460.
- Rivetti, C., Walker, C., and Bustamante, C.** (1998). Polymer chain statistics and conformational analysis of DNA molecules with bends or sections of different flexibility. *J. Mol. Biol.* *280*, 41-59.
- Saitoh, N., Goldberg, I., and Earnshaw, W. C.** (1995). The SMC proteins and the coming of age of the chromosome scaffold hypothesis. *Bioessays* *17*, 759-766.
- Sharples, G. J., and Leach, D. R.** (1995). Structural and functional similarities between the SbcCD proteins of *Escherichia coli* and the RAD50 and MRE11 (RAD32) recombination and repair proteins of yeast. *Mol. Microbiol.* *17*, 1215-1217.
- Stewart, G. S., Maser, R. S., Stankovic, T., Bressan, D. A., Kaplan, M. I., Jaspers, N. G., Raams, A., Byrd, P. J., Petrini, J. H., and Taylor, A. M.** (1999). The DNA double-strand break repair gene hMRE11 is mutated in individuals with an ataxia-telangiectasia-like disorder. *Cell* *99*, 577-587.
- Strunnikov, A. V., and Jessberger, R.** (1999). Structural maintenance of chromosomes (SMC) proteins: conserved molecular properties for multiple biological functions. *Eur. J. Biochem.* *263*, 6-13.

Sung, P., Trujillo, K. M., and van Komen, S. (2000). Recombination factors of *Saccharomyces cerevisiae*. *Mutat. Res.* 451, 257-275.

Trujillo, K. M., Yuan, S. S., Lee, E. Y., and Sung, P. (1998). Nuclease activities in a complex of human recombination and DNA repair factors Rad50, Mre11, and p95. *J. Biol. Chem.* 273, 21447-21450.

Usui, T., Ohta, T., Oshiumi, H., Tomizawa, J., Ogawa, H., and Ogawa, T. (1998). Complex formation and functional versatility of Mre11 of budding yeast in recombination. *Cell* 95, 705-716.

Wyman, C., Rombel, I., North, A. K., Bustamante, C., and Kustu, S. (1997). Unusual oligomerization required for activity of NtrC, a bacterial enhancer-binding protein. *Science* 275, 1658-1661.

Xiao, Y., and Weaver, D. T. (1997). Conditional gene targeted deletion by Cre recombinase demonstrates the requirement for the double-strand break repair Mre11 protein in murine embryonic stem cells. *Nucleic Acids Res.* 25, 2985-2991.

Zhu, J., Petersen, S., Tessarollo, L., and Nussenzweig, A. (2001). Targeted disruption of the Nijmegen breakage syndrome gene NBS1 leads to early embryonic lethality in mice. *Curr. Biol.* 11, 105-109.

Chapter

The coiled coil of the human Rad50

DNA repair protein contains specific segments of

increased flexibility

4

The coiled coil of the human Rad50 DNA repair protein contains specific segments of increased flexibility

John van Noort¹, Thijn van der Heijden¹, Martijn de Jager², Claire Wyman^{2,3}, Roland Kanaar^{2,3}, and Cees Dekker¹

¹Delft University of Technology, Department of Nanoscience and DIMES, Lorentzweg 1, 2628 CJ Delft, The Netherlands, ²Department of Cell Biology & Genetics, Erasmus MC, Dr. Molewaterplein 50, 3000 DR Rotterdam, The Netherlands, and ³Department of Radiation Oncology, Erasmus MC-Daniel, Rotterdam, The Netherlands

Submitted

Protein structural features are usually determined by defining regularities in a large population of homogeneous molecules. However, irregular features such as structural variation and flexibility are likely to be missed, despite their vital role for their biological function. In this paper we report the observation of striking irregularities in the flexibility of the coiled-coil region of the human Rad50 DNA repair protein. Existing methods to quantitatively analyze flexibility are applicable to homogeneous polymers only. Because protein coiled coils cannot be assumed to be homogeneous we develop a method to quantify the *local* flexibility from high-resolution SFM images. Indeed, in Rad50 coiled coils two positions of increased flexibility are observed. We discuss how this dynamic structural feature is integral to Rad50 function.

Introduction

The protein complex containing Rad50 and Mre11 (R/M) plays a pivotal role in maintaining genome stability. Its vital importance is underscored by its conservation from bacteriophages to humans (Cromie et al., 2001). Based on amino acid sequence similarities Rad50 belongs to the structural maintenance of chromosomes (SMC) family of proteins. Their shared amino acid sequence predicts a very distinct structure, including a bipartite globular ATPase domain made up from the N- and C-termini of the protein separated by an extensive central region predicted to form a coiled coil (Wyman and Kanaar, 2002). Accumulated recent evidence reveals that Rad50 and other SMC proteins are arranged as intramolecular coiled coils bringing together the N- and C-termini from one polypeptide to form a functional ATPase at one end of an elongated structure (Figure 1B; de Jager et al., 2001; Chapter 3; Hopfner et al., 2002; Haering et al., 2002). The SMC family members all exist as complexes of two such extended proteins. Their diverse functions must all require this striking structure. Many proposals for the mechanism of action of R/M and other SMC complexes require the coiled coils to be rigid and act as lever arms (Hirano, 1999). However, images of R/M show the coiled coils in a variety of conformations suggesting a high degree of flexibility (de Jager et al., 2001; Chapter 3; Anderson et al., 2001; Figure 1A). This has been confirmed by time-resolved scanning force microscopy (SFM) imaging of R/M partially immobilized in buffer, showing that individual coiled coils are quite flexible (de Jager et al., 2001; Chapter 3). To advance the structural characterization of the Rad50 coiled coils, we developed a method to characterize their flexibility quantitatively from high-resolution SFM images of R/M. For this analysis we used R/M complexes with two separate, well-resolved coiled coils such as shown in Figure 1C. In Figure 1D, a cross-section through the coiled coils is plotted to emphasize the resolution obtained.

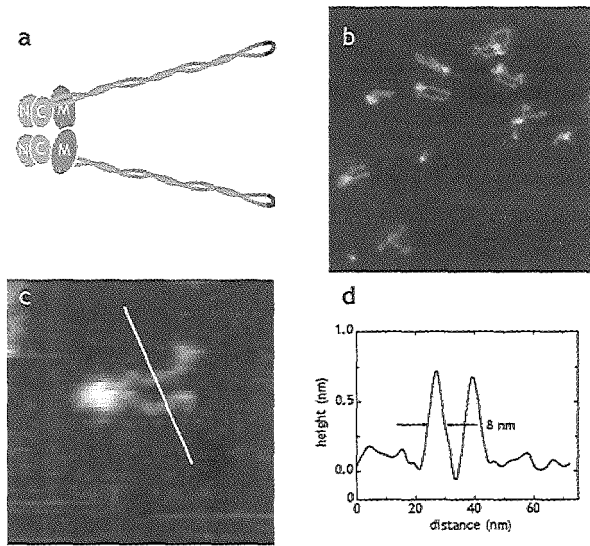


Figure 1. High-resolution SFM images of R/M complexes. (A), Overview of R/M complexes deposited on mica and imaged in air, showing a high variety of conformations. Scan range 500 nm; z range 3 nm. (B) Schematic representation of the architecture of the human R/M complex. Abbreviations: C, Rad50 carboxy-terminal domain; N, Rad50 amino-terminal domain; M, Mre11; Zn²⁺-hook in dark blue. (C) Software zoom of a R/M complex, oriented like panel A, Scan width 125 nm; z range 3 nm. (D) Cross-section through the Rad50 coiled coils of a R/M complex.

The high-resolution images allowed detailed analysis of the trajectory of the coiled coils. In case of a homogeneous polymer, the *local* flexibility F at every position corresponds directly to the inverse of the persistence length P , which is commonly used to describe the *global* bending rigidity of polymers. The persistence length of homogeneous biopolymers can be determined from static images using statistical mechanics. The bending rigidity of DNA for example, has been quantified directly from SFM images (Rivetti et al., 1996). In this method P is determined from measured end-to-end distance R and contour length L using the following equation:

$$\langle R^2 \rangle = 2PL \left[1 - \frac{P}{L} \left(1 - e^{-\frac{L}{P}} \right) \right] \quad (1)$$

For polymers like DNA this method yields an average persistence length that is in good agreement with values obtained by other techniques (Rivetti et al., 1996). This method has been modified to describe known segments of different persistence length (Rivetti et al., 1998). Another method for the determination of overall flexibility of biopolymers involves measuring of polymer extension as a function of the applied force, with optical tweezers (Bustamante et al., 2000) or SFM force spectroscopy (Strunz et al., 1999), and to fit a worm-like-chain model these data (Bustamante et al., 1994). Because structural differences along the polymer chain will be averaged out with these methods, they are applicable to homogeneous polymers only. However, a coiled coil of two interwound amino acid chains cannot be assumed to be homogeneous. To describe this likely

inhomogeneity, we developed a method that allows quantitative analysis of local flexibility along a polymer chain and therefore maps the spatial distribution of the flexibility along the polymer chain.

Local flexibility derived from local curvature distributions.

To locally determine flexibility in a polymer we employed and extended a method derived from quantifying bending angles of protein-DNA complexes (van Noort et al., 1999). A slightly different method has been used to identify subtle sequence dependent differences in flexibility in DNA molecules (Zuccheri et al., 2001). In our analysis, the local curvature κ of a specific polymer at a certain position is defined as the inverse radius of a circle following the trajectory along the molecule at that position. The elastic energy ΔU necessary to deflect the polymer can be expanded around the intrinsic curvature $\langle \kappa \rangle$ by a Taylor series as:

$$U(\kappa) = U(\langle \kappa \rangle) + \frac{1}{2} \frac{\delta^2 U(\langle \kappa \rangle)}{\delta \kappa^2} (\kappa - \langle \kappa \rangle)^2 + \dots \quad (2)$$

Neglecting higher-order terms the elastic bending energy of the polymer can thus be described as a harmonic oscillator:

$$\Delta U(\kappa) = U(\kappa) - U(\langle \kappa \rangle) = \frac{1}{2} k (\kappa - \langle \kappa \rangle)^2 \quad (3)$$

using a spring constant

$$k = \frac{\delta^2 U(\langle \kappa \rangle)}{\delta \kappa^2} \quad (4)$$

The local flexibility F can now be related to this spring constant as:

$$F = \sqrt{\frac{2 k_b T}{k}} \quad (5)$$

where k_b is Boltzmann's constant. Visualization of R/M complexes by SFM reveals the Rad50 coiled coils in a variety of conformations (Figure 1B; de Jager et al., 2001; Chapter 3) imposed by thermal equilibrium, that will follow Boltzmann's law. Thus, using equation 3, the observed curvatures will be distributed according to:

$$N(\kappa) = \sqrt{\frac{k}{2\pi k_b T}} e^{-\frac{k(\kappa - \langle \kappa \rangle)^2}{2k_b T}} \quad (6)$$

giving a normal distribution around average curvature $\langle K \rangle$, with a standard deviation of

$$\sqrt{\frac{k}{k_b T}}$$

Fitting equation 3 to the natural logarithm of this observed curvature distribution directly yields a value for the spring constant k , and thus, via equation 5, also the flexibility F .

Results

Analysis of DNA flexibility with the local curvature method.

First we tested the local curvature method by analysis of 1000 bp DNA molecules. DNA can be considered homogeneous in terms of flexibility, though subtle sequence dependent differences have been reported (Zuccheri et al., 2001). Hundred DNA molecules, were imaged by SFM (Figure 2A) and traced. Applying equation 1 yielded an average persistence length of 45 nm, well within the range of previously reported values (Rivetti et al., 1996).

Using three points at 5 nm spacing along the trajectory of the DNA, iterated at 1 nm intervals, the local curvature was measured. The resulting curvature distribution was found to be constant along the DNA chain, as expected for a homogeneous polymer. The curvature distribution and its calculated bending energy are plotted in Figure 2C and 2D, respectively. In Figure 2D the dotted line shows the calculated bending energy curve for a polymer with a persistence length of 45 nm. For very small curvatures the data closely matched the calculated energy curvature, validating the method.

However, for curvatures exceeding 0.02 nm^{-1} the experimental data deviate substantially from the theoretical curve. Because of resolution limits of SFM imaging high-curvature features are significantly obscured. This effect is enhanced by our tracing method, which moderately filters the coordinates of trajectory of the polymer. Furthermore, to determine the local curvature, we need three points along the trajectory of the molecule, which may average sharp bends within this range. As a consequence of these three effects, sharp kinks will be recorded having a too small curvature, effectively squeezing the tails of the curvature distribution to the center and thus broadening the $U(K)$ curve. Fitting a broader range of curvatures to these data points resulted in an erroneous persistence length of 204 nm.

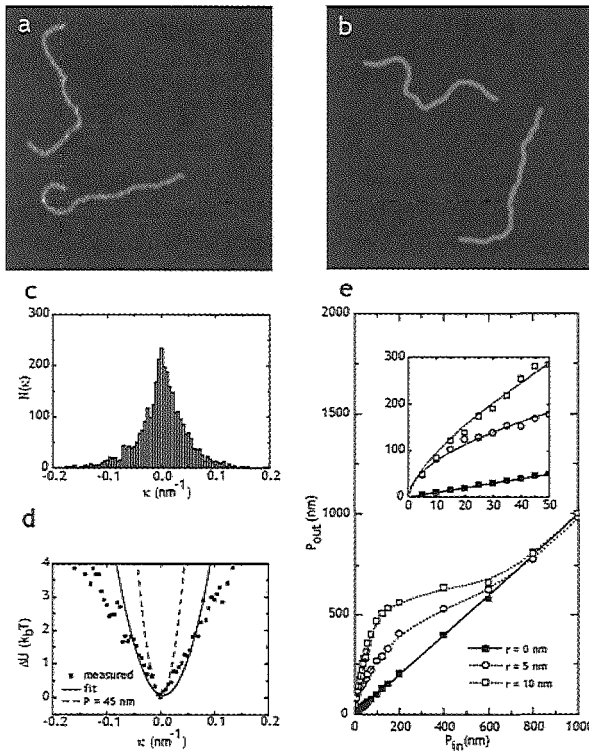


Figure 2. Validation of the local curvature method. (A) Two 1000 bp DNA molecules imaged by tapping mode SFM at a scan range of 500 nm and a z range of 3 nm. (B) Result of simulation of two 1000 bp DNA molecules with a persistence length (P) of 45 nm at a tip radius of 5 nm and a DNA height of 1 nm which corresponds to the height observed in panel A. Image settings are as shown in panel A. (C) Experimentally measured curvature distribution of DNA based on 100 molecules. Curvature was calculated using three 5 nm spaced points along the chain, and iterated every 1 nm, resulting in approximately 290 data points per DNA molecule. (D) Calculated bending energy ΔU for the curvature distribution shown in panel c. Solid line shows a parabolic fit to energy values below 1.5 $k_B T$. Dotted line shows the expected bending energy curve based on a $P = 45$ nm. (E) Persistence length P_{out} as

determined for the simulated homogeneous polymers. Filled squares show persistence length calculated with the end-to-end method. Open circles are measured with the curvature analysis method at a tip radius of 5 nm, while open squares represent data obtained with tip radius 10 nm. The inset shows a zoom for small persistence lengths, in the range of the tip size. The observed persistence length increases monotonously with the inputted persistence length.

To quantify the combined effects of tip-sample convolution and image processing we simulated SFM images of homogenous DNA-like polymers. The simulated polymers had the same dimensions as DNA, but varied in persistence length. The effect of tip-convolution was generated using a parabolic tip, similar to the procedure described by Rivetti et al. (Rivetti and Codeluppi, 2001). Figure 2B shows a simulated image of two 1000 bp DNA molecules with a persistence length of 45 nm, similar to the molecules measured in Figure 2A. Using the end-to-end distance method, the persistence length of the molecules in the simulated images closely matched the input values, κ , confirming the validity of the simulation.

Curvature distributions were generated after tracing 100 molecules in these simulated images. Using the procedure described above the local flexibility was measured. In Figure 2E the resulting values for the persistence length, which correspond to $1/F$, are plotted as a function of the input values. For finite tip radii, the measured persistence length appears to be overestimated by a factor up to 10. Reversibly, based on Figure 2E and the experimentally determined persistence length of DNA according to formula 1, we can estimate the tip radius used to produce the image in Figure 2A to be approximately 6 nm. This fits well with the observed width of the DNA. The measured values converge to the input numbers at persistence lengths beyond 600 nm. Thus, our local curvature method overestimates the persistence length if it is of the same order of magnitude as the image resolution, which is limited in SFM imaging by the finite size of the tip. Despite this overshoot in the absolute value of the calculated persistence length, however, a monotonously increasing observed persistence length was found for small values of the input persistence length (Figure 2E, inset). Thus, our simulations show that a *relative* flexibility can be obtained sensitively and reliably, even though sharp bends are obscured by tip convolution limitations.

Quantitative analysis of flexibility along the Rad50 coiled coil.

To determine the flexibility of the Rad50 coiled coil the contours of 100 R/M complexes were traced. Three typical R/M complexes with their traced coordinates are shown in Figure 3A to 3C. From the traced coordinates we directly obtained an average contour length of 47 nm for a single Rad50 coiled coil and an average end-to-end distance of 42 nm. Naively, neglecting inhomogeneities in the amino acid chains equation 1 results in a global persistence length of 30 nm for a single Rad50 coiled coil. Next, the traced coordinates of the R/M complexes were evaluated using our local curvature method. We defined positive curvature as bending inward forming a circular R/M complex configuration, while outward bends were assigned a negative curvature (Figure 3D).

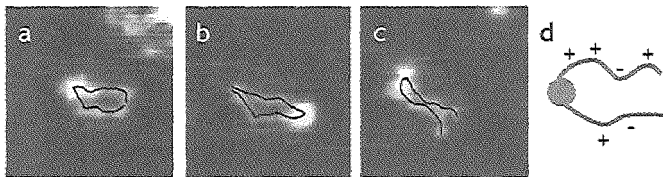


Figure 3. Tracing of R/M complexes. (A to C) display the trajectory of the Rad50 molecules within the R/M complexes as determined by tracing. Scan range 125 nm; z range 3 nm. (D) Schematic representation of a R/M complex with + and - signs denoting our curvature sign convention.

The curvature of all traces was analyzed using three 5 nm-spaced points. This procedure was iterated, following the trajectory of the molecule with 1 nm intervals. The curvatures along 200 Rad50 coiled coils were plotted in equally spaced segments according to the distance from the center of the globular domain. Figure 4A, 4C and 4E for example, show three histograms of the local curvature at 37, 40 and 44 nm from the globular domain, respectively. At 40 nm a significantly broader curvature distribution was observed compared to its neighbouring segments. The curvature distribution represented in terms of the bending energy is plotted in Figure 4B, 4D and 4F. A parabola describing equation 3 was fitted to all data points with a ΔU smaller than $1.5 k_b T$. By adopting this threshold, very high curvatures were omitted, which is justified since the number of these occurrences is underestimated, as described above.

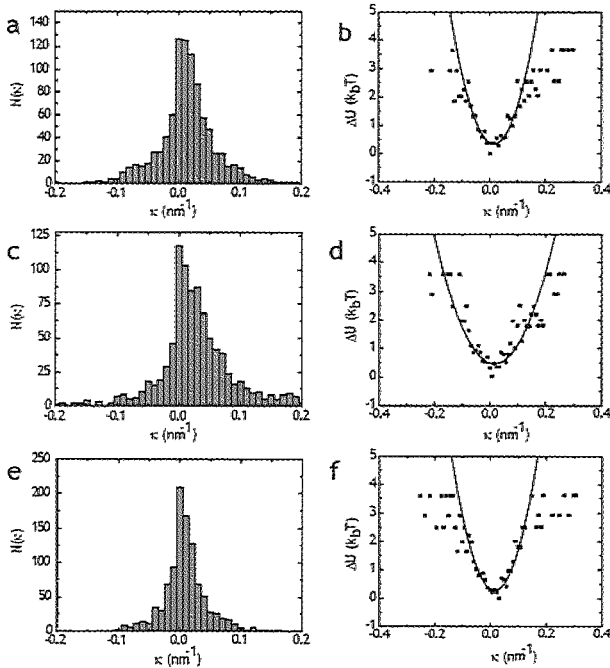


Figure 4. Curvature distributions and corresponding energy plots of Rad50 coiled coils. (A, C, and E) Curvature distributions of specific segments of the Rad50 molecule 37, 40 and 44 nm from the center of the R/M complex globular domain, respectively. (B, D, and F) Corresponding calculated bending energies. Lines represent parabolic fits to values smaller than $1.5 k_b T$.

A major result of this report is that the observed flexibility of the Rad50 coiled coils appears to vary along its length, as shown in Figure 5A. Two sections of clearly increased flexibility could be distinguished at 27 and 40 nm. These two sections of increased flexibility appeared in all curvature distributions, independent of the chosen bin size. While the flexibility of the polymer segments changed along the Rad50 coiled coil, the intrinsic curvature along the coiled coil, deduced from the minimum position of the elastic energy, only moderately varied (Figure 5B), with all sections having a positive

value, i.e. bending toward the centre of the complex. The corresponding radii of curvature, 46 to 86 nm, were all of the same magnitude or larger than the total length of the molecule, giving the molecule a moderately bent average conformation. Thus, the Rad50 coiled coil does not contain segments with locally increased intrinsic curvature and the large variety of coiled coil conformations originates mainly from its two relatively flexible segments.

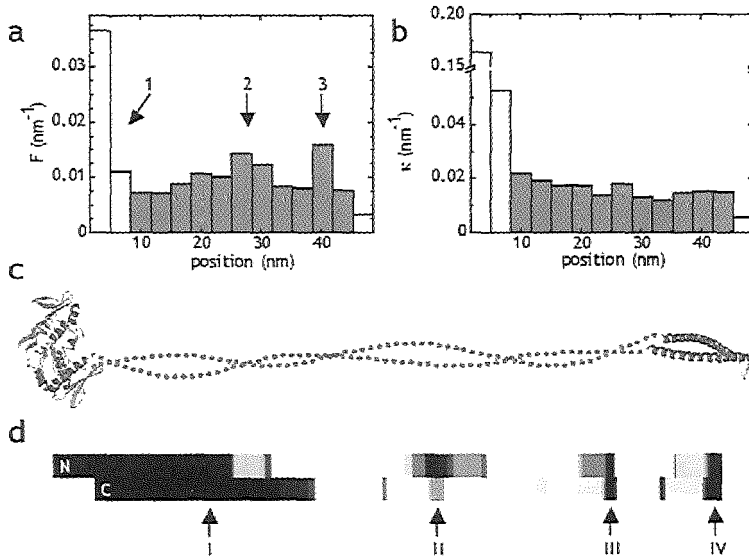


Figure 5. The Rad50 coiled coil contains specific segments of increased flexibility. (A) Flexibility distribution along the Rad50 coiled coil. Segments within 10 nm of the center of the globular R/M complex domain, marked I, are indicated by white bars. These regions do not contribute to the Rad50 coiled coil. The last bin is also displayed in white because end effects distort its value. Gray bars represent segments along the coiled coil. Two segments displaying increased flexibility are marked II and III. (B) Intrinsic curvature distribution along the Rad50 coiled coil. The first bins, indicated in white and corresponding to the R/M complex globular domain, are not relevant with respect to the curvature analysis of the Rad50 coiled coil, the last bin is affected by end effects. (C) Schematic cartoon of Rad50 in ribbon representation derived from the crystal structures of the ATPase domain (left) and the zinc-hook (right) the Rad50 homologue in *Pyrococcus furiosus* (Hopfner et al., 2000; Hopfner et al., 2002). The structure of the coiled coil that connects these two features has not been determined and is indicated by the dotted line. (D) Probability of coiled coil formation along the Rad50 amino acid chain is indicated using a gray scale with black and white representing the lowest and highest probability of forming a coiled coil, respectively. The amino acid chain is folded back onto itself at the position of the zinc-hook, marked IV. The globular domain is marked I. Two positions, marked II and III, appear in the coiled coil where both amino acids chains have a predicted decreased probability in coiled-coil formation. These positions colocalize with increased flexibility segments II and III in panel (A).

Mapping Rad50 regions of increased flexibility on its amino acid sequence.

What is the structural origin of the variation in local flexibility? Crystallographic studies have provided atomic resolution structures for the N- and C- termini of Rad50 (Hopfner et al., 2001), as well as the region in the middle of the predicted coiled coil (Hopfner et al., 2002). The N- and C-termini juxtapose to form a globular ATPase domain. The middle of the predicted coiled coil forms a structure, referred to as a zinc-hook, where the amino acid chain makes a sharp U-turn. However, no high-resolution structural data are available for the predicted coiled coil that connects the globular ATPase domain to the zinc-hook (Figure 5C). The probability of forming a coiled coil along the Rad50 amino acid chain was determined using the program COILS (Lupas et al., 1991). The result is graphically displayed in Figure 5D. Interestingly, in addition to the zinc-hook (denoted IV) and the ATPase domain (denoted I), two positions, denoted II and III, were revealed at in which both strands of the coiled coil had a decreased probability of adopting a coiled-coil structure. Positions II and III are located approximately 110 and 70 amino acids from the zinc-hook, respectively. Assuming a rise of 1.5 Å per amino acid residue and taking into account the broadening effect of tip-convolution which is approximately 4 nm, positions II and III mapped to segments 2 and 3 of locally increased flexibility (Figure 5A). Our results suggest that the observed flexibility of the Rad50 coiled coil resides in segments in the which coiled-coil structure is disrupted.

Discussion

Our detailed analysis of SFM images of a wide variety of molecular conformations has resulted in high-resolution data on the local molecular flexibility. Using high-resolution SFM images of the R/M complex we have revealed structural variations in the Rad50 protein that are spaced 12 nm apart. Although other techniques have been used to quantify polymer flexibility, the method presented here is unique in revealing differences in flexibility within a molecule. The *global* persistence length of a single disrupted aminoacid-chain, determined from force-distance measurements, is 2.0 nm (Kellermayer et al., 1997). Quantitatively we observed the measured flexibility of the Rad50 coiled coils to vary from about 0.007 nm⁻¹ for the stiff segments to 0.016 nm⁻¹ for the more flexible segments. Using a correction based on Figure 1E for a tip radius of 5 nm, this corresponds to an apparent persistence length of 17 and 6.0 nm, respectively. This indicates that the flexible segments approach the flexibility of two non-ordered aminoacid chains.

The remarkable architecture of the R/M complex has led to speculation about its mechanism of action. The flexibility map that we obtained for Rad50 highlights the dynamic nature of its structure and also rules out some mechanistic models. Since the

coiled coils are not stiff they cannot simply transmit changes in conformation of the globular domain to changes in relative orientation of the ends of the coiled coil (Strunnikov and Jessberger, 1999). However, the flexibility we observe is a distinct advantage for other proposed mechanisms for R/M function. We have observed tethering of DNA via apparent interactions between the coiled coil ends of multiple DNA bound R/M complexes (de Jager et al., 2001; Chapter 3). The atomic level structure of the end of an archaeal Rad50 coiled coil has revealed a hook-like structure with a conserved CXXC-motif such that two coiled coil ends can dimerize by coordination of Zn^{2+} (Hopfner et al., 2002). Human Rad50 has a similar CXXC-motif and ability to dimerize in the presence of Zn^{2+} (Hopfner et al., 2002). This mode of dimerization requires the two coiled coil ends to assume a specific orientation relative to each other. The multiple R/M complexes bound to DNA do not appear to be in any regular arrangement (de Jager et al., 2001; Chapter 3). The flexibility of the coiled coils that we demonstrate here would allow the hook ends of multiple DNA bound complexes to form correctly oriented inter-molecular Zn^{2+} -fingers independent of the orientation of their DNA bound globular domains.

The sequence similarity among SMC family members defines a common architecture that likely includes flexible coiled coils. Interestingly, a flexible structure would be advantageous for another set of SMC proteins in the recently proposed mechanism of sister chromatin cohesion by the *Saccharomyces cerevisiae* SMC1/3 cohesin complex. The SMC1 and 3 proteins also have intramolecular coiled coils and dimerize via a globular domain at the apex of the coiled coils (Haering et al., 2002). The ATPase domains of SMC1 and 3 can be bridged by a third cohesin subunit to make a large protein ring. Nasmyth and colleagues have proposed that this protein ring could encircle a chromosome before replication, allow a replication fork to pass through and thus form a topological link around the two resulting daughter chromosomes (Haering et al., 2002). The size of the ring is large enough to allow passage of a replication fork and encircle two 10 nm chromatin fibers. A flexible ring would more easily allow closure in the first place and accommodate replication fork passage, which itself has a dynamic and irregular shape. The SMC proteins function in diverse cellular pathways and likely have diverse mechanistic roles. The flexibility we describe here for human Rad50 coiled coils may be a defining structural feature with exceptional mechanistic versatility.

Materials and Methods

DNA samples were prepared for SFM imaging by depositing 1 ng/ μ l 1000 bp DNA (DNA Quantitation Standard Kit, Eurogentech) in 5 mM $MgCl_2$ and 10 mM Hepes-KOH [pH 7.5] onto freshly cleaved mica. The human R/M complex was purified as described previously (de Jager et

al., 2001; Chapter 3)²⁰. For SFM analysis, 20 μ l containing 400 ng of the protein complex in buffer (150 mM KCl, 25 mM Tris-HCl [pH 7.8], and 10% glycerol) was deposited onto freshly cleaved mica. After about 20 s, the mica was washed with MilliQ-filtered water and blown dry in a stream of nitrogen gas. Samples were imaged in air at room temperature and humidity using a NanoScope IIIa (Digital Instruments), operating in tapping mode with a type E scanner. Tapping mode silicon tips OMCL-AC160TS-W2 (Olympus) were used for imaging DNA and SuperSharpSilicon tips, type SSS-NCH-8 (NanoSensors) were used for imaging R/M complexes. Image processing was done using IDL and consisted only of a background correction. The coordinates of the molecular trajectories were traced manually, using a similar routine as described by Rivetti et al. (Rivetti and Codeluppi, 2001). Further data analysis and simulations were also implemented in IDL.

Acknowledgements

This work was supported by grants from the Dutch Cancer Society (KWF) and the Netherlands Organization for Scientific Research (NWO and FOM-ALW).

References

- Anderson, D. E., Trujillo, K. M., Sung, P., and Erickson, H. P.** (2001). Structure of the Rad50 x Mre11 DNA repair complex from *Saccharomyces cerevisiae* by electron microscopy. *J. Biol. Chem.* 276, 37027-37033.
- Bustamante, C., Marko, J. F., Siggia, E. D., and Smith, S.** (1994). Entropic elasticity of lambda-phage DNA. *Science* 265, 1599-1600.
- Bustamante, C., Smith, S. B., Liphardt, J., and Smith, D.** (2000). Single-molecule studies of DNA mechanics. *Curr. Opin. Struct. Biol.* 10, 279-285.
- Cromie, G. A., Connelly, J. C., and Leach, D. R.** (2001). Recombination at double-strand breaks and DNA ends: conserved mechanisms from phage to humans. *Mol. Cell* 8, 1163-1174.
- de Jager, M., van Noort, J., van Gent, D. C., Dekker, C., Kanaar, R., and Wyman, C.** (2001). Human Rad50/Mre11 is a flexible complex that can tether DNA ends. *Mol. Cell* 8, 1129-1135.
- Haering, C. H., Lowe, J., Hochwagen, A., and Nasmyth, K.** (2002). Molecular architecture of SMC proteins and the yeast cohesin complex. *Mol. Cell* 9, 773-788.
- Hirano, T.** (1999). SMC-mediated chromosome mechanics: a conserved scheme from bacteria to vertebrates? *Genes Dev.* 13, 11-19.

- Hopfner, K. P., Craig, L., Moncalian, G., Zinkel, R. A., Usui, T., Owen, B. A., Karcher, A., Henderson, B., Bodmer, J. L., McMurray, C. T., Carney, J.P., Petrini, J.H., and Tainer, J.A.** (2002). The Rad50 zinc-hook is a structure joining Mre11 complexes in DNA recombination and repair. *Nature* *418*, 562-566.
- Hopfner, K. P., Karcher, A., Craig, L., Woo, T. T., Carney, J. P., and Tainer, J. A.** (2001). Structural biochemistry and interaction architecture of the DNA double-strand break repair Mre11 nuclease and Rad50-ATPase. *Cell* *105*, 473-485.
- Hopfner, K. P., Karcher, A., Shin, D. S., Craig, L., Arthur, L. M., Carney, J. P., and Tainer, J. A.** (2000). Structural biology of Rad50 ATPase: ATP-driven conformational control in DNA double-strand break repair and the ABC-ATPase superfamily. *Cell* *101*, 789-800.
- Kellermayer, M. S., Smith, S. B., Granzier, H. L., and Bustamante, C.** (1997). Folding-unfolding transitions in single titin molecules characterized with laser tweezers. *Science* *276*, 1112-1116.
- Lupas, A., Van Dyke, M., and Stock, J.** (1991). Predicting coiled coils from protein sequences. *Science* *252*, 1162-1164.
- Rivetti, C., and Codeluppi, S.** (2001). Accurate length determination of DNA molecules visualized by atomic force microscopy: evidence for a partial B- to A-form transition on mica. *Ultramicroscopy* *87*, 55-66.
- Rivetti, C., Guthold, M., and Bustamante, C.** (1996). Scanning force microscopy of DNA deposited onto mica: equilibration versus kinetic trapping studied by statistical polymer chain analysis. *J. Mol. Biol.* *264*, 919-932.
- Rivetti, C., Walker, C., and Bustamante, C.** (1998). Polymer chain statistics and conformational analysis of DNA molecules with bends or sections of different flexibility. *J. Mol. Biol.* *280*, 41-59.
- Strunnikov, A. V., and Jessberger, R.** (1999). Structural maintenance of chromosomes (SMC) proteins: conserved molecular properties for multiple biological functions. *Eur. J. Biochem.* *263*, 6-13.
- Strunz, T., Oroszlan, K., Schafer, R., and Guntherodt, H. J.** (1999). Dynamic force spectroscopy of single DNA molecules. *Proc. Natl. Acad. Sci. USA* *96*, 11277-11282.
- van Noort, J., Orsini, F., Eker, A., Wyman, C., de Groot, B., and Greve, J.** (1999). DNA bending by photolyase in specific and non-specific complexes studied by atomic force microscopy. *Nucleic Acids Res.* *27*, 3875-3880.
- Wyman, C., and Kanaar, R.** (2002). Chromosome Organization: Reaching out to Embrace New Models. *Curr. Biol.* *12*, R446-448.
- Zuccheri, G., Scipioni, A., Cavaliere, V., Gargiulo, G., De Santis, P., and Samori, B.** (2001). Mapping the intrinsic curvature and flexibility along the DNA chain. *Proc. Natl. Acad. Sci. USA* *98*, 3074-3079.

Chapter

DNA end-binding specificity of human Rad50/Mre11

is influenced by ATP

5

DNA end-binding specificity of human Rad50/Mre11 is influenced by ATP

Martijn de Jager¹, Claire Wyman^{1,2}, Dik C. van Gent¹ and Roland Kanaar^{1,2}

¹Department of Cell Biology & Genetics, Erasmus MC, Dr. Molewaterplein 50, 3000 DR Rotterdam, The Netherlands, and ²Department of Radiation Oncology, Erasmus MC-Daniel, Rotterdam, The Netherlands

Modified from: *Nucleic Acids Research*, 2002, Vol. 30, No. 20, 4425-4431

The Rad50, Mre11 and Nbs1 complex is involved in many essential chromosomal organization processes dealing with DNA ends, including two major pathways of DNA double-strand break repair, homologous recombination and non-homologous end-joining. Previous data on the structure of the human Rad50 and Mre11 (R/M) complex suggest that a common role for the protein complex in these processes is to provide a physical link between DNA ends such that they can be processed in an organized and coordinated manner. Here we describe the DNA binding properties of the R/M complex. The complex bound to both single-stranded and double-stranded DNA. Scanning force microscopy analysis of DNA binding by R/M showed the requirement for an end to form oligomeric R/M complexes, which could then migrate or transfer away from the end. The R/M complex had a lower preference for DNA substrates with 3'-overhangs compared to blunt or 5'-overhangs. Interestingly, ATP binding, but not hydrolysis, by R/M caused an increased preference for DNA substrates with 3'-overhangs relative to substrates with blunt and 5'-overhangs.

Introduction

DNA ends are a common intermediate in genome metabolism (Cromie et al., 2001). Ends are always present at the termini of linear chromosomes in specialized structure known as telomeres. A DNA end also arises during replication, when a replication fork encounters a single-strand gap, or when the fork reverses due to a DNA lesion that blocks its progress. Pairs of ends occur at DNA double-strand breaks (DSBs), which can be caused by endogenous and exogenous DNA damaging agents. DNA ends are also intermediates in genome rearrangements. For example, DSBs are necessary intermediates during meiotic recombination that creates genetic diversity and during specific mitotic recombination events that create diversity in antibody and T-cell receptor genes.

Despite being frequent intermediates, DNA ends are extremely potent inhibitors of normal cellular function. This is the reason for capture of the natural chromosomal ends into T-loop structures, where the DNA end is not exposed but folded back into a structure, resembling a recombination intermediate (de Lange, 2002). Promiscuous recombination of DNA ends causes deleterious chromosomal rearrangements and genomic instability. These events are often the precursors to mutations, uncontrolled cell growth and carcinogenesis. To prevent these catastrophic events it is essential that DNA ends are sequestered or rapidly repaired. Eukaryotic cells primarily utilize two, mechanistically unrelated, pathways to repair DNA ends, non-homologous end-joining (NHEJ) and homologous recombination. Repair through NHEJ

directly joins two DNA ends at regions of very limited or no sequence homology. Because DSB repair through NHEJ is untemplated, it is error prone. This pathway requires a pair of DNA ends and thus can only repair a true DSB. Homologous recombination, on the other hand, uses the information on a homologous template DNA, such as the sister chromatid, to heal DNA ends. Any DNA sequences missing due to possible degradation at an end can be recovered, making this pathway error-free (Kanaar et al., 1998). In addition, single DNA ends, resulting from, for instance, replication of a gapped template, can be repaired by homologous recombination (Rothstein et al., 2000; Cox et al., 2000; Kowalczykowski, 2000; Michel et al., 2001). Although the NHEJ and recombination pathways for DSB repair are mechanistically unrelated they share the requirement to keep the potential repair partner DNA molecules in close proximity.

An evolutionarily conserved protein complex, containing Rad50, Mre11 and Nbs1 (R/M/N), is involved in diverse aspects of genome metabolism that involve DNA end processing (Haber, 1998). The importance of R/M/N is underscored by the fact that all components are essential in mammalian cells (Xiao and Weaver, 1997; Luo et al., 1999; Zhu et al., 2001; Kang et al., 2002). In addition, mutations in the human *MRE11* and *NBS1* genes cause the cancer predisposition syndromes ataxia telangiectasia-like disorder (ATLD) and Nijmegen breakage syndrome (NBS), respectively (Varon et al., 1998; Stewart et al., 1999). Furthermore, hypomorphic mutations in the murine Rad50 and Nbs1 genes also result in cancer predisposition (Bender et al. 2002; Kang et al., 2002; de Jager and Kanaar, 2002; Chapter 7). Apart from direct involvement in DNA end processing, the R/M/N complex has also been implicated in DNA damage-induced cell cycle regulation via Nbs1 (Carney et al., 1998).

Structural studies of R/M and its components have revealed an interesting architecture and provided clues to understanding aspects of its function. Both the *Pyrococcus furiosus* Mre11 and Rad50 globular domains have been crystallized and models for their atomic level structures have been proposed (Hopfner et al., 2000b; Hopfner et al., 2001). The R/M complex contains two Rad50 molecules and two Mre11 molecules. Dimerization of Mre11 presumably contributes to the stability of the R/M complex (Hopfner et al., 2001). Contrary to previous notions, scanning force microscopy (SFM) studies have demonstrated that Rad50 forms an intramolecular coiled coil by folding back onto itself. The R/M complex contains two of these coiled-coil arms, emanating from a globular domain. DNA is bound by the globular domain while the flexible arms protrude away. The complex can tether DNA molecules, presumably through multiple interactions of the protruding flexible arms (de Jager et al., 2001b; Chapter 3). These observations suggest that a common role of the R/M complex in different aspects of chromosome metabolism is to hold DNA molecules in close proximity.

The R/M/N complex and its components display a variety of biochemical activities relevant to DNA end processing. Mre11, by itself and in the complex, has 3' to 5' exonuclease activity on double-stranded (ds) DNA, as well as endonuclease activity

on single-stranded (ss) DNA (Trujillo et al., 1998; Paull and Gellert, 1998). Small regions of DNA homology in the substrate molecules inhibit the nuclease activity (Paull and Gellert, 2000), perhaps in co-ordination with the annealing activity of Mre11 (de Jager et al., 2001a; Chapter 2). The Rad50 amino acid sequence predicts that the N- and C-termini form globular structures with characteristics of Walker-type A and B ATPase domains, respectively. For one Rad50 homolog, these domains have been shown to associate and form a functional ATPase (Hopfner et al., 2000b). However, no influence of ATP on the biochemical activities of human R/M has been detected to date (Paull and Gellert, 1998; Paull and Gellert, 1999). Only for *S. cerevisiae* R/M the presence of ATP does result in additional activity to degrade 3'-overhangs (Trujillo and Sung, 2001). The human complex of R/M including Nbs1 does have activities that are influenced by ATP. In this case, the presence of ATP promotes opening of fully paired DNA hairpins, induces a relatively weak DNA unwinding activity and alters endonuclease specificity (Paull and Gellert, 1999). Crystallography revealed that ATP binding causes a change in the relative orientation of two domains of *P. furiosus* Rad50, which has been suggested to affect DNA binding (Hopfner et al., 2001). We therefore investigated the influence of ATP on the interaction of human R/M with DNA. The complex bound to both ss- and dsDNA and had a preference for binding to DNA substrates containing blunt ends or ends with 5'-overhangs relative to DNA molecules ending in 3'-overhangs. Interestingly, ATP binding, but not hydrolysis, changed the preference for R/M association with the different DNA substrates.

Results

Production and purification of the human Rad50/Mre11 complex

The human R/M complex was purified from Sf21 cells coinfecting with baculoviruses expressing histidine-tagged Rad50 and untagged Mre11. A protein profile of fractions from the purification is shown in Figure 1A. The final fraction (lane 5) was estimated to contain Rad50 and Mre11 in approximately stoichiometric amounts. The identity of the proteins in this fraction was confirmed by immunoblot analysis (Figure 1B) using α -Rad50 and α -Mre11 antibodies (lanes 2 and 4, respectively). Size fractionation showed that the purified Rad50 and Mre11 were present in a complex (Figure 1C). The complex eluted at a position corresponding to a molecular mass of approximately 1.5 MDa, as compared to elution pattern of molecular weight standards in a parallel analysis. Because the complex does not have a globular shape (de Jager et al., 2001b; Chapter 3) its elution profile cannot be used to estimate its molecular mass or the stoichiometry of its components. However, previous biophysical analyses of an archaeal R/M complex

have shown that it consists of a heterotetramer containing two Rad50 and two Mre11 molecules (Hopfner et al., 2001), which would yield a molecular mass of approximately 470 kDa.

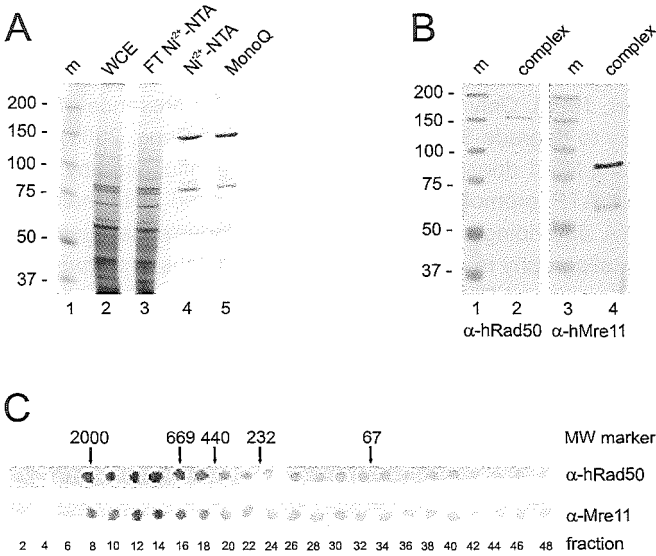


Figure 1. Purification of the human R/M complex. (A) SDS-PAGE analysis of human R/M complex purification, stained with Coomassie Brilliant Blue. Lane 1, m, molecular size markers (molecular mass indicated in kDa); lane 2, WCE, soluble fraction of extracted infected Sf21 cells; lane 3, flow through of a Ni²⁺-NTA column; lane 4, pool of eluted fractions of the Ni²⁺-NTA column; lane 5, R/M preparation eluted from MonoQ column.

(B) Immunoblot analysis of the purified complex. Lanes 1 and 3, m, molecular size markers (molecular mass indicated in kDa); lanes 2 and 4, 500 ng of protein from the MonoQ fractions. Lane 2 was probed with anti-Rad50 antibodies and lane 4 with anti-Mre11 antibodies. (C) Size fractionation analysis of the protein complex. Fractions from a Superose 6 column were analyzed by immuno-spot blotting with anti-Rad50 and anti-Mre11 antibodies as indicated. Positions of molecular size markers relative to eluted fraction numbers are indicated (molecular mass indicated in kDa).

Rad50/Mre11 binds ss- and dsDNA

The R/M complex was tested in DNA binding reactions including either a radiolabeled 160-nt ss- or 160-bp dsDNA fragment (see Materials and Methods). Distinct DNA-protein complexes were formed with both ss- and dsDNA (Figure 2). Binding to ssDNA resulted in at least two complexes that differed in mobility, while binding to dsDNA resulted in at least 3 distinct complexes. Stable complexes formed at lower protein concentrations on ssDNA than on dsDNA (compare lanes 4 and 5 to 9 and 10). Binding to short (50-nt or bp) ss- or dsDNA fragments did not result in the formation of DNA-protein complexes that were stable enough to be detected as discrete bands in gel

mobility shift experiments (data not shown). The presence or absence of divalent cations and/or ATP did not influence R/M binding to DNA as assayed by this method.

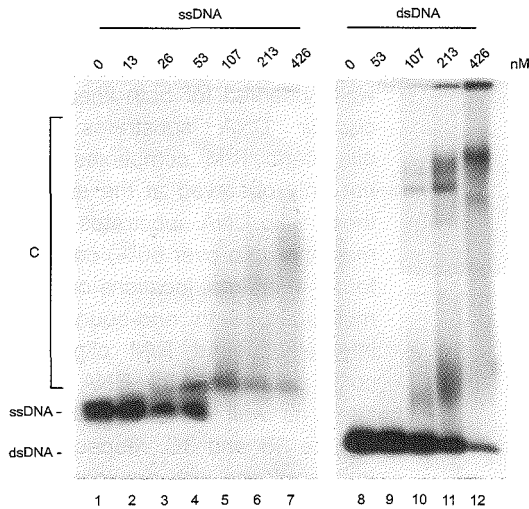


Figure 2. DNA binding by the R/M complex. Radiolabeled 160 nt ssDNA or 160 bp dsDNA fragments were incubated at a concentration of 2.5 nM of DNA fragments with the indicated concentrations of R/M for 20 min at 25°C. Samples were analyzed by agarose gel electrophoresis, followed by autoradiography. Positions of unbound ssDNA, dsDNA and DNA-protein complexes (C) are indicated.

Formation of Rad50/Mre11 oligomers at different DNA end structures

The biochemical activities of the R/M complex that have been described to date differ for various DNA end structures and therefore we investigated the influence of the type of DNA ends on R/M binding. To analyze the DNA binding properties of the human R/M complex in more detail, we used SFM. Protein-DNA complexes can be detected by SFM at much lower, presumably more physiologically relevant, protein to DNA ratios than are needed for gel assays (Wyman et al., 1997; de Jager et al., 2001b; Chapter 3). Furthermore, by directly observing protein-DNA complexes, different architectures can be distinguished. DNA substrates were prepared from the same plasmid DNA digested with restriction endonucleases to produce substrates with either blunt ends or ss-overhangs with either 3' or 5' polarity. As shown in Figure 3A to 3C, different distinct classes of R/M-DNA complexes were observed. The first class consisted of single or small multimeric R/M complexes (with up to 10 coiled-coil arms) bound to the linear DNA via their globular domains (Figure 3A). The second class consisted of much larger oligomeric R/M complexes bound to DNA (Figure 3B and 3C). Previous experiments indicated that a DNA end is required for the formation of oligomeric R/M complexes (de Jager et al., 2001b; Chapter 3). Therefore, we quantitated this behavior of the R/M complex by performing competition experiments with a mixture of linear 5-kb DNA substrates and nicked circular 3-kb DNA substrates (Figure 3D). While 14% of the linear

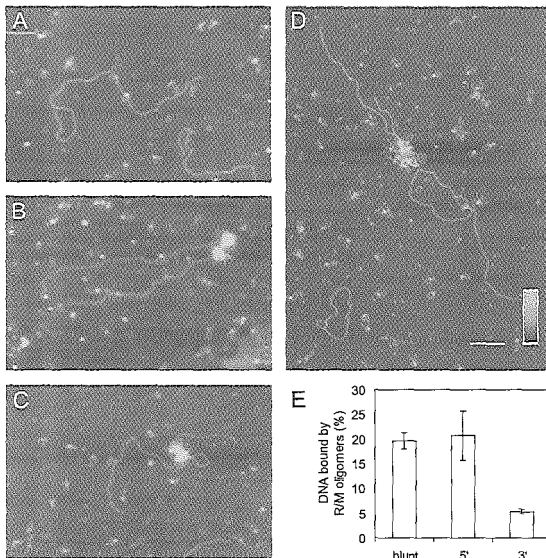


Figure 3. Influence of DNA end structure on R/M binding. Examples of R/M binding to 5 kb linear DNA molecules. DNA molecules were incubated at 3 nM with 56 nM R/M in the absence of ATP. (A) Monomeric R/M protein complexes bound to linear DNA. (B) Binding of oligomeric complexes to linear DNA substrates. In the example shown, oligomeric complexes are located at DNA ends and tether two DNA molecules. (C) An example of internally bound oligomeric complexes, resulting in intramolecular tethering. (D) Scanning force micrograph of a reaction mixture containing 5 kb linear DNA substrates and 3 kb nicked circular DNA substrates at a 1:1 ratio. R/M forms oligomeric complexes only on linear DNA substrates. The scale bar is 200 nm and color represents height from 0 to 1 nm (dark to light) as shown by the key insert. (E) Quantification of R/M binding to different DNA substrates. Blunt-ended DNA or DNA with either 3'- or 5'-overhangs was incubated at ~ 3 nM with 56 nM of R/M in the absence of ATP. Shown is the percentage of DNA molecules bound by R/M oligomeric complexes for different DNA substrates. Error bars indicate SEM of independent triplicate experiments with at least 100 DNA molecules analyzed for each datapoint.

DNA molecules were bound by oligomeric R/M complexes, only 2% of the circular DNA substrates was bound by this form of R/M. In contrast, for monomeric R/M complexes an equal binding efficiency, to approximately 35%, was observed for both linear and circular DNA substrates. The oligomeric R/M complexes were not only observed at the ends of these 5-kb DNA substrates, but a majority (upto over 80%) could be found at internal locations on DNA molecules. Both end-bound and internally bound R/M oligomers could tether distant DNA sites, inter- as well as intramolecularly (Figure 3B and 3C, respectively). In accordance with previous data, tethering of DNA by single or small multimeric R/M complexes was never observed (de Jager et al., 2001b; Chapter 3). The percentage of DNA molecules bound by R/M oligomers was determined for each DNA substrate (Figure 3E). Approximately 20% of the substrate molecules with blunt ends and 5'-overhangs were bound by R/M oligomers. In contrast, only 5% of the DNA substrates with 3'-overhangs were bound by R/M oligomers. Of the DNA molecules bound by R/M oligomers, the relative contribution of end-bound, internally bound and tethered DNA molecules did not differ significantly among the different DNA substrates.

ATP hydrolysis by the Rad50/Mre11 complex

The human Rad50 amino acid sequence, as well as that of other Rad50 homologs, includes an N-terminal Walker A motif and a C-terminal Walker B motif (Walker et al., 1982; Aravind et al., 1999), indicating potential ATPase activity. ATP-dependent DNA binding activities in the absence of the Mre11 subunits have been demonstrated for *S. cerevisiae* Rad50 and the catalytic domains of the *P. furiosus* structural Rad50 homolog (Raymond and Kleckner, 1993; Hopfner et al., 2000a). ATP hydrolysis has only been directly demonstrated for *P. furiosus* Rad50 (Hopfner et al., 2000b). Furthermore, for the structural R/M homolog of *E. coli*, SbcCD, ATP-dependent DNA binding and nuclease activities have been revealed (Connelly et al., 1997). We measured the ATPase activity of the purified human R/M complex by determining the rate of ATP hydrolysis at different substrate concentrations (Figure 4A). The K_m for ATP of the R/M complex was 33 nM and its V_{max} was 222 fmol.min⁻¹. Thus, the R/M complex has a relatively weak ATPase activity with a turnover rate of 0.026 min⁻¹ per complex molecule. The ATPase activity of a number of other proteins involved in DSB repair, such as Rad51 and Rad54, dramatically increases in the presence of ss- and dsDNA, respectively (Benson et al., 1994; Swagemakers et al., 1998). However, the kinetics of the R/M complex ATPase activity did not change dramatically upon addition of either ss- or dsDNA (data not shown).

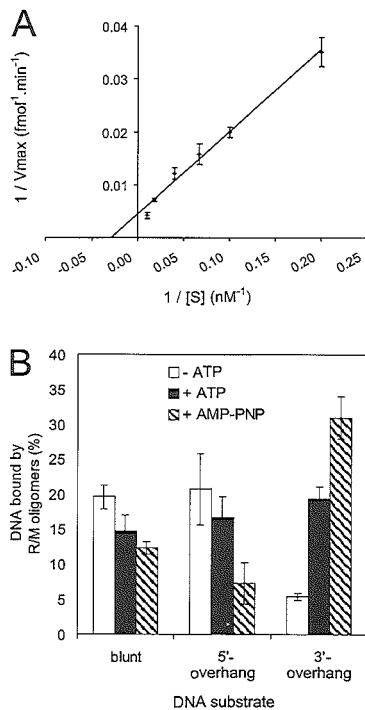


Figure 4. R/M possesses a low ATPase activity that influences the affinity for different DNA ends. (A) Analysis of the ATPase activity of the human R/M complex. The rate of ATP hydrolysis (V) was determined by analysis of the first 20 minutes of the reaction at different ATP concentrations, ($[S]$). Shown is a double reciprocal plot of $1/V$ against $1/[S]$ from which the K_m and V_{max} values were determined. Error bars indicate SEM of independent triplicate experiments. (B) Quantification of R/M affinity for different DNA substrates in the presence of ATP. Blunt-ended DNA or DNA with either 3'- or 5'-overhangs was incubated at 3 nM with 56 nM of R/M in the presence of DNA molecules bound by R/M oligomeric complexes for different substrates either in the absence of ATP (white bars), the presence of ATP (black bars) or the presence of AMP-PNP (hatched bars). Error bars indicate SEM of independent triplicate experiments with at least 100 DNA molecules analyzed for each datapoint.

Influence of ATP on R/M oligomer formation at different DNA end structures

To investigate whether ATP affected DNA binding by R/M, we analyzed binding of R/M to the different DNA substrates in the presence of ATP. The efficiency of formation of large R/M oligomers on the different DNA substrates, in the presence (black bars) and absence of ATP (white bars) is graphically represented in Figure 4B. Binding of DNA substrates containing either blunt ends or 5'-overhangs was slightly reduced in the presence of ATP, while binding to substrates ending in 3'-overhangs was increased significantly. The addition of ATP restored binding to DNA substrates with 3'-overhangs to approximately 20%, just as was observed for DNA substrates with blunt ends and 5'-overhangs in the absence of ATP.

Subsequently, we tested whether ATP hydrolysis was required to influence the formation of R/M oligomers on the different DNA substrates. ATP was replaced with the non-hydrolyzable ATP analog, AMP-PNP, in the DNA binding reactions. As shown in Figure 4B (hatched bars), the presence of AMP-PNP enhanced the effect observed with ATP. The binding to DNA substrates with blunt ends or 5'-ss overhangs was further decreased to about half of the binding in the absence of ATP. In contrast, R/M oligomer formation on 3'-overhangs was increased 1.5-fold compared to binding in the presence of ATP, and 6-fold compared to binding in the absence of ATP.

Discussion

The Rad50/Mre11 complex is essential for many aspects of chromosomal metabolism. Here, we characterized the DNA binding properties of the human R/M complex by SFM. R/M preferentially binds to particular DNA end structures and this preference can be modified by addition of ATP. R/M requires a DNA end to form oligomers which can subsequently migrate or transfer on the DNA.

The crystal structure of *P. furiosus* Mre11 has revealed a likely DNA binding pocket with two manganese ions at the nuclease active site. Modelling of DNA substrates into this pocket suggests that dsDNA substrates need to be deformed to get the phosphodiester backbone of the DNA close enough to the active site metal ions for catalysis to occur. In contrast, the inherently more flexible ssDNA can easily be positioned in close proximity to the metal ions (Hopfner et al., 2001). The analysis of DNA binding by gel retardation experiments showed that R/M binds both to ss- and dsDNA substrates (Figure 2). The geometry of the DNA binding pocket has implications for the specificity of the Mre11 nuclease activity. Mre11 and the R/M complex display a manganese-dependent, 3' to 5' exonuclease activity on DNA substrates with blunt ends or 5'-overhangs, while substrates with 3'-overhangs are not degraded (Paull and Gellert, 1998; Trujillo and Sung, 2001). The results of the experiments we describe here

suggest that the nuclease activity of the R/M complex might be linked to its DNA binding properties. In the absence of ATP, the R/M complex prefers binding to DNA substrates with blunt ends or 5'-overhangs compared to substrates with 3'-overhangs (Figure 3E).

Biochemical experiments have shown that addition of ATP stimulates the degradation of substrates with 3'-overhangs by *S. cerevisiae* R/M complex (Trujillo and Sung, 2001). For the human R/M/N complex, ATP has also been shown to stimulate degradation of DNA substrates with 3'-overhangs (Paull and Gellert, 1999). This ATP-induced effect on Mre11 is likely to be mediated through Rad50, although a direct influence of ATP on the catalytic domain of Mre11 can not be excluded. The crystal structure of *P. furiosus* Rad50 catalytic domains provides some insight into how ATP binding by Rad50 might influence DNA binding by Mre11. The *P. furiosus* Rad50 catalytic domain dimer forms two ATPase sites. The presence of AMP-PNP in the Rad50 crystals induces a 30° rotation of the N-terminal globular domain with respect to the C-terminal globular domain. Furthermore, the crystal structure has revealed that the Rad50 dimer contains a positively charged groove, which could be a potential DNA binding site (Hopfner et al., 2000b). From these observations it has been suggested that the structural change in Rad50 induced by ATP binding could alter the conformation of DNA bound to the R/M complex, thereby influencing the position of the DNA in the Mre11 DNA binding pocket and active site. Alternatively, the structural change in Rad50 could directly modify the conformation of the Mre11 DNA binding pocket. Our results show that the presence of ATP stimulates the binding of the R/M complex to DNA substrates with 3'-overhangs, while the binding to substrates with blunt ends and 5'-overhangs decreases slightly. A similar, but more pronounced, effect is observed in the presence of AMP-PNP (Figure 4B). Because AMP-PNP can not be hydrolyzed to ADP, the presence of AMP-PNP results in a R/M complex that is presumably continuously in its 'ATP-bound' conformation, which apparently has the most dramatic effect on preference for binding to different ends. These data show that the ATP-binding by Rad50 affects the DNA binding specificity of the complex and could therefore, by extension, influence the nuclease activities of Mre11.

In addition to ATP influencing human R/M end-binding preference (Figure 4B), DNA ends themselves influence the interaction among R/M complexes. Human R/M binds both to circular and linear DNA molecules (de Jager et al., 2001b; Chapter 3). However, R/M forms larger oligomeric complexes on linear DNA molecules and not on circular DNA molecules (Figure 3D). Interestingly, although R/M requires a DNA end to oligomerize, the position of the R/M oligomers is not restricted to the DNA end of the 5-kb DNA molecules used in our study (Figure 3B to 3D). The R/M complexes formed on circular and linear DNA are functionally different; the smaller R/M complexes found on circular DNA do not interact with each other even if they are present on the same DNA molecule. In contrast, tethering of different DNA molecules via interactions of larger R/M oligomers, most likely through the coiled-coil arms, is observed for approximately 30% of linear DNA molecules bound by R/M oligomers (Figure 3B). We also observe intramolecular DNA tethering via two R/M oligomers bound at internal positions on a

DNA molecule (Figure 3C). R/M oligomers observed at internal positions on linear DNA are possibly a consequence of migration or transfer of the complex along the DNA after end binding, since in direct competition experiments large R/M oligomers are almost never observed on circular DNA (Figure 3D; de Jager et al., 2001b; Chapter 3).

Interestingly, a similar mode of DNA binding with respect to DNA ends and inward migration, is observed for another end-binding protein complex, the Ku70/Ku86 heterodimer. The ring structure of Ku70/Ku86 requires the complex to initially interact with a DNA end, after which it can migrate along the DNA (Paillard and Strauss, 1991; Walker et al., 2001). *In vitro* and *in vivo* experiments have demonstrated that the R/M and the Ku70/86 protein complexes are involved in DNA end metabolism. They are key components of DSB repair pathways, but are also implicated in V(D)J recombination and telomere length maintenance (Haber, 1998; Featherstone, 1999 #93; Casellas et al., 1998; Manis et al., 1998; Hsu et al., 1999; Zhu et al., 2000; Chen et al., 2000 Nbs at VDJ). Based on their structures, the R/M complex and the Ku70/86 heterodimer have been proposed to recognize and structurally organize DNA ends (de Jager et al., 2001b; Chapter 3; Walker et al., 2001; Jones et al., 2001; Hopfner et al., 2002). The inward migration or transfer of the R/M and Ku70/86 complexes is probably a key aspect of their function because it allows a molecular hand-off between proteins required for structural organization of DNA ends and end-processing factors. Due to chromatin structure or other interacting factors, the inward migration is likely to be limited, which has two advantages. It will allow access of factors with specific functions, such as (further) nucleolytic processing, nucleotide addition, or strand ligation, to the very DNA ends, while it still enables protein complexes such as R/M to function in proximity of the DNA ends to keep them organized.

Materials and Methods

Protein expression and purification

Human R/M was produced by co-infection of Sf21 cells with baculoviruses expressing C-terminally 6-histidine tagged human Rad50 and untagged human Mre11 (generous gifts of T. Paull and M. Gellert) at a multiplicity of infection of approximately 8 and 5, respectively. Cells were harvested after 72 hours. The purification was performed as described previously (de Jager et al., 2001a; Chapter 2). Equilibrium density centrifugation experiments with the truncated versions of the archaeal structural homologs of Rad50 and Mre11 have shown that this complex is a heterotetramer (R_2/M_2 ; Hopfner et al., 2001). Therefore, we assumed a molecular mass of 470 kDa for the human R/M complex. The functionality of the R/M preparation was confirmed by testing the nuclease activity (Paull and Gellert, 1998). As described previously for human Mre11 by itself, the

R/M complex was also able to stimulate annealing of complementary oligonucleotides although at a reduced frequency (de Jager et al., 2001a; Chapter 2; data not shown).

Antibodies

The α -hRad50 antibodies (affinity purified, # 551), used for immunoblotting were a generous gift of C. Heyting. The α -hMre11 antibodies (serum, # 2244) used for immunoblotting were generated as described previously (de Jager et al., 2001a; Chapter 2).

Size fractionation

Fifty μ g of purified R/M was loaded on a Superose 6 PC 3.2/30 size fractionation column (Amersham Biosciences). Protein buffer (150 mM KCl, 25 mM Tris-HCl, (pH 7.8) and 10% glycerol) was used for equilibration and fractionation. Fifty- μ l fractions were collected, of which 10 μ l was analyzed by immuno-spotblotting with α -Rad50 and α -Mre11 antibodies.

DNA substrates

The 160 basepair (bp) dsDNA fragment used in gel retardation experiments was obtained by a PCR reaction with M13 ssDNA as a template, using 22 nucleotide (nt) primers that hybridized to positions 6425 and 6584. The 160-nt ssDNA fragment used in gel retardation experiments was obtained by a PCR reaction as described above with one biotinylated primer. After the PCR reaction, DNA was bound to magnetic streptavidin beads (Dyna) following manufacturers protocols. The non-biotinylated DNA strand was eluted by incubating the DNA-bound beads in 0.1 M NaOH for 3 min. The ssDNA containing supernatant was removed and neutralized with an equal volume of 0.1 M HCl. Both the ss- and dsDNA fragments were subsequently purified using a Qiaquick PCR purification kit (Qiagen).

The DNA substrates used for SFM were produced by digestion of pcDNA3.1(+) (Invitrogen). A 5.4-kb blunt-ended fragment was created by *Stu*I (New England Biolabs) digestion, after which the DNA was phenol extracted. To create a 4.8-kb fragment with non-complementary 4-nt and 3-nt 3'-overhangs, plasmid DNA was digested with *Kpn*I and *Dra*III (NEB), respectively. To create a 4.5-kb fragment with non-complementary 4-nt 5'-overhangs, plasmid DNA was digested with *Bgl*III and *Xho*I (NEB). After double-digestions, DNA fragments were separated by electrophoresis and the desired fragments were isolated from the gel with the use of a Qiaquick gel extraction kit (Qiagen). A singly-nicked circular 3-kb DNA substrate was generated by DNaseI treatment of pBlueScript (Stratagene) as described (Ristic et al., 2001).

Gel retardation experiments

Binding of R/M to DNA was analyzed using gel mobility shift assays as described (de Jager et al., 2001a; Chapter 2). Briefly, a 32 P end-labeled 160 nt or bp DNA fragment was incubated at 2.5 nM

with R/M at the indicated concentrations in binding buffer (50 mM Hepes-KOH pH 8.0, 10 mM Tris-HCl, 100 mM KCl, 4.2% glycerol and 0.5 mg/ml BSA). Binding reactions were separated on a 0.3 % agarose gel in $0.5 \times$ TBE.

ATPase assays

To assay ATPase activity, radiolabeled γ - ^{32}P ATP at 5 nM, supplemented with non-labeled ATP to indicated concentrations, was incubated with 825 nM R/M in 100 mM KCl, 10 mM Tris-HCl (pH 7.8), 4 % glycerol, 10 mM Hepes-KOH (pH 8.0), 5 mM MgCl_2 , 0.2 mg/ml BSA for 0, 5, 10 and 20 min at 30 °C. Reactions were terminated by the addition of EDTA to 167 mM. Samples were analyzed by thin layer chromatography (Merck TLC plates), run in 0.75 M KH_2PO_4 (pH 4.5) and subsequently quantified by phospho-imaging.

The maximal rate of R/M-mediated ATP hydrolysis was determined from a plot of the hydrolysis rates, V , during the first 20 min of the reaction at different substrate concentrations, $[S]$. These data are plotted in a double reciprocal plot (Figure 4A).

Scanning force microscopy

DNA-protein complexes for SFM were formed in 20- μl reactions as described for the gel mobility shift experiments, with the exception of the inclusion of 2 mM MgCl_2 and the omission of BSA. ATP, when present, was at a concentration of 2 mM. DNA and protein concentrations were as described in the figure legend. Reactions were diluted 10-fold in deposition buffer (10 mM Hepes-KOH pH 7.5 and 10 mM MgCl_2) and deposited on freshly cleaved mica. After approximately 1 min the mica was washed with water (glass distilled, SIGMA) and exposed to a stream of filtered air. Samples were imaged in air at room temperature and humidity, using a NanoScope IIIa (Digital Instruments), operating in tapping mode with a type E scanner. Silicon tips (Nanoprobes) were from Digital Instruments or Nanofactory.

The binding of the R/M complex to DNA was quantified by counting different types of R/M complex bound to the different DNA substrates. Specifically, monomeric R/M complexes or small multimers with less than ten protein arms were distinguished from oligomeric complexes. The protein-DNA complexes were further categorized according to whether they were located at the end or internally on the DNA molecule, or whether they tethered multiple DNA molecules.

Acknowledgements

We thank K.P. Hopfner and M. Modesti for helpful discussions. This work was supported by grants from the Dutch Cancer Society (KWF) and the section Chemical Sciences (CW) of the Netherlands Organization for Scientific Research (NWO).

References

- Aravind, L., Walker, D. R., and Koonin, E. V.** (1999). Conserved domains in DNA repair proteins and evolution of repair systems. *Nucleic Acids Res.* *27*, 1223-1242.
- Bender, C. F., Sikes, M. L., Sullivan, R., Huye, L. E., Le Beau, M. M., Roth, D. B., Mirzoeva, O. K., Oltz, E. M., and Petrini, J. H.** (2002). Cancer predisposition and hematopoietic failure in Rad50^{S/S} mice. *Genes Dev.* *16*, 2237-2251.
- Benson, F. E., Stasiak, A., and West, S. C.** (1994). Purification and characterization of the human Rad51 protein, an analogue of *E. coli* RecA. *EMBO J.* *13*, 5764-5771.
- Carney, J. P., Maser, R. S., Olivares, H., Davis, E. M., Le Beau, M., Yates, J. R., Hays, L., Morgan, W. F., and Petrini, J. H.** (1998). The hMre11/hRad50 protein complex and Nijmegen breakage syndrome: linkage of double-strand break repair to the cellular DNA damage response. *Cell* *93*, 477-486.
- Casellas, R., Nussenzweig, A., Wuerffel, R., Pelanda, R., Reichlin, A., Suh, H., Qin, X. F., Besmer, E., Kenter, A., Rajewsky, K., and Nussenzweig, M. C.** (1998). Ku80 is required for immunoglobulin isotype switching. *EMBO J.* *17*, 2404-2411.
- Chen, H. T., Bhandoola, A., Difilippantonio, M. J., Zhu, J., Brown, M. J., Tai, X., Rogakou, E. P., Brotz, T. M., Bonner, W. M., Ried, T., and Nussenzweig, A.** (2000). Response to RAG-mediated VDJ cleavage by NBS1 and gamma-H2AX. *Science* *290*, 1962-1965.
- Connelly, J. C., de Leau, E. S., Okely, E. A., and Leach, D. R.** (1997). Overexpression, purification, and characterization of the SbcCD protein from *Escherichia coli*. *J. Biol. Chem.* *272*, 19819-19826.
- Cox, M. M., Goodman, M. F., Kreuzer, K. N., Sherratt, D. J., Sandler, S. J., and Marians, K. J.** (2000). The importance of repairing stalled replication forks. *Nature* *404*, 37-41.
- Cromie, G. A., Connelly, J. C., and Leach, D. R.** (2001). Recombination at double-strand breaks and DNA ends: conserved mechanisms from phage to humans. *Mol. Cell* *8*, 1163-1174.
- de Jager, M., Dronkert, M. L., Modesti, M., Beerens, C. E., Kanaar, R., and van Gent, D. C.** (2001a). DNA-binding and strand-annealing activities of human Mre11: implications for its roles in DNA double-strand break repair pathways. *Nucleic Acids Res.* *29*, 1317-1325.
- de Jager, M., van Noort, J., van Gent, D. C., Dekker, C., Kanaar, R., and Wyman, C.** (2001b). Human Rad50/Mre11 is a flexible complex that can tether DNA ends. *Mol. Cell* *8*, 1129-1135.
- de Jager, M. and Kanaar, R.** (2002). Genome instability and Rad50^S: subtle yet severe. *Genes Dev.* *16*, 2173-2178.
- de Lange, T.** (2002). Protection of mammalian telomeres. *Oncogene* *21*, 532-540.
- Haber, J. E.** (1998). The many interfaces of Mre11. *Cell* *95*, 583-586.
- Hopfner, K. P., Karcher, A., Craig, L., Woo, T. T., Carney, J. P., and Tainer, J. A.** (2001). Structural biochemistry and interaction architecture of the DNA double-strand break repair Mre11 nuclease and Rad50-ATPase. *Cell* *105*, 473-485.

- Hopfner, K. P., Karcher, A., Shin, D., Fairley, C., Tainer, J. A., and Carney, J. P.** (2000a). Mre11 and Rad50 from *Pyrococcus furiosus*: cloning and biochemical characterization reveal an evolutionarily conserved multiprotein machine. *J. Bacteriol.* *182*, 6036-6041.
- Hopfner, K. P., Karcher, A., Shin, D. S., Craig, L., Arthur, L. M., Carney, J. P., and Tainer, J. A.** (2000b). Structural biology of Rad50 ATPase: ATP-driven conformational control in DNA double-strand break repair and the ABC-ATPase superfamily. *Cell* *101*, 789-800.
- Hopfner, K. P., Putnam, C. D., and Tainer, J. A.** (2002). DNA double-strand break repair from head to tail. *Curr. Opin. Struct. Biol.* *12*, 115-122.
- Hsu, H. L., Gilley, D., Blackburn, E. H., and Chen, D. J.** (1999). Ku is associated with the telomere in mammals. *Proc. Natl. Acad. Sci. USA* *96*, 12454-12458.
- Jones, J. M., Gellert, M., and Yang, W. (2001). A Ku bridge over broken DNA. *Structure* *9*, 881-884.
- Kanaar, R., Hoeijmakers, J. H., and van Gent, D. C.** (1998). Molecular mechanisms of DNA double strand break repair. *Trends Cell Biol.* *8*, 483-489.
- Kang, J., Bronson, R. T., and Xu, Y.** (2002). Targeted disruption of NBS1 reveals its roles in mouse development and DNA repair. *EMBO J.* *21*, 1447-1455.
- Kowalczykowski, S. C.** (2000). Initiation of genetic recombination and recombination-dependent replication. *Trends Biochem. Sci.* *25*, 156-165.
- Luo, G., Yao, M. S., Bender, C. F., Mills, M., Bladl, A. R., Bradley, A., and Petrini, J. H.** (1999). Disruption of mRad50 causes embryonic stem cell lethality, abnormal embryonic development, and sensitivity to ionizing radiation. *Proc. Natl. Acad. Sci. USA* *96*, 7376-7381.
- Manis, J. P., Gu, Y., Lansford, R., Sonoda, E., Ferrini, R., Davidson, L., Rajewsky, K., and Alt, F. W.** (1998). Ku70 is required for late B cell development and immunoglobulin heavy chain class switching. *J. Exp. Med.* *187*, 2081-2089.
- Michel, B., Flores, M. J., Viguera, E., Grompone, G., Seigneur, M., and Bidnenko, V.** (2001). Rescue of arrested replication forks by homologous recombination. *Proc. Natl. Acad. Sci. USA* *98*, 8181-8188.
- Paillard, S., and Strauss, F.** (1991). Analysis of the mechanism of interaction of simian Ku protein with DNA. *Nucleic Acids Res.* *19*, 5619-5624.
- Paul, T. T., and Gellert, M.** (1998). The 3' to 5' exonuclease activity of Mre 11 facilitates repair of DNA double-strand breaks. *Mol. Cell* *1*, 969-979.
- Paul, T. T., and Gellert, M.** (1999). Nbs1 potentiates ATP-driven DNA unwinding and endonuclease cleavage by the Mre11/Rad50 complex. *Genes Dev.* *13*, 1276-1288.
- Paul, T. T., and Gellert, M.** (2000). A mechanistic basis for Mre11-directed DNA joining at microhomologies. *Proc. Natl. Acad. Sci. USA* *97*, 6409-6414.
- Raymond, W. E., and Kleckner, N.** (1993). RAD50 protein of *S. cerevisiae* exhibits ATP-dependent DNA binding. *Nucleic Acids Res.* *21*, 3851-3856.
- Ristic, D., Wyman, C., Paulusma, C., and Kanaar, R.** (2001). The architecture of the human Rad54-DNA complex provides evidence for protein translocation along DNA. *Proc. Natl. Acad. Sci. USA* *98*, 8454-8460.
- Rothstein, R., Michel, B., and Gangloff, S.** (2000). Replication fork pausing and recombination or "gimme a break". *Genes Dev.* *14*, 1-10.

- Stewart, G. S., Maser, R. S., Stankovic, T., Bressan, D. A., Kaplan, M. I., Jaspers, N. G., Raams, A., Byrd, P. J., Petrini, J. H., and Taylor, A. M.** (1999). The DNA double-strand break repair gene hMRE11 is mutated in individuals with an ataxia-telangiectasia-like disorder. *Cell* 99, 577-587.
- Swagemakers, S. M., Essers, J., de Wit, J., Hoeijmakers, J. H., and Kanaar, R.** (1998). The human RAD54 recombinational DNA repair protein is a double-stranded DNA-dependent ATPase. *J. Biol. Chem.* 273, 28292-28297.
- Trujillo, K. M., and Sung, P.** (2001). DNA structure-specific nuclease activities in the *Saccharomyces cerevisiae* Rad50.Mre11 complex. *J. Biol. Chem.* 276, 35458-35464.
- Trujillo, K. M., Yuan, S. S., Lee, E. Y., and Sung, P.** (1998). Nuclease activities in a complex of human recombination and DNA repair factors Rad50, Mre11, and p95. *J. Biol. Chem.* 273, 21447-21450.
- Varon, R., Vissinga, C., Platzer, M., Cersaletti, K. M., Chrzanowska, K. H., Saar, K., Beckmann, G., Seemanova, E., Cooper, P. R., Nowak, N. J., Stumm, M., Weemaes, C. M., Gatti, R. A., Wilson, R. K., Digweed, M., Rosenthal, A., Sperling, K., Concannon, P., and Reis, A.** (1998). Nibrin, a novel DNA double-strand break repair protein, is mutated in Nijmegen breakage syndrome. *Cell* 93, 467-476.
- Walker, J. E., Saraste, M., Runswick, M. J., and Gay, N. J.** (1982). Distantly related sequences in the alpha- and beta-subunits of ATP synthase, myosin, kinases and other ATP-requiring enzymes and a common nucleotide binding fold. *EMBO J.* 1, 945-951.
- Walker, J. R., Corpina, R. A., and Goldberg, J.** (2001). Structure of the Ku heterodimer bound to DNA and its implications for double-strand break repair. *Nature* 412, 607-614.
- Wyman, C., Rombel, I., North, A. K., Bustamante, C., and Kustu, S.** (1997). Unusual oligomerization required for activity of NtrC, a bacterial enhancer-binding protein. *Science* 275, 1658-1661.
- Xiao, Y., and Weaver, D. T.** (1997). Conditional gene targeted deletion by Cre recombinase demonstrates the requirement for the double-strand break repair Mre11 protein in murine embryonic stem cells. *Nucleic Acids Res.* 25, 2985-2991.
- Zhu, J., Petersen, S., Tessarollo, L., and Nussenzweig, A.** (2001). Targeted disruption of the Nijmegen breakage syndrome gene NBS1 leads to early embryonic lethality in mice. *Curr. Biol.* 11, 105-109.
- Zhu, X. D., Kuster, B., Mann, M., Petrini, J. H., and Lange, T.** (2000). Cell-cycle-regulated association of RAD50/MRE11/NBS1 with TRF2 and human telomeres. *Nat Genet.* 25, 347-352.

Chapter

SMC family members: functional diversity

through differential arrangements of

conserved building blocks

6

SMC family members: functional diversity through differential arrangements of conserved building blocks

Martijn de Jager¹, Claire Wyman^{1,2}, John van Noort³, Thijn van der Heijden³, Cees Dekker³, and Roland Kanaar^{1,2}

¹Department of Cell Biology & Genetics, Erasmus MC, Dr. Molewaterplein 50, 3000 DR Rotterdam, The Netherlands, and ²Department of Radiation Oncology, Erasmus MC-Daniel, Rotterdam, The Netherlands, and ³Delft University of Technology, Department of Applied Physics and DIMES, Lorentzweg 1, 2628 CJ Delft, The Netherlands

Structural maintenance of chromosomes (SMC) proteins are classified as a family based on the predicted similarity of their structure. They are all proposed to have structural functions in DNA metabolism. Here, we describe a structural analysis of different SMC family members by scanning force microscopy. We show that, although SMC proteins are composed of structural similar components, the different arrangement of these components results in variety of complex architectures. We discuss how these structural differences can account for functional diversity of SMC family members in DNA metabolism.

Introduction

Within the limited volume in the cell nucleus an enormous amount of DNA is present to encode the essential information that is required for cellular function. Therefore, it is not surprising that mechanisms evolved that organize the genome to guide it through complex processes. Key players in these mechanisms are the structural maintenance of chromosome (SMC) proteins. The first SMC proteins were identified as essential components during the replication process (reviewed in Strunnikov and Jessberger, 1999; Hirano, 2002). After replication, the resulting sister chromatids are linked by cohesin, a multiprotein complex containing the SMC1 and SMC3 heterodimer, to prevent them from drifting apart before cell division and to assure proper segregation. The condensin complex, containing the SMC2 and SMC4 heterodimer, is essential for chromosome condensation before cell division.

The SMC proteins share structural properties that can be predicted from their amino acid sequences. The amino (N) – and carboxy (C) – termini are predicted to contain Walker A- and Walker B-type ATPase motifs, respectively. As described for the ABC transporter proteins, the halves of this bipartite ATPase domain can come together to form a functional ATPase (Lowe et al., 2001). The two ATPase domains are separated by an extended region of approximately 900 amino acids that is predicted to adopt a α -helical structure.

Based on sequence similarity that predicts comparable structural components, the SMC family contains additional members, such as the evolutionary conserved Rad50 protein. Rad50 forms a protein complex with the non-SMC component Mre11. The human and *Saccharomyces cerevisiae* Rad50 complexes are implicated in double-strand break repair and other processes of DNA end metabolism (reviewed in Chapter 1). The homologous complex in *Escherichia coli*, SbcCD, is proposed to maintain genomic integrity by removing secondary DNA structures that have arisen during or after DNA replication (reviewed in Leach, 1994). The function of the *Pyrococcus furiosus* Rad50 complex in DNA metabolism is still unknown.

Electron microscopic images of bacterial SMC proteins show that the overall structure of these proteins consists of two globular domains that are separated by an extended structure (Melby et al., 1998). This observation led to a model in which two SMC proteins dimerize to form two active ATPase domains that are separated by an intermolecular coiled coil, composed of two anti-parallel arranged α -helices. However, more recent experiments show that SMC family proteins form intramolecular coiled coils (de Jager et al., 2001; Chapter 3; Haering et al., 2002; Hopfner et al., 2002). Thus, the two halves of the bipartite ATPase domain come together to form a functional ATPase domain at one side of an intramolecular coiled-coil arm. At the other side of this arm the Rad50 homologs contain a CXXC-motif. For the *P. furiosus* Rad50 homolog two coiled coils can dimerize by coordinated binding of a zinc atom (Hopfner et al., 2002). The cohesin complex lacks this CXXC-motif. Instead it contains a globular domain at the apex of the coiled coil, that provides a strong heterodimerization domain (Haering et al., 2002).

To achieve a functional structure, SMC family proteins form complexes with non-SMC accessory proteins. The Rad50 homologs associate with the conserved Mre11 protein. For the *P. furiosus* complex, Mre11 interacts with the Rad50 coiled-coil region, adjacent to the ATPase domain (Hopfner et al., 2001). For the human Rad50 complex this results in an overall structure that consists of a globular domain from which two coiled-coil arms protrude (de Jager et al., 2001; Chapter 3). The SMC1 and SMC3 heterodimer interacts with the non-SMC components Scc1 and Scc3 (Losada et al., 1998). The N- and C- termini of Scc1 interact specifically with the SMC3 and SMC1 ATPase domains, respectively. This interaction has been proposed to result in a ring-like structure (Haering et al., 2002). Likewise, the SMC2 and SMC4 could heterodimerize through the globular domains at the apexes of their coiled coils and form a ring like structure through the interaction with three non-SMC components Cnd1, 2 and 3 (Freeman et al., 2000; Yoshimura et al., 2002).

The differential arrangement of the SMC complex components could result in a variety of conformations. Presumably these conformations are important for the diverse functions of SMC proteins in genome maintenance. In this study we use scanning force microscopy (SFM) to directly compare the architecture of a collection of SMC proteins at nanometer resolution. We catalog a variety of conformations and their occurrence in these SMC protein preparations. The results are correlated with what is known about the biological function of SMC proteins.

Results

Sequence comparison of SMC family members

To investigate the structural properties of different SMC family members, we first compared the amino acid sequences of human, *S. cerevisiae*, *P. furiosus* and *E. coli* Rad50 homologs as well as the *S. cerevisiae* SMC1 and SMC3 cohesin complex components. As shown in Figure 1A, a high degree of similarity is observed at the N- and C- termini of the proteins. In all family members these two parts contain the Walker A- and B-type motifs of an ATPase domain, respectively. The sequence in between these two motifs is much less conserved. However, this region of all SMC proteins is predicted to have a high probability of forming a α -helix. The organization in these three parts (Walker A-type motif, α -helical region and Walker B-type motif) is the basis for their classification as members of the SMC family of proteins (Aravind et al., 1999). A CXXC-motif is found half way along the α -helix of different Rad50 homologs. Two coiled-coil arms of the *P. furiosus* homolog can dimerize by intermolecular coordination of a zinc atom by the four cysteine residues (Hopfner et al., 2002). This specific motif is absent in *S. cerevisiae* SMC1 and SMC3. Instead, these proteins contain a larger region with low coiled coil forming probability and limited sequence similarity. This region, often referred to as the 'hinge' region, forms a globular domain that provides a strong interaction interface between SMC1 and SMC3 (Haering et al., 2002).

The N- and C-terminal Walker A- and B-type motifs together form an active ATPase domain. SFM analysis of human Rad50 complex and electron microscopic analysis of *S. cerevisiae* SMC1 and SMC3 complex show that their α -helical regions are folded into an intramolecular coiled-coil conformation (de Jager et al., 2001; Chapter 3; Haering et al., 2002). The crystal structures of the CXXC-motif of *P. furiosus* Rad50 and the interaction domain of the *Thermotoga maritima* SMC1 and SMC3 cohesin complex components confirm that the α -helical regions of these family members are folded to form intramolecular coiled coils as well (Haering et al., 2002; Hopfner et al., 2002). The COILS program (Lupas et al., 1991) was used to determine the probability of the α -helical segment to form a coiled coil. Figure 1B aligns both α -helical segments in an anti-parallel manner and graphically represents the probability of coiled coil formation along the amino acid sequence. In this representation a low probability of coiled coil formation is indicated in black and a high probability is indicated in white. The amino acid chains of the Rad50 homologs are folded at the CXXC-motif, since this motif is located at the apex of the intramolecular coiled coil (Hopfner et al., 2002). As expected, the ATPase domains have a low probability to form a coiled coil. The folding of the SMC1 and SMC3 amino acid chains is based on the crystal structure of the globular domain in between the α -helical regions. From this domain an intramolecular coiled coil

protrudes (Haering et al., 2002). Furthermore, within the coiled-coil regions of the SMC family members small segments with low coiled-coil probability were found. For the human Rad50/Mre11 complex these disruptions correlate with locally increased flexibility of the coiled-coil structure (Chapter 4; van Noort et al., submitted).

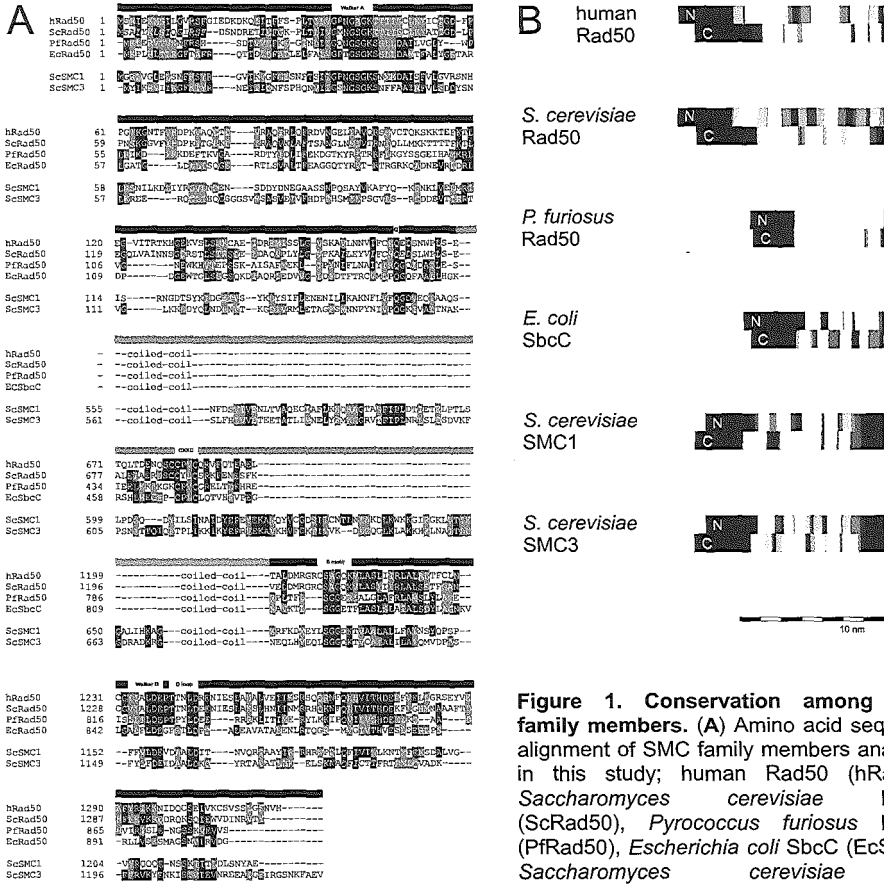


Figure 1. Conservation among SMC family members. (A) Amino acid sequence alignment of SMC family members analyzed in this study; human Rad50 (hRad50), *Saccharomyces cerevisiae* Rad50 (ScRad50), *Pyrococcus furiosus* Rad50 (PfRad50), *Escherichia coli* SbcC (EcSbcC), *Saccharomyces cerevisiae* SMC1 (ScSMC1) and *Saccharomyces*

cerevisiae SMC3 (ScSMC3). Conserved motifs, Walker A-type motif, Q-loop, CXXC-motif, S-motif, Walker B-type motif and D-loop are indicated. Globular domains and coiled-coil region are indicated by black and gray bars, respectively. Identical residues are black, similar residues are gray. **(B)** Probability of coiled coil formation along the amino acid chain for SMC family members is indicated using a gray scale with black and white representing the lowest and highest probability of forming a coiled coil, respectively. The amino acid chain is folded back onto itself to form an intramolecular coiled coil. The human, *S. cerevisiae*, *P. furiosus* and *E. coli* Rad50 homologs are folded back at the position of the CXXC-motif. Folding of *S. cerevisiae* SMC1 and SMC3 is based on the structure of the globular domain located in between the coiled coil forming regions. The amino- and carboxy-termini are indicated by 'N' and 'C', respectively. The predicted length of the coiled-coil region is indicated by the scale bar.

Architecture and structural features of SMC family members

We used SFM to investigate the architectural features of the *S. cerevisiae*, *P. furiosus* and *E. coli* Rad50/Mre11 homologs as well as *S. cerevisiae* SMC1/SMC3. SFM imaging provides three-dimensional structural information with nanometer resolution. The dimensions of the SMC proteins are within this scale of resolution and can thus be accurately imaged. In this study we investigated and compared the arrangement of components with respect to multimerization status and association of coiled coil ends that result in the structural features of these protein complexes.

Representative images obtained from the reconstituted *S. cerevisiae* Rad50/Mre11 protein complex are shown in Figure 2A to 2D. The data are summarized in Figure 6. The most frequently occurring form (71% of all molecules) likely represents a heterotetramer (R_2/M_2), based on analogous observations for the human Rad50/Mre11 complex (de Jager et al., 2001; Chapter 3). It consisted of a large globular domain, containing the Rad50 ATPase domains and Mre11, from which two coiled-coil arms protruded. The coiled-coil arms were either in open or closed conformation (Figure 2A and 2B; 43% and 28%, respectively), which could be a result of interactions between the CXXC-motifs of the two arms. In addition, as observed for the human complex, multimers containing two to ten heterotetrameric Rad50/Mre11 complexes ($[R_2/M_2]_n$) were observed at low frequency (Figure 2C; 6%; de Jager et al., 2001; Chapter 3). The remaining 23% of molecules interacted through the apices of the coiled-coil arms (Figure 2D). The average overall contour length of coiled-coil arm and globular domain was 45 ± 6 nm.

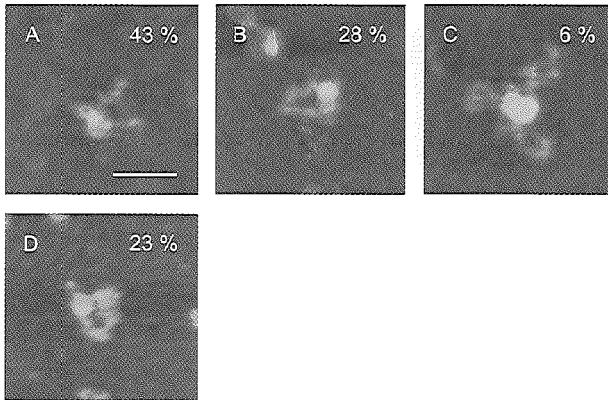


Figure 2. Analysis of the *S. cerevisiae* Rad50/Mre11 protein complex by SFM. (A to D) Representative SFM images of Rad50/Mre11 complexes in different conformations. The percentage of complexes in the different conformations is indicated in each panel (146 molecules were analyzed). The scale bar is 50 nm. Color represents height from 0 to 2 nm, black to white.

Representative images of the *P. furiosus* Rad50/Mre11 complex are shown in Figure 3A to 3F. The architectures observed for this protein were clearly distinct from those observed for *S. cerevisiae* Rad50/Mre11. First, about half (45% of all molecules) of the *P. furiosus* Rad50/Mre11 molecules were heterodimeric (R_1/M_1) with a large globular domain, presumably consisting of the Rad50 ATPase domain and Mre11, from

which one Rad50 coiled-coil arm protruded (Figure 3A). These heterodimers could interact to form heterotetramers (R_2/M_2) with two globular domains and two arms. Unlike the *S. cerevisiae* and human Rad50/Mre11 complex (see Figure 2; de Jager et al., 2001; Chapter 3), the two coiled coils were juxtaposed in most of these heterotetrameric structures (Figure 3B to 3D; 51% of all molecules). However, it is unclear from these images whether the superimposed coiled-coil arms interacted through the CXXC-motif at the apex of the coiled-coil arm. Almost one third of all molecules had closely juxtaposed coiled-coil arms as well as globular domains (Figure 3C to 3E). For 23% of all molecules the arms appeared close together and might be wound around each other (Figure 3C and 3D). Winding of the coiled-coil arms would result in shortening of the coiled-coil arms as appeared to be the case for the molecule in Figure 3D. Seven percent of all molecules interacted through both the coiled-coil arm ends as well as the globular domains and adopted a circular conformation (Figure 3E). The classes of conformations represented by Figure 3B to 3E might not be distinct arrangements, but could represent flexibility of the coiled coils. Only a very small number of molecules interacted exclusively through the globular domains (Figure 3F; 3% of all molecules). The overall contour length of a Rad50/Mre11 heterodimer (R_1/M_1) was 44 ± 3 nm. To get an indication of the flexibility of the coiled-coil arms we determined the overall persistence length, as described in Materials and Methods. The persistence length of the Rad50/Mre11 heterodimer was 58 nm. Figure 6 summarizes the results of this analysis.

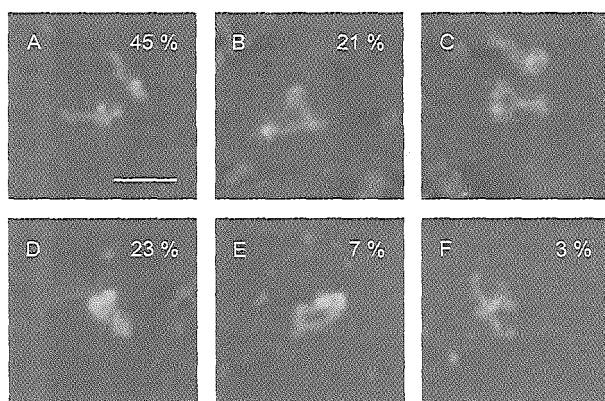


Figure 3. Analysis of the *P. furiosus* Rad50/Mre11 protein complex by SFM. (A to F) Representative SFM images of Rad50/Mre11 complexes in different conformations. The percentage of complexes in the different conformations is indicated in each panel (217 molecules were analyzed). The scale bar is 50 nm. Color represents height from 0 to 2 nm, black to white.

A similar basic organization of complex components was observed for the *E. coli* SbcCD complex (with SbcC and SbcD being homologs of Rad50 and Mre11, respectively; Sharples and Leach, 1995). Twenty-one percent of all complexes were heterodimeric (C_1/D_1 ; Figure 4A). However, the majority of complexes was heterotetrameric (C_2/D_2 ; Figure 4B to 4E; 73% of all molecules). The heterotetrameric

complexes showed a very heterogeneous length that ranged from 24 to 57 nm (compare Figure 4D and 4E). A small number of heterotetrameric molecules appeared to interact through their globular domains, forming a dimer of two heterotetramers ($[C_2/D_2]_2$; Figure 4F; 4% of all molecules). The conformation where both the apexes of the arms and the globular domains interact was never observed. The overall length of a heterodimer was 39 ± 7 nm. In this case the persistence length was 97 nm for the heterotetrameric complex (C_2/D_2). The results of this analysis are summarized in Figure 6.

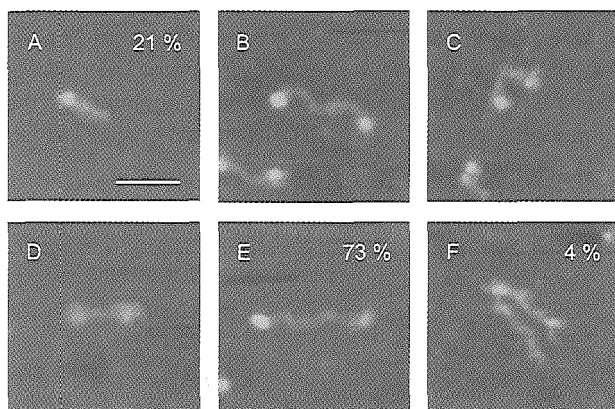


Figure 4. Analysis of the *E. coli* SbcCD protein complex by SFM. (A to F) Representative SFM images of SbcCD complexes in different conformations. The percentage of complexes in the different conformations is indicated in each panel (280 molecules were analyzed). The scale bar is 50 nm. Color represents height from 0 to 2 nm, black to white.

The architecture of the *S. cerevisiae* SMC1/SMC3 complex is different from the Rad50/Mre11 homologs. Electron microscopic images show that SMC1 and SMC3 form a heterodimeric complex ($SMC1_1/SMC3_1$). SMC1 and SMC3 both have a globular ATPase domain and dimerize through globular domains at the end of the intramolecular coiled-coil arms. These findings are supported by crystal structures of both the ATPase domains and the interaction domain (Lowe et al., 2001; Haering et al., 2002). Our SFM images showed similar structures. Figure 5A and 5B show representative images of SMC3 and the SMC1/SMC3 complex, respectively. As indicated in Figure 6, the overall contour length of SMC3 was 33 ± 5 nm.

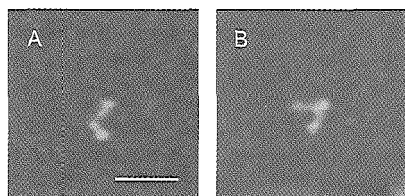


Figure 5. Analysis of the *S. cerevisiae* SMC1/SMC3 protein complex by SFM. (A) Representative SFM image of SMC3. The scale bar is 50 nm. (B) Representative SFM image of the SMC1/SMC3 complex. Color represents height from 0 to 2 nm, black to white.

Discussion

Similar building blocks but different architectures

In this work we describe a comparison of the architectures of the *S. cerevisiae*, *P. furiosus* and *E. coli* Rad50/Mre11 homologs as well as the *S. cerevisiae* SMC1/SMC3 components of the cohesin complex by SFM imaging. The amino acid sequence similarity of these different SMC family members is reflected in the fact that they contain similar structural building blocks. However, the different arrangements of the building blocks results in distinct architectures of these complexes. Figure 6 summarizes the different architectures and conformations that are observed for the analyzed SMC family members.

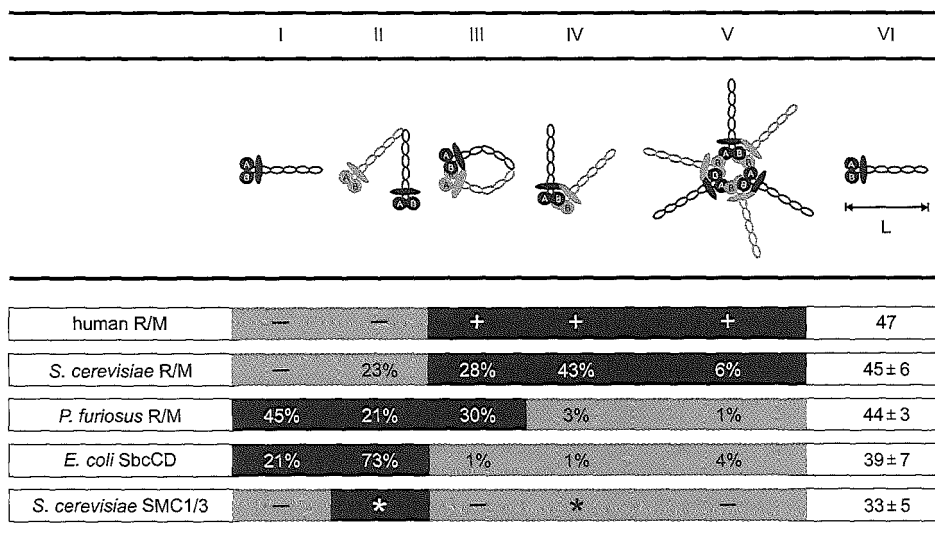


Figure 6. Comparison of conformations of SMC family members. For the SMC family members used in this study and human Rad50/Mre11 complex, the occurrence of different conformations, as could be observed by SFM, is indicated. From left to right: heterodimer (I), heterotetramer interacting through the apices of coiled-coil arms (II), heterotetramer interacting through the globular domains (III), heterotetramer interacting through both the apices of the coiled-coil arms and the globular domains (IV), multimer formed by multiple heterotetramers (V) and average heterodimer contour length [nm] (VI). The Rad50 homolog ATPase domains are indicated by a sphere, Mre11 homolog by an oval. The observed frequency of a conformation in the protein preparation is indicated. Black background indicates the most frequently observed conformations. (*) For the *S. cerevisiae* SMC1/SMC3 complex the difference between class II and III could not be distinguished by our SFM analysis but is based on published data. See text and Materials and Methods for more information.

An important difference in complex architecture is the occurrence of heterodimeric complexes consisting of one Rad50 and one Mre11 homolog. This conformation can only be observed in preparations of the bacterial and archaeal homologs, but not in preparations of the human and *S. cerevisiae* homologs. As discussed below, this might be a consequence of the relative contribution of different interaction interfaces for the different SMC family members. The occurrence of this conformation for *E. coli* SbcC suggests that, like for the other family members, the coiled coil of SbcC is also intramolecular.

Another difference is observed in the mode of heterotetramer formation. Human Rad50/Mre11 heterodimeric complexes always interact through the globular domains to form heterotetramers (R_2/M_2 ; de Jager et al., 2001; Chapter 3). For the *S. cerevisiae* Rad50/Mre11 complexes this is also the predominant type of interaction (Figure 2). For both homologs this mode of interaction results in complexes with a large globular domain from which two arms protrude. The tips of the coiled-coil arms can touch, resulting in a circular conformation (Figure 2A and 2B). However, an interaction through the tips of the coiled-coil arms only is never observed for the human complex. This mode of interaction can be observed at a frequency of 23% for the *S. cerevisiae* Rad50/Mre11 complex (Figure 2D). This difference may reflect the reconstituted nature of the latter protein preparation. Our data show that for these homologs the interaction through the globular domains is predominant under the used conditions.

In contrast, archaeal Rad50/Mre11 heterodimers interact mainly through the tips of the coiled-coil regions to form heterotetramers (R_2/M_2 ; Figure 3). The heterodimers of the *P. furiosus* complex can interact through the tips of the coiled-coil region and the globular domains simultaneously (Figure 3C and 3D). This can result in a conformation where both arms lie closely together side-by-side (Figure 3C and 3D) or a circular conformation (Figure 3E). An interaction through the globular domains only is rare (Figure 3F), arguing that the major interaction interface is located at the tips of the coiled-coil arms. This observation fits with the demonstration that the apex of the coiled-coil region contains a CXXC-motif (Figure 1) that functions as half of a zinc finger. For the *P. furiosus* Rad50 homolog two CXXC-motifs can provide an interaction interface between two heterodimers through the intermolecular coordination of a zinc atom (Hopfner et al., 2002). The interaction of *E. coli* SbcCD heterodimers to form heterotetramers (C_2/D_2) appears to occur exclusively through the tips of the coiled-coil arms (Figure 4B to 4E). In analogy with the *P. furiosus* homolog this interaction is likely to occur through the CXXC-motif. Interestingly, a simultaneous interaction through the tips of the coiled-coil region and globular domains is never observed. A possible explanation for this finding could be that the *E. coli* SbcCD coiled coils are less flexible. This is consistent with the large persistence length (97 nm) of the *E. coli* SbcCD complex, compared to the human and *P. furiosus* complexes (30 nm and 58 nm, respectively). For both the *E. coli* and *P. furiosus* complexes the persistence length is larger than the contour length, which indicates that the arms are almost never bend. In addition, the interacting CXXC-motifs orient the coiled coils in opposing directions

(Hopfner et al., 2002). This might result in a kink of the coiled-coil arms as shown in Figure 4B. The combination of these features might thus prevent the interaction of the globular domains. These results show that for the prokaryotic Rad50/Mre11 homologs the interaction through the CXXC-motifs is predominant at least under our experimental conditions.

For the *S. cerevisiae* SMC1/SMC3 complex, the SFM images do not distinguish between interactions through the globular ATPase domain or the globular domain at the end of the coiled-coil region as these globular domains have a similar size. However, these components interact exclusively through globular domains at the apexes of the coiled-coil regions (Haering et al., 2002).

Another major difference is observed for the interaction between heterotetrameric complexes. Both the human and *S. cerevisiae* Rad50/Mre11 complexes form larger multimers with up to 10 heterotetrameric complexes ($[(R_2/M_2)_n]$; Figure 2C; de Jager et al., 2001; Chapter 3). This type of complex might be a precursor of the large oligomers that form on DNA, as observed for the human Rad50/Mre11 complex (de Jager et al., 2001; Chapter 3; de Jager et al., 2002; Chapter 5). This arrangement in oligomers has not been observed for the other SMC family members. The heterotetramers of *E. coli* SbcCD do occasionally interact to form a larger complex (Figure 4F). However, in the absence of experiments that examine the interaction of SbcCD with DNA, the functional relevance of these SbcCD oligomers is unclear.

The source of different architectures

One intriguing question is how it is possible that these family members show these dramatic differences in architecture, even though their sequences are conserved. Based on their structures, the Rad50/Mre11 homologs can be divided in two classes. In the first class (human and *S. cerevisiae*), the complexes exist as heterotetramers of which the heterodimeric components interact almost exclusively through the globular domains. In this class of complexes free heterodimers are absent. In the second class (*P. furiosus* and *E. coli*), separate heterodimers are frequently present. The heterodimers interact mainly through the tips of the coiled-coil regions. One difference between the sequences of these two classes can be found in the CXXC-motif at the tip of the coiled-coil arm. While the *P. furiosus* and *E. coli* homologs have this basic motif, in both the human and *S. cerevisiae* sequences an additional cysteine is present, resulting in a $C_1C_2XXC_3$ -motif. In addition, the interaction between Mre11 molecules might influence the complex conformation. The Mre11 homolog, present in each heterodimer, can dimerize and could stabilize the heterotetramer by doing so (Johzuka and Ogawa, 1995; Paull and Gellert, 1998; Hopfner et al., 2001). An interesting observation in this light is that in a preparation of *S. cerevisiae* Rad50 without Mre11, the predominant conformation is the monomer (79%; data not shown). However, in the presence of Mre11 heterodimers cannot be observed. In contrast, in the *P. furiosus* and *E. coli* Rad50/Mre11 preparations heterodimers do exist (45% and 21%, respectively) and do

almost not interact through the globular domains that contain Mre11 and SbcD, respectively. Taken together, a weak interaction through the CXXC-motif could coincide with a strong interaction through the Mre11 homolog and *visa versa*, thus determining the conformation of the complex.

From the amino acid sequences of the *S. cerevisiae* SMC1 and SMC3 can be predicted that the apexes of the coiled-coil arms form a larger structure. The crystal structures of bacterial SMC1 and SMC3 homologs show that these structures fold into globular domains that interact strongly. The ATPase domain of SMC1 and SMC3 interact separately with different domains of Scc1 (Haering et al., 2002).

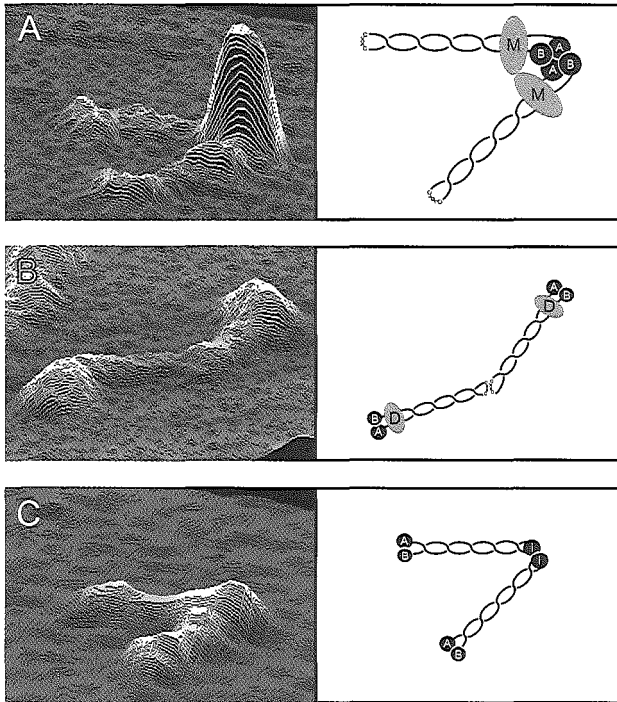


Figure 7. Functional diversity through differential arrangements of conserved building blocks in three classes of SMC proteins. SFM images of human Rad50/Mre11 (A), *E. coli* SbcCD (B) and *S. cerevisiae* SMC1/SMC3 (C) are presented in a tilted view to stress their structural similarities and architectural differences. Schematic representations of models for the arrangements of the complex components are depicted besides the images. Walker A- and B-type motifs of Rad50, SbcC and SMC1 and SMC3 are represented by 'A' and 'B', respectively. 'M' and 'D' indicate Mre11 and SbcD, respectively. CXXC-motifs and SMC1 and SMC3 interaction domains ('i') are indicated.

Complex architecture and DNA binding properties

In all Rad50/Mre11 homologs Mre11 possesses DNA binding and nuclease activities (Sharples and Leach, 1995; Paull and Gellert, 1998; Usui et al., 1998; Hopfner et al., 2000). The Mre11 interaction domain on Rad50 is located on the coiled-coil region of Rad50, adjacent to its ATPase domains (Hopfner et al., 2001). The activities of Mre11 in the human, *S. cerevisiae* and *P. furiosus* Rad50/Mre11 complexes might be altered by an ATP-induced structural switch in Rad50 (Trujillo and Sung, 2001; Hopfner et al.,

2001; de Jager et al., 2002; Chapter 5). Therefore, it is likely that the Rad50/Mre11 homologs will interact with DNA through their Mre11-containing globular domains. Since the architecture of the eukaryotic and prokaryotic complexes is different, this can also be expected to be reflected in their DNA binding properties and, by extension, biological functions. The human Rad50/Mre11 complex is involved in DNA end processing pathways such as homologous recombination, DNA end-joining and telomere length maintenance (reviewed in Chapter 1). The complex binds to DNA through its globular domain with the arms protruding away from the DNA. Large multimers of the complex can tether DNA molecules through multiple, presumably flexible interactions (de Jager et al., 2001; Chapter 3). These observations could explain the biological function of the complex in DNA end metabolism. The *S. cerevisiae* Rad50/Mre11 complex has a very similar architecture and is a functional homolog of the human complex.

The *P. furiosus* Rad50/Mre11 homolog also binds DNA through the globular domains (Hopfner et al., 2001). However, for both the *P. furiosus* and *E. coli* Rad50/Mre11 homologs a function in DNA end metabolism has not been described so far. Furthermore, the prokaryotic complex architectures show essential differences from eukaryotic complexes. Therefore, these complexes might not be functional, but only structural Rad50/Mre11 homologs. The *E. coli* SbcCD complex has been implicated in cleavage of hairpin structures that can arise during replication (Connelly and Leach, 1996; Connelly et al., 1998; Connelly et al., 1999). Likely, the complex architecture with two independent DNA binding sites evolved to be optimal for its specific functions.

The *S. cerevisiae* SMC1/SMC3 components of cohesin do not contain DNA binding sites. A third complex component, Scc1, binds specifically to the ATPase domains of both SMC1 and SMC3, thus forming a proteinaceous circle. It has been hypothesized that this circle embraces a chromatid before replication. After passage of the replication machinery the cohesin complex would embrace the two resulting sister chromatids (Haering et al., 2002). The diameter of the circle (approximately 40 nm) is large enough to allow passage of the replication fork. The flexibility that is required to allow passage of an irregular shaped particle like the replication machinery is probably achieved through small disruptions in the coiled-coil regions that make the otherwise relatively stiff coiled coils more flexible. The globular interaction domains of the coiled-coil arms provide the strong interaction that is required to resist the force of the kinetochores that are pulling the sister chromatids into opposite directions during alignment on the metaphase plate. During the metaphase to anaphase transition of mitotic cell division, Scc1 is proteolytically cleaved by separase (reviewed in Uhlmann, 2001). This cleavage would allow the sister chromatids to be separated by opening the circle that embraces them (Haering et al., 2002).

We believe that the SMC family proteins exploit the different architectural arrangements of their common building blocks to perform their distinct functions in DNA metabolism. The eukaryotic Rad50/Mre11 complexes use their flexible arms and central DNA binding domain to provide a flexible bridge between broken DNA molecules. The cohesin complexes on the other hand use their flexibility to hold sister chromatids in an

embrace that does not necessarily require physical contact with DNA. The relevance of the structure of prokaryotic Rad50/Mre11 complexes, that contain two separate DNA binding domains that are connected by a coiled coil, is currently unclear. Experiments that analyze the action of the SMC complexes on DNA will surely provide further insights.

Materials and Methods

Protein preparations

The protein preparations used in this study were kind gifts of K. M. Trujillo and P. Sung (*S. cerevisiae* Rad50 and Rad50/Mre11), K.P. Hopfner, J. P. Carney and J. A. Tainer (*P. furiosus* Rad50 and Rad50/Mre11), C. Connelly and D. R. F. Leach (*E. coli* SbcCD), C. H. Haering and K. Nasmyth (*S. cerevisiae* SMC3 and SMC1/SMC3 complex). Their purification and characterization were described previously (Connelly et al., 1997; Hopfner et al., 2000; Trujillo and Sung, 2001; Haering et al., 2002).

Scanning Force Microscopy

Protein preparations were diluted in protein buffer (150 mM KCl, 25 mM Tris-HCl, pH 8 and 10% glycerol). Hundred to 500 ng of protein was deposited on freshly cleaved mica. After approximately 1 min the mica was rinsed with glass distilled water (Sigma) and dried with filtered air. Samples were imaged in air at room temperature and humidity using a Nanoscope IIIa or IV (Digital Instruments) operating in tapping mode, using an E-type scanner. Scanning probes were obtained from Veeco and MikroMasch.

Software, image processing and measurements

Multiple sequence alignments were performed using the CLUSTALW program (Thompson et al., 1994). The probability of regions to adopt a coiled coil was assessed with COILS (Lupas et al., 1991) and visualized using an IDL software routine. Image processing was done using Nanoscope software (Digital Instruments) or IDL and consisted only of a background correction. The coordinates of the molecular trajectories were traced manually to determine contour lengths. All data analysis was implemented in IDL.

Since the reconstituted *S. cerevisiae* Rad50/Mre11 complex did not contain heterodimers and was not homogenous, the contour lengths of Rad50 monomers in a Rad50 preparation were determined. This preparation was more homogenous and contained mostly monomers (80% of all

molecules). In the *E. coli* SbcCD preparation heterodimers cannot easily be distinguished from heterotetramers. Therefore, contour lengths were determined for unambiguous heterotetramers only. The length of a heterodimer was defined as half this value. Persistence lengths were determined using a similar routine as described by Rivetti et al. (Rivetti et al., 1998). This persistence length expresses the flexibility of homogenous polymers. Since the coiled-coil arms are known not to be homogenous, determination of the local persistence length would be preferred (Chapter 4; van Noort et al., submitted). However, with the current data set, the resolution of our images does not allow this type of analysis. Therefore, to get an indication of the flexibility of the coiled-coil arms, we determined the overall persistence length for heterodimeric *P. furiosus* Rad50/Mre11 complex and heterotetrameric *E. coli* SbcCD complexes. The overall persistence length of human Rad50 was determined in Chapter 4 (van Noort et al., submitted).

Acknowledgements

We are grateful to the following persons for kind gifts of the SMC family proteins used in this study: K. M. Trujillo and P. Sung for *S. cerevisiae* Rad50 and Rad50/Mre11 complex, K.P. Hopfner, J. P. Carney and J. A. Tainer for *P. furiosus* Rad50 and Rad50/Mre11 complex, J. C. Connelly and D. R. F. Leach for *E. coli* SbcCD, and C. H. Haering and K. Nasmyth for *S. cerevisiae* SMC3 and SMC1/SMC3 complex. This work was supported by grants from the Dutch Cancer Society (KWF) and the Netherlands Organization for scientific Research (NWO – Chemical Sciences).

References

- Aravind, L., Walker, D. R., and Koonin, E. V. (1999). Conserved domains in DNA repair proteins and evolution of repair systems. *Nucleic Acids Res.* 27, 1223-1242.
- Connelly, J. C., de Leau, E. S., and Leach, D. R. (1999). DNA cleavage and degradation by the SbcCD protein complex from *Escherichia coli*. *Nucleic Acids Res.* 27, 1039-1046.
- Connelly, J. C., Kirkham, L. A., and Leach, D. R. (1998). The SbcCD nuclease of *Escherichia coli* is a structural maintenance of chromosomes (SMC) family protein that cleaves hairpin DNA. *Proc. Natl. Acad. Sci. USA* 95, 7969-7974.
- Connelly, J. C., de Leau, E. S., Okely, E. A., and Leach, D. R. (1997). Overexpression, purification, and characterization of the SbcCD protein from *Escherichia coli*. *J. Biol. Chem.* 272, 19819-19826.

Connelly, J. C., and Leach, D. R. (1996). The *sbcC* and *sbcD* genes of *Escherichia coli* encode a nuclease involved in palindrome inviability and genetic recombination. *Genes Cells* 1, 285-291.

de Jager, M., van Noort, J., van Gent, D. C., Dekker, C., Kanaar, R., and Wyman, C. (2001). Human Rad50/Mre11 is a flexible complex that can tether DNA ends. *Mol. Cell* 8, 1129-1135.

de Jager, M., Wyman, C., van Gent, D. C., and Kanaar, R. (2002). DNA end-binding specificity of human Rad50/Mre11 is influenced by ATP. *Nucleic Acids Res.* 30, 4425-4431.

Freeman, L., Aragon-Alcaide, L., and Strunnikov, A. (2000). The condensin complex governs chromosome condensation and mitotic transmission of rDNA. *J. Cell. Biol.* 149, 811-824.

Haering, C. H., Lowe, J., Hochwagen, A., and Nasmyth, K. (2002). Molecular architecture of SMC proteins and the yeast cohesin complex. *Mol. Cell* 9, 773-788.

Hirano, T. (2002). The ABCs of SMC proteins: two-armed ATPases for chromosome condensation, cohesion, and repair. *Genes Dev.* 16, 399-414.

Hopfner, K. P., Craig, L., Moncalian, G., Zinkel, R. A., Usui, T., Owen, B. A., Karcher, A., Henderson, B., Bodmer, J. L., McMurray, C. T., Carney, J.P., Petrini, J.H., and Tainer, J.A. (2002). The Rad50 zinc-hook is a structure joining Mre11 complexes in DNA recombination and repair. *Nature* 418, 562-566.

Hopfner, K. P., Karcher, A., Craig, L., Woo, T. T., Carney, J. P., and Tainer, J. A. (2001). Structural biochemistry and interaction architecture of the DNA double-strand break repair Mre11 nuclease and Rad50-ATPase. *Cell* 105, 473-485.

Hopfner, K. P., Karcher, A., Shin, D., Fairley, C., Tainer, J. A., and Carney, J. P. (2000). Mre11 and Rad50 from *Pyrococcus furiosus*: cloning and biochemical characterization reveal an evolutionarily conserved multiprotein machine. *J. Bacteriol.* 182, 6036-6041.

Johzuka, K., and Ogawa, H. (1995). Interaction of Mre11 and Rad50: two proteins required for DNA repair and meiosis-specific double-strand break formation in *Saccharomyces cerevisiae*. *Genetics* 139, 1521-1532.

Leach, D. R. (1994). Long DNA palindromes, cruciform structures, genetic instability and secondary structure repair. *Bioessays* 16, 893-900.

Losada, A., Hirano, M., and Hirano, T. (1998). Identification of *Xenopus* SMC protein complexes required for sister chromatid cohesion. *Genes Dev.* 12, 1986-1997.

Lowe, J., Cordell, S. C., and van den Ent, F. (2001). Crystal structure of the SMC head domain: an ABC ATPase with 900 residues antiparallel coiled-coil inserted. *J. Mol. Biol.* 306, 25-35.

Lupas, A., Van Dyke, M., and Stock, J. (1991). Predicting coiled coils from protein sequences. *Science* 252, 1162-1164.

Melby, T. E., Ciampaglio, C. N., Briscoe, G., and Erickson, H. P. (1998). The symmetrical structure of structural maintenance of chromosomes (SMC) and MukB proteins: long, antiparallel coiled coils, folded at a flexible hinge. *J. Cell. Biol.* 142, 1595-1604.

Paul, T. T., and Gellert, M. (1998). The 3' to 5' exonuclease activity of Mre 11 facilitates repair of DNA double-strand breaks. *Mol. Cell* 1, 969-979.

Rivetti, C., Walker, C., and Bustamante, C. (1998). Polymer chain statistics and conformational analysis of DNA molecules with bends or sections of different flexibility. *J. Mol. Biol.* 280, 41-59.

- Sharples, G. J., and Leach, D. R.** (1995). Structural and functional similarities between the SbcCD proteins of *Escherichia coli* and the RAD50 and MRE11 (RAD32) recombination and repair proteins of yeast. *Mol. Microbiol.* 17, 1215-1217.
- Strunnikov, A. V., and Jessberger, R.** (1999). Structural maintenance of chromosomes (SMC) proteins: conserved molecular properties for multiple biological functions. *Eur. J. Biochem.* 263, 6-13.
- Thompson, J. D., Higgins, D. G., and Gibson, T. J.** (1994). CLUSTAL W: improving the sensitivity of progressive multiple sequence alignment through sequence weighting, position-specific gap penalties and weight matrix choice. *Nucleic Acids Res.* 22, 4673-4680.
- Trujillo, K. M., and Sung, P.** (2001). DNA structure-specific nuclease activities in the *Saccharomyces cerevisiae* Rad50.Mre11 complex. *J. Biol. Chem.* 276, 35458-35464.
- Uhlmann, F.** (2001). Secured cutting: controlling separase at the metaphase to anaphase transition. *EMBO Rep.* 2, 487-492.
- Usui, T., Ohta, T., Oshiumi, H., Tomizawa, J., Ogawa, H., and Ogawa, T.** (1998). Complex formation and functional versatility of Mre11 of budding yeast in recombination. *Cell* 95, 705-716.
- van Noort, J., van der Heijden, T., de Jager, M., Wyman, C., Kanaar, R., and Dekker, C.** (2003). The coiled-coil of the human Rad50 DNA repair protein contains specific segments of increased flexibility. submitted
- Yoshimura, S. H., Hizume, K., Murakami, A., Sutani, T., Takeyasu, K., and Yanagida, M.** (2002). Condensin architecture and interaction with DNA: regulatory non-SMC subunits bind to the head of SMC heterodimer. *Curr. Biol.* 12, 508-513.

Chapter

Genome instability and *Rad50^S*: subtle yet severe

7

Chapter 7

Genome instability and *Rad50^S*: subtle yet severe

Martijn de Jager ¹ and Roland Kanaar ^{1,2}

¹Department of Cell Biology & Genetics, Erasmus MC, Dr. Molewaterplein 50, 3000 DR Rotterdam, The Netherlands, and ²Department of Radiation Oncology, Erasmus MC-Daniel, Rotterdam, The Netherlands

Modified from: *Genes & Development*, 2002, Vol. 16, No. 17, 2173-2178

In the early 1980s, a primary hurdle on the track to understanding the function of a protein was the isolation of its gene. Over the last two decades, we have seen subsequent hurdles in the race to decipher protein function, including atomic structure resolution and the creation of viable mouse mutants, being cleared at an ever-increasing pace. The genome surveillance protein Rad50 has now leapt over these modern-day hurdles. In the last two years, rapid progress has been made in understanding structural aspects of Rad50 (Hopfner et al., 2000, 2001, 2002; de Jager et al., 2001; Chapter 3). John Petrini and colleagues recently reported on the phenotypes of mice carrying a hypomorphic *Rad50* allele named *Rad50^S* (Bender et al., 2002).

Rad50 is part of an evolutionarily conserved protein complex containing Mre11 and Nbs1 (D'Amours and Jackson, 2002) that is referred to as the Mre11 complex by Petrini and colleagues. The Mre11 complex has been implicated in diverse aspects of genome metabolism that involve DNA end processing, including cell cycle checkpoint activation in response to DNA double-strand breaks (DSBs), DSB repair, and telomere length maintenance (Haber, 1998; Lombard and Guarente, 2000; Petrini, 2000; Zhu et al., 2000). All three components of the mammalian Mre11 complex are essential for cellular viability (Xiao and Weaver, 1997; Luo et al., 1999; Yamaguchi-Iwai et al., 1999; Zhu et al., 2001). However, hypomorphic mutations in the human *NBS1* and *MRE11* genes cause the genome instability and cancer predisposition syndromes Nijmegen breakage syndrome (NBS) and ataxia telangiectasia-like disorder (ATLD), respectively (Carney et al., 1998; Matsuura et al., 1998; Varon et al., 1998; Stewart et al., 1999). In addition, two different engineered reduced-function alleles of murine *Nbs1* resulted in viable mice (Kang et al., 2002; Williams et al., 2002). No viable mutations in mammalian *RAD50* had been identified thus far. This void has now been filled by the *Rad50^{S/S}* mice.

Rad50^{S/S} mice

To derive a viable mouse *Rad50* allele, Bender et al. (2002) took their clues from genetic analyses of the *RAD50* gene from the yeast *Saccharomyces cerevisiae*. *RAD50*-deficient *S. cerevisiae* cells are viable but display mitotic and meiotic phenotypes. The cells are sensitive to the DNA-damaging agent methyl methanesulfonate (MMS) and are defective in the formation of viable spores. Alani et al. (1990) had isolated separation-of-function (*rad50S*) alleles of *RAD50* that conferred no overt MMS sensitivity to the cells, but still blocked viable spore formation. All of the nine different mutations that resulted in the *rad50S* phenotype mapped to the N terminus of Rad50 and were located in the vicinity of the Walker A-type ATPase domain of Rad50 (Fig. 1A). Bender et al. (2002) mimicked three of these mutations in mouse embryonic stem (ES) cells. Two resulted in inviable cells, but one, a methionine substitution for lysine at amino acid position 22 (K22M), did support cell growth. This allele was used to derive *Rad50^{S/S}* mice.

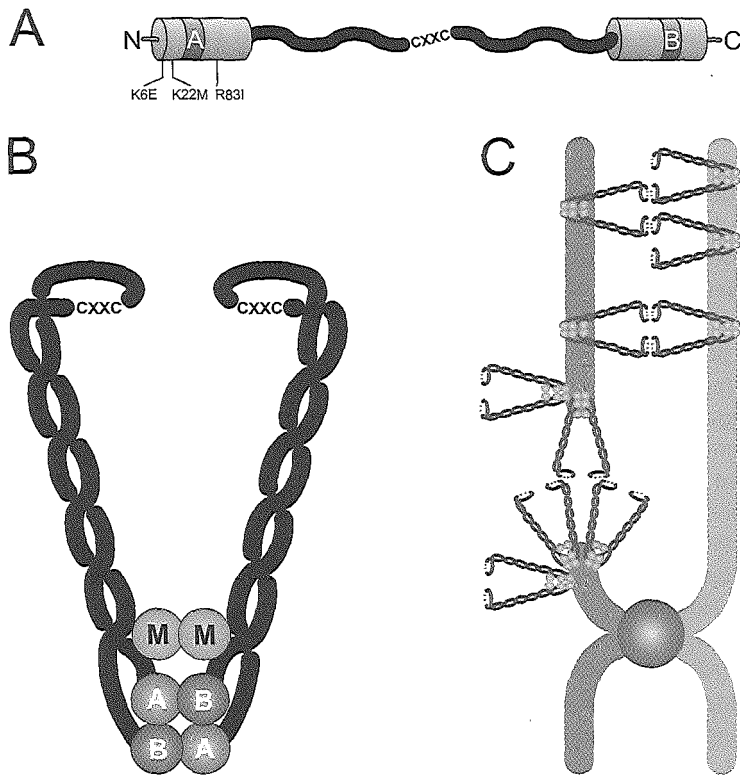


Figure 1. Architectural features of the Rad50 protein and its interaction with DNA. (A) Schematic representation of protein domains in Rad50, as predicted from its primary amino acid sequence. N-terminal and C-terminal globular domains (N and C, respectively) are separated by a region with the potential to form an extended coiled coil. The Walker A- and B-type ATPase domains (A and B, respectively) and the CXXC-motif in the middle of the coiled-coil region are indicated. The three different hypomorphic mutations located in the N-terminal globular domain and tested by Bender et al. (2002) are depicted. (B) Model for the architecture of the Rad50 and Mre11 components in the Mre11 complex. Rad50 Walker A- and B-type ATPase domains are connected by an intramolecular coiled coil. A Mre11 dimer binding to the base of the coiled-coil regions is represented by M. The conserved CXXC-motif at the distal tip of the coiled coils is indicated. (C) Schematic representation of potential DNA-repair functions of the Mre11 complex. The complex has been proposed to keep DNA fragments within close proximity, either within a sister chromatid or between sister chromatids. This tethering can occur through multiple interactions of the zinc-hook structures by intermolecular coordination of a zinc ion between Rad50 CXXC-motifs.

A remarkable aspect of the *Rad50^S* allele is its dramatically different consequence at the cellular versus the organismal level (Bender et al., 2002). *Rad50^{S/S}* mouse embryonic fibroblasts (MEFs) show almost none of the phenotypes that might be expected of perturbed Mre11 complex function (Table 1). The cells display no growth defect, no defect in ionizing radiation-induced relocalization of the complex, and no hypersensitivity to DNA-damaging agents such as ionizing radiation and mitomycin C. In addition, although NBS and ATLD cells are defective in the ionizing-radiation-induced intra-S-phase checkpoint, *Rad50^{S/S}* cells are not (Table 1). However, even though no overt cellular phenotype of the *Rad50^S* allele could be detected, its effect on mice is profound. *Rad50^{S/S}* mice are susceptible to partial embryonic lethality. Animals that make it through birth are small, and most of them die within three months of severe anemia caused by hematopoietic stem cell depletion, whereas longer-lived animals are predisposed to cancer. How to reconcile these severe phenotypes with the subtle mutation in the Mre11 complex is a challenge, given that the complex plays pivotal roles in diverse aspect of DNA metabolism.

phenotype	Human Nijmegen breakage syndrome	Human AT-like disorder	Murine <i>Rad50^S</i>	Murine <i>Nbs</i>
cancer predisposition	Y	ND	Y	Y/N ^a
cellular radiosensitivity	Y	Y	N	Y
spontaneous chromosomal instability	Y	Y	Y	N
radioresistant DNA synthesis	Y	Y	N	Y
defective ionizing radiation-induced foci formation	Y	Y	N	Y

Table 1. Comparison of genome instability-related phenotypes associated with mutations in the Mre11 complex in humans and mice.

Y, phenotype observed; N, phenotype not observed; ND, not determined.

^a depends on specific *Nbs* allele (Kang et al., 2002; Williams et al., 2002)

Rad50 structure

Because a specific mutation in Rad50, K22M, causes reduced function of the Mre11 complex, it is useful to consider the architecture of Rad50 and the complex. Based on its primary amino acid sequence, Rad50 has traditionally been declared a member of

the structural maintenance of chromosomes (SMC) protein family, which organizes chromosomes during their replication and segregation (Nasmyth, 2001; Hirano, 2002; Wyman and Kanaar, 2002). The amino acid sequence of proteins in this family suggests that they consist of N- and C-terminal globular domains, separated by an extended coiled-coil region (Fig. 1A). The terminal globular domains contain Walker A- and B-type ATPase domains, respectively, that reconstitute into a bipartite ATPase domain (Fig. 1B). The combination of electron microscopy, scanning force microscopy (SFM), and X-ray crystallography confirmed this predicted structure (Melby et al., 1998; Hopfner et al., 2000; Anderson et al., 2001, 2002; de Jager et al., 2001; Chapter 3; Haering et al., 2002; Hopfner et al., 2002). However, these studies also revealed a number of highly interesting surprises.

SMC family proteins function either as homo- or heterodimers. The Mre11 complex contains a Rad50 homodimer. A previously unexpected aspect of the architecture of the coiled-coil regions is that they do not form intermolecular coiled coils, but intramolecular coiled coils that are highly flexible (Fig. 1B; de Jager et al., 2001; Chapter 3; Haering et al., 2002; Hopfner et al., 2002). The intramolecular coiled coil forms because the predicted coiled-coil region of a single molecule folds back onto itself. In the case of Rad50 homologs, the coiled coil is interrupted by a conserved CXXC-motif, where C stands for cysteine and X for any amino acid (Fig. 1A). Recently, it was shown that this motif is located at the tip of the coiled coil in an archaeal Rad50 structural homolog. It provides a dimerization domain, referred to as a zinc-hook, between the two Rad50 coiled-coil arms by coordination of a zinc ion by the sulfhydryl groups of the four cysteines (Fig. 1B and 1C; Hopfner et al., 2002).

A molecular picture of the architecture of the human Mre11 complex and its mode of interaction with DNA is now beginning to emerge. Mre11, which has exo- and endonuclease activities (Sharples and Leach, 1995; Paull and Gellert, 1998; Trujillo et al., 1998), binds to the coiled-coil regions of Rad50 near the globular ATPase domain (Hopfner et al., 2001). A dimer of Mre11 interacts with two Rad50 molecules, resulting in a large globular domain from which the coiled-coil arms emanate (Fig. 1B; de Jager et al., 2001; Chapter 3). An intriguing unanswered question about the architecture of the Mre11 complex is the location of Nbs1. This component interacts with Mre11 (D'Amours and Jackson, 2002), but exactly how it fits in the complex is still unknown. SFM analysis of the complex between human Rad50 and Mre11 showed that it binds DNA through its globular domain with the arms protruding away. The complex oligomerizes on linear DNA and can tether DNA molecules, presumably through interactions between the tips of its coiled coils (de Jager et al., 2001; Chapter 3; Hopfner et al., 2002). Importantly, oligomerization requires a DNA end, allowing the complex to specifically tether broken DNA molecules either within a sister chromatid or between a broken and an intact sister chromatid (Fig. 1C).

The deleterious effects of the Rad50 K22M mutation in mice invite biochemical analysis of the activities of the Mre11 complex containing this mutation. Because it is located close to the ATPase domain of Rad50, it is of interest to determine the effect of

this mutation on the nuclease activities of the complex, given that ATP stimulates the endonuclease activity of the complex on DNA substrates containing 3' single-stranded overhangs (Paull and Gellert, 1999; Trujillo and Sung, 2001). Effects of the mutation on the nuclease activity could impinge on the DNA repair function of the Mre11 complex or on its involvement in DNA damage checkpoint signaling, because the nucleolytic processing of DNA lesions could be required to effectively signal them to the cell cycle checkpoint machinery (Lydall and Weinert, 1995; Lee et al., 1998; D'Amours and Jackson, 2001).

The Mre11 complex and S-phase progression

Deficiencies in the Mre11 complex, such as those that occur in cells derived from NBS and ATLD patients, can result in the inefficient inhibition of DNA synthesis upon ionizing radiation treatment (Table 1; Shiloh, 1997; Stewart et al., 1999). This response, known as radioresistant DNA synthesis (RDS), is indicative of the inability of cells to fully induce an intra-S-phase checkpoint (Shiloh, 1997). Several recent studies provide new insights into the position of the Mre11 complex in the cascades of events that are required to protect cells from RDS. Near the top of these cascades is the ataxia telangiectasia mutated (ATM) protein kinase, which is defective in patients suffering from the genome instability, and cancer predisposition syndrome ataxia telangiectasia (AT; Khanna and Jackson, 2001). In response to ionizing-radiation-induced DSBs, ATM phosphorylates Nbs1, which is required to inhibit DNA synthesis (D'Amours and Jackson, 2002). Interestingly, the extent of RDS is greater in cells from AT patients than in cells from NBS and ATLD patients, suggesting the possibility of parallel pathways leading to DNA synthesis inhibition that diverge at ATM (Falck et al., 2002). Indeed, recent evidence suggests that one branch is formed by the ATM-dependent phosphorylation of Chk2, which results in inhibition of DNA replication origin firing through the Chk2–Cdc25A–cyclin E/Cdk2 cascade (Falck et al., 2001), whereas ATM-dependent phosphorylation of the Mre11 complex is required for a parallel branch of the intra-S-phase checkpoint (Falck et al., 2002). An intriguing downstream substrate in the Mre11 complex-dependent branch could be SMC1, a component of the multiprotein cohesion complex required for establishment of sister-chromatid cohesion during S-phase (Nasmyth, 2001; Hirano, 2002). Ionizing-radiation-induced phosphorylation of SMC1 by ATM is dependent on Nbs1 and required for inhibition of DNA synthesis (Kim et al., 2002; Yazdi et al., 2002). However, the results of Bender et al. (2002) support the argument that the checkpoint-related functions of the Mre11 complex in *Rad50^{S/S}* cells are not significantly affected. When *Rad50^{S/S}* cells were treated with ionizing radiation they were as efficient as wild-type cells in inhibiting DNA synthesis.

The Mre11 complex in DNA repair and replication

Given that mutations in the components of the *S. cerevisiae* Mre11 complex (in which the Nbs1-like component is encoded by the *XRS2* gene) resulted in ionizing radiation sensitivity, much attention has been given over the years to defining its role in repair of DSBs. Multiple lines of evidence suggest that the complex participates in two mechanistically distinct pathways of DSB repair: homologous recombination and nonhomologous DNA end joining (Bressan et al., 1999; Lewis and Resnick, 2000; Chen et al., 2001; Huang and Dynan, 2002). The former depends on a homologous DNA template, that is, the undamaged sister chromatid, to accurately restore the continuity of the broken sister chromatid, whereas the latter religates DNA ends without any requirement for a template. Important as the role of the Mre11 complex in repair of exogenously induced DSBs might be, the complex is also pivotally important in protecting cells from spontaneous chromosomal rearrangements (Chen and Kolodner, 1999; Myung et al., 2001). These latter observations are consistent with a role of the Mre11 complex in preventing genome instability during DNA replication.

Indeed, the dependence of genome duplication on homologous recombination in general is presently a topic of vigorous reinvestigation (Cox et al., 2000). Evidence from genetic, cytological, and biochemical approaches points to a possible central position of the Mre11 complex in this link. *S. cerevisiae rad50S* and *mre11* nuclease-deficient alleles are synthetically lethal with the structure-specific endonuclease Rad27/FEN1 (Moreau et al., 1999; Debrauwere et al., 2001). Given the role of Rad27/FEN1 in processing intermediates in laggingstrand DNA synthesis, these results suggest the involvement of the Mre11 complex in this process. Furthermore, the complex plays a role in the resolution of aberrant DNA structures that arise when replication forks pass through repeated sequences (Cromie et al., 2001; Farah et al., 2002; Lobachev et al., 2002). In addition, certain DSB repair pathways that are directly coupled to extensive DNA replication, such as break-induced replication in *S. cerevisiae* and replication restart in phages, require Rad50 and Mre11 homologs (George et al., 2001; Signon et al., 2001). Finally, the Mre11 complex localizes to replication sites (Maser et al., 2001), and its presence is required to prevent the accumulation of DSBs during DNA replication in extracts from *Xenopus laevis* cells (Costanzo et al., 2001).

Cells derived from *Rad50^{S/S}* mice are not sensitive to exogenously induced DSBs, yet they show increases in spontaneous levels of γ -H2AX foci, a marker for DSBs (Modesti and Kanaar, 2001), and cytologically detectable chromosome breaks (Bender et al., 2002). These phenotypes are consistent with the idea that the Mre11 complex is important for correcting problems arising during DNA replication. If so, *Rad50^{S/S}* cells would be under continuous genotoxic stress, which could cause the underlying phenotype of the mice. The age-dependent attrition of cells in the bone marrow and testis can be explained in this context because these tissues contain rapidly proliferating cells derived from a small stem-cell compartment. Furthermore, interference with the ability of *Rad50^{S/S}* cells to activate cell cycle checkpoints and

induce apoptosis by deletion of *p53* results in an increased life span of the mice and decreased tumor latency (Bender et al., 2002). This is also in accordance with the idea that reduced function of the Mre11 complex leads to chronic genotoxicity.

Rad50S: conservation between yeast and mouse?

Based on their amino acid sequences, it is clear that components of the yeast and mammalian Mre11 complex are highly conserved. It is interesting, then, that the K22M amino acid change in Rad50 yields contrasting phenotypes in yeast and mice. The differential effect is most dramatic in meiosis: Whereas the failure to form viable spores owing to the inability to further process meiotic DSBs is a defining feature of *rad50S* yeast strains, no overt meiotic defect is observed in *Rad50^{S/S}* mice (Bender et al., 2002). However, in addition to differences in phenotypes, there are also similarities, particularly with respect to telomere metabolism. In yeast the Mre11 complex is involved in telomere homeostasis (Haber, 1998). In mammalian cells the complex has been localized at telomeres, but a biological effect on telomeres had not been shown (Zhu et al., 2000). Now Bender et al. (2002) show that in *Rad50^{S/S}* tumor cells, telomere-to-telomere fusions are increased. A more detailed analysis of the molecular nature of these defective telomeres will undoubtedly provide new insight into the mechanism of telomere maintenance in mammalian cells. Given the presence of repetitive DNA sequences at telomeres and their unusual structure (Griffith et al., 1999), the role of the Mre11 complex might be related to its role in resolving aberrant DNA secondary structures arising during replication of sequences with a high propensity to form secondary structures.

The murine *Rad50^S* allele underscores the fact that very subtle changes in protein activity can have dramatic phenotypic consequences. It also shows that even in the context of a highly conserved protein, it is not trivial to predict the behavior of mammalian mutant alleles based on yeast genetics. Two of the mimicked yeast *rad50S* alleles resulted in nonviable murine ES cells, whereas a third resulted in mice on the threshold of viability. The severity of the murine *Rad50^S* phenotype caused by a subtle mutation provides a prime example of the importance of polymorphisms in genome-surveillance proteins for conferring differences in cancer predisposition in the human population. Now that a biological effect of the mammalian *Rad50^S* protein has been shown, it is an interesting venture to link this biological effect to one or more of the many biochemical and structural functions of the Mre11 complex. Certainly, we can expect many more surprises with regard to this protein complex in the not-too-distant future, given that the keyword “Rad50” pulls up just as many references in PubMed in the last two and half years as in the preceding 23.

References

- Alani, E., Padmore, R., and Kleckner, N.** (1990). Analysis of wildtype and *rad50* mutants of yeast suggests an intimate relationship between meiotic chromosome synapsis and recombination. *Cell* 61, 419-436.
- Anderson, D.E., Trujillo, K.M., Sung, P., and Erickson, H.P.** (2001). Structure of the Rad50 · Mre11 DNA repair complex from *Saccharomyces cerevisiae* by electron microscopy. *J. Biol. Chem.* 276, 37027-37033.
- Anderson, D.E., Losada, A., Erickson, H.P., and Hirano, T.** (2002). Condensin and cohesin display different arm conformations with characteristic hinge angles. *J. Cell. Biol.* 156, 419-424.
- Bender, C.F., Sikes, M.L., Sullivan, R., Erskine Huye, L., Le Beau, M.M., Roth, D.B., Mirzoeva, O.K., Oltz, E.M., and Petrini, J.H.J.** (2002). Cancer predisposition and hematopoietic failure in *Rad50^{SS}* mice. *Genes Dev.* 16, 2237-2251.
- Bressan, D.A., Baxter, B.K., and Petrini, J.H.** (1999). The Mre11–Rad50–Xrs2 protein complex facilitates homologous recombination-based double-strand break repair in *Saccharomyces cerevisiae*. *Mol. Cell. Biol.* 19, 7681-7687.
- Carney, J.P., Maser, R.S., Olivares, H., Davis, E.M., Le Beau, M., Yates III, J.R., Hays, L., Morgan, W.F., and Petrini, J.H.** (1998). The hMre11/hRad50 protein complex and Nijmegen breakage syndrome: Linkage of double-strand break repair to the cellular DNA damage response. *Cell* 93, 477-486.
- Chen, C. and Kolodner, R.D.** (1999). Gross chromosomal rearrangements in *Saccharomyces cerevisiae* replication and recombination defective mutants. *Nat. Genet.* 23, 81-85.
- Chen, L., Trujillo, K., Ramos, W., Sung, P., and Tomkinson, A.E.** (2001). Promotion of Dnl4-catalyzed DNA end-joining by the Rad50/Mre11/Xrs2 and Hdf1/Hdf2 complexes. *Mol. Cell* 8, 1105-1115.
- Costanzo, V., Robertson, K., Bibikova, M., Kim, E., Grieco, D., Gottesman, M., Carroll, D., and Gautier, J.** (2001). Mre11 protein complex prevents double-strand break accumulation during chromosomal DNA replication. *Mol. Cell* 8, 137-147.
- Cox, M.M., Goodman, M.F., Kreuzer, K.N., Sherratt, D.J., Sandler, S.J., and Marians, K.J.** (2000). The importance of repairing stalled replication forks. *Nature* 404, 37-41.
- Cromie, G.A., Connelly, J.C., and Leach, D.R.** (2001). Recombination at double-strand breaks and DNA ends: Conserved mechanisms from phage to humans. *Mol. Cell* 8, 1163-1174.
- D'Amours, D. and Jackson, S.P.** (2001). The yeast Xrs2 complex functions in S phase checkpoint regulation. *Genes Dev.* 15, 2238-2249.
- D'Amours, D. and Jackson, S.P.** (2002). The Mre11 complex: At the crossroads of DNA repair and checkpoint signalling. *Nat. Rev. Mol. Cell Biol.* 3, 317-327.
- Debrauwere, H., Loeillet, S., Lin, W., Lopes, J., and Nicolas, A.** (2001). Links between replication and recombination in *Saccharomyces cerevisiae*: A hypersensitive requirement for

homologous recombination in the absence of Rad27 activity. *Proc. Natl. Acad. Sci. USA* 98, 8263-8269.

de Jager, M., van Noort, J., van Gent, D.C., Dekker, C., Kanaar, R., and Wyman, C. (2001). Human Rad50/Mre11 is a flexible complex that can tether DNA ends. *Mol. Cell* 8, 1129-1135.

Falck, J., Mailand, N., Syljuasen, R.G., Bartek, J., and Lukas, J. (2001). The ATM-Chk2-Cdc25A checkpoint pathway guards against radioresistant DNA synthesis. *Nature* 410, 842-847.

Falck, J., Petrini, J.H., Williams, B.R., Lukas, J., and Bartek, J. (2002). The DNA damage-dependent intra-S phase checkpoint is regulated by parallel pathways. *Nat. Genet.* 30, 290-294.

Farah, J.A., Hartsuiker, E., Mizuno, K., Ohta, K., and Smith, G.R. (2002). A 160-bp palindrome is a Rad50 · Rad32-dependent mitotic recombination hotspot in *Schizosaccharomyces pombe*. *Genetics* 161, 461-468.

George, J.W., Stohr, B.A., Tomso, D.J., and Kreuzer, K.N. (2001). The tight linkage between DNA replication and double-strand break repair in bacteriophage T4. *Proc. Natl. Acad. Sci. USA* 98, 8290-8297.

Griffith, J.D., Comeau, L., Rosenfield, S., Stansel, R.M., Bianchi, A., Moss, H., and de Lange T. (1999). Mammalian telomeres end in a large duplex loop. *Cell* 97, 503-514.

Haber, J.E. (1998). The many interfaces of Mre11. *Cell* 95, 583-586.

Haering, C.H., Lowe, J., Hochwagen, A., and Nasmyth, K. (2002). Molecular architecture of SMC proteins and the yeast cohesin complex. *Mol. Cell* 9, 773-788.

Hirano, T. (2002). The ABCs of SMC proteins: Two-armed ATPases for chromosome condensation, cohesion, and repair. *Genes Dev.* 16, 399-414.

Hopfner, K.P., Karcher, A., Shin, D.S., Craig, L., Arthur, L.M., Carney, J.P., and Tainer, J.A. (2000). Structural biology of Rad50 ATPase: ATP-driven conformational control in DNA double-strand break repair and the ABC-ATPase superfamily. *Cell* 101, 789-800.

Hopfner, K.P., Karcher, A., Craig, L., Woo, T.T., Carney, J.P., and Tainer, J.A. (2001). Structural biochemistry and interaction architecture of the DNA double-strand break repair Mre11 nuclease and Rad50-ATPase. *Cell* 105, 473-485.

Hopfner, K.P., Craig, L., Moncalian, G., Zinkel, R.A., Usui, T., Owen, B.A.L., Karcher, A., Henderson, B., Bodmer, J.L., Mc-Murray, C.T., Carney, J.P., Petrini, J.H., and Tainer, J.A. (2002). The Rad50 zinc-hook is a structure joining Mre11 complexes in DNA recombination and repair. *Nature* 418, 562-566.

Huang, J. and Dynan, W.S. (2002). Reconstitution of the mammalian DNA double-strand break end-joining reaction reveals a requirement for an Mre11/Rad50/NBS1-containing fraction. *Nucleic Acids Res.* 30, 667-674.

Kang, J., Bronson, R.T., and Xu, Y. (2002). Targeted disruption of NBS1 reveals its roles in mouse development and DNA repair. *EMBO J.* 21, 1447-1455.

Khanna, K.K. and Jackson, S.P. (2001). DNA double-strand breaks: Signaling, repair and the cancer connection. *Nat. Genet.* 27, 247-254.

Kim, S.T., Xu, B., and Kastan, M.B. (2002). Involvement of the cohesin protein, Smc1, in Atm-dependent and independent responses to DNA damage. *Genes Dev.* 16, 560-570.

- Lee, S.E., Moore, J.K., Holmes, A., Umezu, K., Kolodner, R.D., and Haber, J.E.** (1998). *Saccharomyces* Ku70, mre11/rad50 and RPA proteins regulate adaptation to G2/M arrest after DNA damage. *Cell* 94, 399-409.
- Lewis, L.K. and Resnick, M.A.** (2000). Tying up loose ends: Nonhomologous end-joining in *Saccharomyces cerevisiae*. *Mutat. Res.* 451, 71-89.
- Lobachev, K.S., Gordenin, D.A., and Resnick, M.A.** (2002). The Mre11 complex is required for repair of hairpin-capped double-strand breaks and prevention of chromosome rearrangements. *Cell* 108, 183-193.
- Lombard, D.B. and Guarente, L.** (2000). Nijmegen breakage syndrome disease protein and MRE11 at PML nuclear bodies and meiotic telomeres. *Cancer Res.* 60, 2331-2334.
- Luo, G., Yao, M.S., Bender, C.F., Mills, M., Bladi, A.R., Bradley, A., and Petrini, J.H.** (1999). Disruption of mRad50 causes embryonic stem cell lethality, abnormal embryonic development, and sensitivity to ionizing radiation. *Proc. Natl. Acad. Sci. USA* 96, 7376-7381.
- Lydall, D. and Weinert, T.** (1995). Yeast checkpoint genes in DNA damage processing: Implications for repair and arrest. *Science* 270, 1488-1491.
- Maser, R.S., Mirzoeva, O.K., Wells, J., Olivares, H., Williams, B.R., Zinkel, R.A., Farnham, P.J., and Petrini, J.H.J.** (2001). Mre11 complex and DNA replication: Linkage to E2F and sites of DNA synthesis. *Mol. Cell. Biol.* 21, 6006-6016.
- Matsuura, S., Tauchi, H., Nakamura, A., Kondo, N., Sakamoto, S., Endo, S., Smeets, D., Solder, B., Belohradsky, B. H., Der Kaloustian, V. M., Oshimura, M., Isomura, M., Nakamura, Y., and Komatsu, K.** (1998). Positional cloning of the gene for Nijmegen breakage syndrome. *Nat. Genet.* 19, 179-181.
- Melby, T.E., Ciampaglio, C.N., Briscoe, G., and Erickson, H.P.** (1998). The symmetrical structure of structural maintenance of chromosomes (SMC) and MukB proteins: Long, antiparallel coiled coils, folded at a flexible hinge. *J. Cell Biol.* 142, 1595-1604.
- Modesti, M. and Kanaar, R.** (2001). DNA repair: Spot(light)s on chromatin. *Curr. Biol.* 11, R229-R232.
- Moreau, S., Ferguson, J.R., and Symington, L.S.** (1999). The nuclease activity of Mre11 is required for meiosis but not for mating type switching, end joining, or telomere maintenance. *Mol. Cell. Biol.* 19, 556-566.
- Myung, K., Datta, A., and Kolodner, R.D.** (2001). Suppression of spontaneous chromosomal rearrangements by S phase checkpoint functions in *Saccharomyces cerevisiae*. *Cell* 104, 397-408.
- Nasmyth, K.** (2001). Disseminating the genome: Joining, resolving, and separating sister chromatids during mitosis and meiosis. *Annu. Rev. Genet.* 35, 673-745.
- Paull, T.T. and Gellert, M.** (1998). The 3' to 5' exonuclease activity of Mre 11 facilitates repair of DNA double-strand breaks. *Mol. Cell* 1, 969-979.
- Paull, T.T. and Gellert, M.** (1999). Nbs1 potentiates ATP-driven DNA unwinding and endonuclease cleavage by the Mre11/Rad50 complex. *Genes Dev.* 13, 1276-1288.
- Petrini, J.H.** (2000). The Mre11 complex and ATM: Collaborating to navigate S phase. *Curr. Opin. Cell Biol.* 12, 293-296.

- Sharples, G.J. and Leach, D.R.** (1995). Structural and functional similarities between the SbcCD proteins of *Escherichia coli* and the RAD50 and MRE11 (RAD32) recombination and repair proteins of yeast. *Mol. Microbiol.* *17*, 1215-1217.
- Shiloh, Y.** (1997). Ataxia-telangiectasia and the Nijmegen breakage syndrome: Related disorders but genes apart. *Annu. Rev. Genet.* *31*, 635-662.
- Signon, L., Malkova, A., Naylor, M.L., Klein, H., and Haber, J.E.** (2001). Genetic requirements for RAD51- and RAD54-independent break-induced replication repair of a chromosomal double-strand break. *Mol. Cell. Biol.* *21*, 2048-2056.
- Stewart, G.S., Maser, R.S., Stankovic, T., Bressan, D.A., Kaplan, M.I., Jaspers, N.G., Raams, A., Byrd, P.J., Petrini, J.H., and Taylor, A.M.** (1999). The DNA double-strand break repair gene hMRE11 is mutated in individuals with an ataxia-telangiectasia-like disorder. *Cell* *99*, 577-587.
- Trujillo, K.M. and Sung, P.** (2001). DNA structure-specific nuclease activities in the *Saccharomyces cerevisiae* Rad50 · Mre11 complex. *J. Biol. Chem.* *276*, 35458-35464.
- Trujillo, K.M., Yuan, S.S., Lee, E.Y., and Sung, P.** (1998). Nuclease activities in a complex of human recombination and DNA repair factors Rad50, Mre11, and p95. *J. Biol. Chem.* *273*, 21447-21450.
- Varon, R., Vissinga, C., Platzer, M., Cerosaletti, K. M., Chrzanowska, K. H., Saar, K., Beckmann, G., Seemanova, E., Cooper, P. R., Nowak, N. J., Stumm, M., Weemaes, C. M., Gatti, R. A., Wilson, R. K., Digweed, M., Rosenthal, A., Sperling, K., Concannon, P., and Reis, A.** (1998). Nibrin, a novel DNA double-strand break repair protein, is mutated in Nijmegen breakage syndrome. *Cell* *93*, 467-476.
- Williams, B.R., Mirzoeva, O.K., Morgan, W.F., Lin, J., Dunnick, W., and Petrini, J.H.** (2002). A murine model of Nijmegen breakage syndrome. *Curr. Biol.* *12*, 648-653.
- Wyman, C. and Kanaar, R.** (2002). Chromosome organization: Reaching out to embrace new models. *Curr. Biol.* *12*, R446-R448.
- Xiao, Y. and Weaver, D.T.** (1997). Conditional gene targeted deletion by Cre recombinase demonstrates the requirement for the double-strand break repair Mre11 protein in murine embryonic stem cells. *Nucleic Acids Res.* *25*, 2985-2991.
- Yamaguchi-Iwai, Y., Sonoda, E., Sasaki, M. S., Morrison, C., Haraguchi, T., Hiraoka, Y., Yamashita, Y. M., Yagi, T., Takata, M., Price, C., Kakazu, N., and Takeda, S.** (1999). Mre11 is essential for the maintenance of chromosomal DNA in vertebrate cells. *EMBO J.* *18*, 6619-6629.
- Yazdi, P.T., Wang, Y., Zhao, S., Patel, N., Lee, E.Y., and Qin, J.** (2002). SMC1 is a downstream effector in the ATM/NBS1 branch of the human S-phase checkpoint. *Genes Dev.* *16*, 571-582.
- Zhu, J., Petersen, S., Tessarollo, L., and Nussenzweig, A.** (2001). Targeted disruption of the Nijmegen breakage syndrome gene NBS1 leads to early embryonic lethality in mice. *Curr. Biol.* *11*, 105-109.
- Zhu, X.D., Kuster, B., Mann, M., Petrini, J.H., and Lange, T.** (2000). Cell-cycle-regulated association of RAD50/MRE11/NBS1 with TRF2 and human telomeres. *Nat. Genet.* *25*, 347-352.

Abbreviations

Å	Ångstrom (10^{-10} meter)	Ni	nickel
AMP-PNP	adenosine 5'-(β,γ -imido)-triphosphate tetralithium	nm	nanometer (1.10^{-9} meter)
AT	ataxia telangiectasia	nt	nucleotide
ATLD	ataxia telangiectasia - like disorder	<i>P</i>	persistence length
ATM	ataxia telangiectasia mutated	PAGE	polyacrylamide gel electrophoresis
ATP	adenosine 5'-triphosphate	<i>R</i>	end-to-end distance
bp	basepair	RDS	radioresistant DNA synthesis
C-	carboxy-	R/M	Rad50 and Mre11 protein complex
CXXC	(cysteine - any amino acid - any amino acid - cysteine)	RPA	replication protein A
Da	dalton ($1,66.10^{-27}$ kg)	[<i>S</i>]	substrate concentration
DNA	deoxyribonucleic acid	SCID	severe combined immunodeficiency
DNA-PK	DNA-dependent protein kinase	SFM	scanning force microscopy, also called atomic force microscopy
DNA-PK _{cs}	DNA-dependent protein kinase catalytic subunit	SMC	structural maintenance of chromosomes
DSB	double-strand break	ssDNA	single-stranded DNA
dsDNA	double-stranded DNA	<i>U</i>	elastic energy
EM	electron microscope	<i>V</i>	reaction velocity
ES cell	embryonic stem cell	<i>V</i> _{max}	maximal reaction velocity
<i>F</i>	flexibility	V(D)J	variable, diverse and joining segments
<i>k</i>	spring constant	Zn	zinc
<i>K</i>	intrinsic curvature		
kb	kilo basepairs (1000 basepairs)		
<i>k_b</i>	Boltzmann's constant		
kDa	kilo dalton (1000 daltons)		
<i>K_m</i>	Michaelis-Menten constant		
<i>L</i>	contour length		
<i>M</i>	molarity ($6,0.10^{23}$ molecules per liter)		
MEF	mouse embryonic fibroblast		
N-	amino-		
NBS	Nijmegen breakage syndrome		
Nbs1	Nijmegen breakage syndrome protein		
NHEJ	non-homologous end-joining		

Summary of the thesis

The integrity of DNA, the carrier of genetic information, is under continuous threat of damage by DNA damaging agents and processes. Persistent DNA damages can interfere with normal cellular functions and can ultimately result in cell death or carcinogenesis. In order to counteract these deleterious effects, the cell utilizes specialized DNA repair mechanisms for the different types of DNA damages. DNA double-strand breaks (DSBs) and DNA ends are among the most genotoxic lesions. They can be induced by exogenous and endogenous agents but are also intentionally induced in specialized cellular processes. If DNA ends are left unprocessed they can cause genetic rearrangements that can trigger carcinogenesis. To process DNA ends appropriately, different mechanisms exist that are utilized depending on the type of break and the circumstances under which it occurs. These distinct mechanisms all use dedicated sets of proteins with specialized functions. The complex of Rad50 with Mre11 and Nbs1, however, is involved in many different DNA metabolic processes: both meiotic and mitotic recombination, DSB repair, telomere length maintenance and cell cycle regulation.

To identify the common mechanistic function needed for multiple cellular processes, the biochemical activities of the Rad50 complex components were investigated. Rad50 possesses a weak ATPase activity that might be indicative of a molecular switch. One interesting activity of Mre11, in addition to its DNA binding and nuclease activities is the potential to anneal complementary single-stranded DNA molecules. Despite the biochemical knowledge that is available to date the exact function of the complex remains illusive.

Intriguing information, however, comes from the architecture of the Rad50 complex. Scanning force microscopic (SFM) analyses shows that the overall complex architecture consists of a globular DNA binding globular domain from which two intramolecular coiled coils extend. Time-resolved SFM of individual molecules shows these coiled coils to be highly flexible structures. Using high-resolution SFM images of the Rad50 complex, we map local flexibility along the coiled coil. The high flexibility is likely due to localized disruptions of the coiled-coil structure. SFM analyses of Rad50 complexes bound to DNA shows that the complex binds to DNA through the globular domain with the coiled-coil arms protruding away. Large oligomers consisting of many Rad50 complex molecules can form on the DNA. Although the complex binds to both linear and circular DNA molecules, a DNA end is required to form these large oligomers. The position of the large oligomers is not restricted to the DNA end, but are also found at internal positions on linear DNA molecules as well, which indicates that the complex could translocate on DNA. Interestingly, the type of single-stranded overhang at the

DNA end influences the affinity of the complex for its substrate. Furthermore, this affinity appears to be influenced by ATP. This indicates that Rad50 might indeed be an ATP-operated structural switch for the binding of the complex to DNA. An essential clue to the function of the Rad50 complex in DNA end processing comes from the observation that large DNA-bound oligomeric complexes can tether DNA molecules through multiple interactions of the coiled-coil arms. In view of the high flexibility of the Rad50 coiled coils it is tempting to speculate that the many coiled coils provide a strong, but flexible interaction interface. Together these data indicate that the essential function of the Rad50 complex in the different DNA metabolic processes might be to hold DNA ends together in a flexible manner. The nuclease and annealing activities of Mre11 might be required for processing of DNA ends. Alternatively, the inward movement of the complex would allow other factors to perform their specialized functions at the DNA end. Since the inward migration will be limited due to chromatin structure, this would still allow the complex to keep the ends structurally organized.

The overall structure of the Rad50 complex is highly conserved through evolution and homologs of the complex have been identified in evolutionary distant species. The presence of a bipartite ATPase domain and a coiled-coil region make the Rad50 homologs members of the structural maintenance of chromosomes (SMC) family of proteins. A comparative SFM analysis of human, yeast, bacterial, archaeal Rad50 homologs and SMC family members shows that these proteins share the same structural elements such as globular ATPase domains and an extended coiled-coil region. Interestingly, the arrangement of these elements is different for the various family members, which indicates that these proteins use similar structural elements in different arrangements that are optimally suited for their specific functions.

Samenvatting van het proefschrift

Iedere cel in het menselijk lichaam bevat een enorme hoeveelheid DNA. Al dit DNA bevat gecodeerde informatie die essentieel is voor het functioneren van de cellen waaruit een organisme bestaat. Ieder DNA molecuul bestaat uit twee complementaire strengen die samen een dubbele helix vormen. Het DNA is georganiseerd in zogenaamde chromosomen die elk bestaan uit een lang stuk DNA dat heel compact opgevouwen is. De mens heeft 23 chromosomen in iedere celkern. Hoewel DNA erg belangrijk is, is het ook erg kwetsbaar. Het wordt continu blootgesteld aan stoffen en processen die het fysiek kunnen beschadigen. Als de beschadigingen aanwezig blijven zal dit een negatieve invloed hebben op het functioneren van de cel. Zo kan de cel doodgaan of, in tegenstelling, ongeremd gaan groeien. Deze ongeremde groei kan resulteren in tumor formatie. Gelukkig bestaan er verschillende manieren om DNA beschadigingen te herstellen. Elk type DNA beschadiging kan herkend en gerepareerd worden door daarin gespecialiseerde groepjes eiwitten die werken in verschillende processen.

Bij een heel gevaarlijke soort DNA beschadiging, de dubbelstrengs breuk, zijn de beide strengen waaruit DNA moleculen bestaan gebroken. Deze breuken kunnen veroorzaakt worden door stoffen die van nature voorkomen in de cel, maar ook door invloeden van buitenaf, zoals röntgenstraling en chemicaliën. Behalve deze ongewenste breuken worden DNA breuken ook met opzet gemaakt in zeer gespecialiseerde processen in de cel die bepaalde stukken DNA herrangschikken om zo variatie in genetische informatie te creëren. Verder komen DNA einden ook voor aan de uiteinden van de chromosomen. Als deze breuken en uiteinden niet juist worden behandeld en/of gerepareerd is er een grote kans dat stukken DNA verdwijnen of op een verkeerde manier aan elkaar worden geplakt, wat kan leiden tot de dood van cellen of de vorming van tumorcellen. Om DNA uiteinden op de juiste manier te verwerken bestaan verschillende processen die afhankelijk van de omstandigheden kunnen worden gebruikt. Een groepje van drie eiwitten, Rad50, Mre11 en Nbs1, ook wel Rad50 complex genaamd is betrokken bij een aantal geheel verschillende processen die DNA behandelen, waaronder ook het herstel van breuken.

Om te onderzoeken wat de gemeenschappelijke functie van het Rad50 complex in de verschillende processen zou kunnen zijn werden eerst de biochemische eigenschappen van het Rad50 complex onderzocht. Rad50 kan ATP, een stof die bijdraagt aan de energie voorziening van de cel, langzaam omzetten en zou deze energie kunnen gebruiken voor een kleine verandering in zijn vorm. Een ander eiwit uit het complex, Mre11, kan aan DNA binden en dit knippen. Verder kan dit eiwit twee complementaire strengen DNA 'samensmelten' tot dubbelstrengs DNA. Ondanks alle

kennis over de biochemische eigenschappen van het Rad50 complex is nog steeds niet duidelijk wat nu de precieze functie van dit complex is.

Veel inzicht komt echter van het bestuderen van de vorm van het Rad50 complex. Met behulp van de zogenaamde 'scanning force' microscoop, die met een minuscuul soort naaldje heel kleine voorwerpen affast, laten we zien dat het Rad50 complex een heel bijzondere vorm heeft. Het bestaat uit een bolletje met twee armpjes, die elk 50 miljoenste millimeter lang zijn. Door het bekijken van één Rad50 complex gedurende een bepaalde tijd werd duidelijk dat de armpjes flexibel zijn. De meting van de locale flexibiliteit over de lengte van de armpjes laat zien dat deze op twee plaatsen extra flexibel zijn. Als we DNA toevoegen aan het Rad50 complex blijkt dat het eiwit aan DNA bindt via het bolletje, terwijl de armpjes weg wijzen van het DNA. Op DNA moleculen met een uiteinde kan het Rad50 complex grote structuren, oligomeren, vormen die bestaan uit meerdere complexen. Deze structuren blijven niet bij het uiteinde van het DNA, maar kunnen naar binnen toe bewegen. De affiniteit van het Rad50 complex voor verschillende typen DNA uiteinden wordt beïnvloed door ATP, wat past bij de hierboven beschreven mogelijke vormverandering in Rad50 door ATP binding. De observatie dat oligomeren van het Rad50 complex verschillende DNA moleculen bij elkaar kunnen brengen door interacties van de uiteinden van de eiwit armpjes, is een hele belangrijke aanwijzing voor de mogelijke functie van het Rad50 complex. De flexibiliteit van de armpjes kan zorgen voor een sterke maar ook flexibele binding, vergelijkbaar met klittenband. Deze vindingen geven aan dat het Rad50 complex een functie heeft in het bij elkaar houden van DNA moleculen op een flexibele manier, terwijl andere eiwitten die bijvoorbeeld DNA moleculen bewerken en aan elkaar plakken nog steeds goed bij het DNA uiteinde kunnen komen. Deze activiteit past precies bij alle processen waarbij het Rad50 complex betrokken is.

Alle organismen hebben eiwit complexen waarvan de globale vorm veel lijkt op dat van het Rad50 complex. Samen vormen deze eiwitten een familie waarvan de leden verschillende structurele functies hebben in de organisatie van chromosomen. Een analyse van verschillende eiwitten uit deze familie met behulp van de 'scanning force' microscoop laat zien dat ze inderdaad bestaan uit dezelfde onderdelen, maar dat deze onderdelen op verschillende manieren gerangschikt zijn. De precieze rangschikking van de onderdelen is hoogstwaarschijnlijk toegespitst op de specifieke functie van de familieleden.

List of publications

Kamiuchi, S., Saijo, M., Citterio, E., de Jager, M., Hoeijmakers, J. H. J., and Tanaka, K. (2002). Translocation of Cockayne syndrome group A protein to the nuclear matrix: possible relevance to transcription-coupled DNA repair. *Proc. Natl. Acad. Sci. USA* 99, 201-206.

de Jager, M., Dronkert, M. L., Modesti, M., Beerens, C.E., Kanaar, R., and van Gent, D. C. (2001). DNA-binding and strand-annealing activities of human Mre11: implications for its roles in DNA double-strand break repair pathways. *Nucleic Acids Res.* 29, 1317-1325.

de Jager, M., van Noort, J., van Gent, D.C., Dekker, C., Kanaar, R., and Wyman, C. (2001). Human Rad50/Mre11 is a flexible complex that can tether DNA ends. *Mol. Cell* 8, 1129-1135.

de Jager, M., and Kanaar R. (2002). Genome instability and *Rad50^S*: subtle yet severe. *Genes Dev.* 16, 2173-2178.

de Jager, M., Wyman, C., van Gent, D.C., and Kanaar R. (2002). DNA end-binding specificity of human Rad50/Mre11 is influenced by ATP. *Nucleic Acids Res.* 30, 4425-4431.

van Noort, J., van der Heijden, T., de Jager, M., Wyman, C., Kanaar, R. and Dekker, C. (2003). The coiled coil of the human Rad50 DNA repair protein contains specific segments of increased flexibility. Submitted.

Curriculum Vitae

naam	Martijn de Jager
geboren	9 januari 1977 te Gouda
1989-1991	HAVO (jaar 1 en 2) Rijks Scholen Gemeenschap te Gouda
1991-1994	HAVO (jaar 3 t/m 5) Gertrudis Lyceum te Roosendaal
1994-1998	Hogere Laboratorium Opleiding Hogeschool West-Brabant te Etten-Leur richting Medisch, specialisatie Biotechnologie
1997-1998	stage en afstuderen Erasmus Universiteit Rotterdam, afdeling Celbiologie en Genetica titel afstudeeronderzoek: ' A study of the role of Cockayne syndrome group A protein in transcription-coupled DNA repair' onder begeleiding van Prof. dr. J.H.J. Hoeijmakers, Dr. W. Vermeulen en Drs. E. Citterio
1998-2002	promotie onderzoek Erasmus MC Rotterdam, afdeling Celbiologie en Genetica promotoren: Prof. dr. R. Kanaar en Prof. dr. J.H.J. Hoeijmakers co-promotor: Dr. C. Wyman
2002-	Erasmus MC Rotterdam, afdeling Celbiologie en Genetica wetenschappelijk onderzoeksmedewerker in tijdelijke dienst

Dankwoord

Allereerst heel veel dank aan Jan Hoeymakers. Je bent niet alleen een fantastische wetenschapper, maar ook een buitengewone persoonlijkheid. Het is geweldig hoe je altijd geïnteresseerd bent in ieders wel een wee. Bedankt dat je het aandurfte om mij als AIO aan te nemen en heel veel dank voor je enthousiasme en steun.

Anderen die deze stap durften te nemen zijn Dik en Roland. Dik, bedankt voor het eerste jaar begeleiding, ik heb hier heel veel van geleerd. Roland, heel erg bedankt dat je het over wilde nemen toen het even niet zo lekker liep. Ik denk dat je in vele opzichten een topwetenschapper bent. Ik heb heel veel van je geleerd en met veel plezier onder jouw begeleiding gewerkt. Also a lot of thanks to your 'partner in crime': Claire, I've enjoyed your excellent scientific input in this work as well as your warm personality.

Hennie, bedankt voor de samenwerking en steun gedurende het eerste jaar. 'Ome' Coen en Jeroen, bedankt voor jullie steun en wijze raad. Coen, het was een geweldige (muzikale) ervaring met jou in het lab. Jeroen, bedankt verder voor je hulp als paranimf. Another uncle to me is Mauro. You're a great scientist and person, thanks for everything!

A lot of thanks also to everybody of the department, and especially to the 738-ies: bedankt André, Cecile, Mies en Raoul; dziękuję Justia and Asia; shukriya Sheba; huala lepo DeJane; arigato gozaimasu Katsu (hiro)!!! Deborah, bedankt voor het delen van deze promotie-ervaring en heel veel succes! Verder bedankt Jan Jos (voor de avontuurlijke wandelingen en weekends), de computer-experts en Tom, Jasparina, Rita en Mariete voor de 'logistische' ondersteuning. John, Thijn, Peter en Cees, bedankt voor de plezierige samenwerking. Michiel, bedankt, ook voor je hulp als paranimt en veel succes met je eigen promotie.

Papa en mama, bedankt voor jullie veelzijdige steun door de jaren heen! Maaike, Eric en opa, bedankt voor jullie belangstelling. Du, thank you for your support, understanding, and love, and good luck with your own thesis. Huala ra sie!

Nogmaals bedankt allemaal, zonder jullie had dit boekje hier zeker niet gelegen!
Martijn